

OUTPUT FEEDBACK ADAPTIVE CONTROL IN THE PRESENCE OF UNMODELED DYNAMICS

A Thesis
Presented to
The Academic Faculty

by

Rajeev Chandramohan

In Partial Fulfillment
of the Requirements for the Degree
Doctor of Philosophy in the
School of Aerospace Engineering

Georgia Institute of Technology
December 2016

Copyright © 2016 by Rajeev Chandramohan

OUTPUT FEEDBACK ADAPTIVE CONTROL IN THE PRESENCE OF UNMODELED DYNAMICS

Approved by:

Professor Anthony J Calise,
Committee Chair
School of Aerospace Engineering
Georgia Institute of Technology

Professor Anthony J Calise, Advisor
School of Aerospace Engineering
Georgia Institute of Technology

Assoc.Professor Eric N Johnson
School of Aerospace Engineering
Georgia Institute of Technology

Professor J.V.R. Prasad
School of Aerospace Engineering
Georgia Institute of Technology

Professor James E Steck
Aerospace Engineering
Wichita State University

Assist.Professor Tansel Yucelen
Mechanical Engineering
University of South Florida

Date Approved: 15 September 2016

To,
My Parents,

ACKNOWLEDGEMENTS

I would like to thank my advisors, Dr. Anthony J Calise and Dr. Eric N Johnson for their guidance and support throughout my doctoral studies at Georgia Institute of Technology. I would like to extend my gratitude to the other members of my committee for their helpful comments and suggestions. Thanks are also due to Dr. James E Steck who introduced me to the world of adaptive flight control during the course of my graduate studies at Wichita State University. I also want to thank my family and friends for their help and support during the course of my studies at Georgia Institute of Technology.

TABLE OF CONTENTS

| | |
|---|-------------|
| DEDICATION | iii |
| ACKNOWLEDGEMENTS | iv |
| LIST OF TABLES | vii |
| LIST OF FIGURES | viii |
| SUMMARY | x |
| I INTRODUCTION | 1 |
| 1.1 Model Reference Adaptive Control | 2 |
| 1.2 Function Approximators | 5 |
| 1.3 Research in Output Feedback Adaptive Control | 8 |
| 1.4 Research in Adaptive Control Of Systems with Unmodeled Dynamics | 10 |
| 1.5 Thesis Contributions and Overview | 15 |
| II ADAPTIVE OUTPUT FEEDBACK CONTROL FOR MATCHED UNMODELED DYNAMICS | 17 |
| 2.1 Introduction | 17 |
| 2.2 Problem Formulation | 17 |
| 2.3 Boundedness of Signals | 25 |
| 2.4 Wing Rock Dynamics | 32 |
| 2.5 Control of Flexible Spacecraft | 40 |
| 2.6 Summary | 45 |
| III REDUCING THE EFFECT OF NOISE IN ADAPTIVE CONTROL | 46 |
| 3.1 Introduction | 46 |
| 3.2 The effect of noise on adaptive control | 46 |
| 3.3 Reducing the effect of sensor noise | 48 |
| 3.4 Boundedness Analysis | 48 |
| 3.5 Control of Flexible Spacecraft | 50 |

| | | |
|-------------------|---|------------|
| 3.6 | Summary | 52 |
| IV | ADAPTIVE OUTPUT FEEDBACK CONTROL FOR SYSTEMS WITH INPUT UNCERTAINTY | 53 |
| 4.1 | Introduction | 53 |
| 4.2 | Problem Formulation | 54 |
| 4.3 | Boundedness of signals | 56 |
| 4.4 | Control of Flexible Spacecraft in the presence of Input Uncertainties | 61 |
| 4.5 | Reducing the effect of sensor noise for systems with input uncertainty | 68 |
| 4.6 | Attitude control of flexible spacecraft with input uncertainty in the presence of noise | 69 |
| 4.7 | Summary | 72 |
| V | ADAPTIVE CONTROL OF A FLEXIBLE UNMANNED AERIAL VEHICLE | 73 |
| 5.1 | Introduction | 73 |
| 5.2 | Flexible UAV Model | 74 |
| 5.3 | Nominal Control Design | 78 |
| 5.4 | Adaptive Control Design | 84 |
| 5.5 | Adaptive Control For Uncertain Control Effectiveness | 88 |
| 5.6 | Conclusion | 93 |
| VI | SUMMARY AND FUTURE RESEARCH | 95 |
| 6.1 | Future Research | 96 |
| APPENDIX A | — FLEXIBLE UAV MODEL | 100 |
| APPENDIX B | — CONVERTING FROM MODAL FORM TO STATE SPACE | 110 |
| REFERENCES | | 112 |
| VITA | | 119 |

LIST OF TABLES

| | | |
|---|---|----|
| 1 | Eigenvalues derived from stability derivative model | 75 |
| 2 | Eigenvalues derived from eight state model | 75 |
| 3 | Eigenvalues derived from forty four state model | 77 |

LIST OF FIGURES

| | | |
|----|--|----|
| 1 | Model Reference Adaptive Control Architecture | 3 |
| 2 | Linear in the parameter neural network with 3 inputs and a bias | 7 |
| 3 | Neural Network with a single hidden layer | 8 |
| 4 | Adaptive Control Architecture for Systems With Unmodeled Dynamics | 23 |
| 5 | Geometric representation of sets | 29 |
| 6 | Limit value of $\bar{\mu}$ for $Q_0 = I_2$ | 35 |
| 7 | Bank angle response of the nominal controller without uncertainty and unmodeled dynamics. | 37 |
| 8 | Nominal control input without uncertainty and unmodeled dynamics. | 37 |
| 9 | Comparison of bank angle responses with uncertainty and unmodeled dynamics. | 38 |
| 10 | Comparison of control inputs with uncertainty and unmodeled dynamics. | 38 |
| 11 | Comparison of bank angle responses for two different adaptive laws. | 39 |
| 12 | Comparison of control inputs for two different adaptive laws. | 39 |
| 13 | Response of the rigid spacecraft model under nominal control. | 43 |
| 14 | Response of the rigid spacecraft model under adaptive controller that employs delayed inputs and outputs. | 44 |
| 15 | Response of the flexible spacecraft model under Ref.[41] adaptive control. | 44 |
| 16 | Response of the flexible spacecraft model under adaptive controller that employs delayed inputs and outputs. | 45 |
| 17 | Adaptive control response of the spacecraft model in the presence of noise with the weight update developed in Chapter 2. | 51 |
| 18 | Adaptive control response of the spacecraft model in the presence of noise with filtered error signal. | 52 |
| 19 | Response of the rigid spacecraft model under nominal control. | 63 |
| 20 | Response of the flexible nonlinear spacecraft model under nominal control. | 64 |
| 21 | Response of the nonlinear flexible spacecraft model without input uncertainty for the adaptive design with $\gamma_d = 0$, $\Gamma_{W_2} = 0$ | 66 |

| | | |
|----|--|----|
| 22 | Response of the nonlinear flexible spacecraft model with input uncertainty for the adaptive design with $\gamma_d = 0$, $\Gamma_{W_2} = 0$ | 67 |
| 23 | Response of the nonlinear flexible spacecraft model with input uncertainty with input uncertainty for the adaptive design with $\gamma_d = 10$, $\Gamma_{W_2} = 5$ | 68 |
| 24 | Response of the flexible spacecraft model with sensor noise using the weight update law in Equations (4.18), (4.19) and (4.20) and the same adaptation parameter values as in Figure 23. | 71 |
| 25 | Response of the flexible spacecraft model with sensor noise using the weight update law in Equations (4.59), (4.60) and (4.61) and the same adaptation parameter values as in Figure 23. | 72 |
| 26 | Response of the rigid stability derivative UAV model under nominal control. | 82 |
| 27 | Response of the eight state UAV model under nominal control. | 83 |
| 28 | Response of the forty four state UAV model under nominal control. | 84 |
| 29 | Response of the forty four state UAV model under adaptive control. | 86 |
| 30 | Response of the forty four state UAV model under adaptive control with noisy measurements. | 87 |
| 31 | Response of the forty four state UAV model under adaptive control using filtered error signal in the adaptive law with noisy measurements. | 88 |
| 32 | Response of the forty four state UAV model under adaptive control developed in Chapter 2 with input uncertainty. | 90 |
| 33 | Response of the forty four state UAV model under adaptive control developed in Chapter 4 with Input Uncertainty. | 91 |
| 34 | Response of the forty four state UAV model under adaptive control developed in Chapter 4 with noisy measurements. | 92 |
| 35 | Response of the forty four state UAV model under adaptive control developed in Chapter 4 using filtered error signal with noisy measurements. | 93 |

SUMMARY

This thesis outlines a method of output feedback adaptive control in the presence of matched unmodeled dynamics, uncertain control effectiveness and matched parametric uncertainties. An adaptive feedback controller that augments an assumed existing observer based linear controller is developed. The adaptive approach outlined here assumes that the uncertainty within the system can be linearly parameterized in terms of current and delayed values of inputs and measured outputs. New weight update laws are developed to show that all the signals in the system are uniformly ultimately bounded using a Lyapunov like analysis that depends on the existence of a positive definite solution of a parameter dependent Riccati equation in the presence of unmodeled dynamics, uncertain control effectiveness and parametric uncertainties. The unique attributes of this approach are that it can be used to augment an existing linear controller without modifying the parameters of that controller, it does not rely on the use of high gains in the adaptation law, and is adaptive to the presence of matched parametric uncertainties and unmodeled dynamics. One key difference between the proposed design and existing methods is that it does not rely on the use of a high gain observer or high gain error observer in the weight update law. The thesis also addresses the effect of noisy measurements on the performance of adaptive controllers by filtering the error signal employed in the weight update laws. Uniform ultimate boundedness of all signals is shown utilizing concepts of singular perturbation theory by treating the filter as a fast subsystem and the system dynamics together with weight update law as a slow subsystem. The design procedure is evaluated by augmenting an existing observer based controller with an adaptive controller to compensate for unmodeled dynamics, unknown control effectiveness and

parametric uncertainties in the presence of noisy measurements for several aerospace applications that include a flexible satellite example and a 44-state highly flexible aircraft example.

CHAPTER I

INTRODUCTION

Linear control theory provides a basis for designing controllers for systems to meet performance and robustness specifications. One of the major disadvantages of linear controllers is that the system to be controlled must be modeled by linear ordinary differential equations. Most physical systems contain nonlinearities to some degree, as well as unmodeled dynamics. In order to design linear controllers for practical systems, systems are linearized about an operating point and a set of controllers are designed at the operating points using linear control theory. Linear controllers designed about a specified operating point provide adequate performance in a neighborhood of the operating point which deteriorates as the system moves away from the operating point due to the presence of nonlinearities and other forms of uncertainty. Therefore for systems with a large operating envelope, such as flight control systems, it is necessary to gain schedule a controller as the system moves from the neighborhood of one operating point to another. If these transitions occur rapidly, then the validity of such an approach becomes questionable.

Robust control theory provides theoretical methods to design linear controllers to compensate for uncertainty between the mathematical model and the actual system. Controllers designed using robust control theory result in linear controllers with fixed parameters that can maintain performance specifications in the presence of a specified amount of uncertainty. However, such designs may be overly conservative when applied to highly uncertain systems.

Adaptive control theory can be used to design nonlinear controllers whose parameters vary with time based on an adaptation law. An adaptive controller can

be expected to perform better in the presence of large uncertainty than a fixed gain controller, or a controller whose gains are scheduled as a function of flight condition, particularly if the uncertainty is matched. However this advantage comes at a price, because adaptive controllers are inherently nonlinear and require concepts from nonlinear system theory to establish stability of systems controlled with such controllers. One of the major challenges in adaptive controller design involves the design of a learning algorithm to update the parameters of the adaptive controller such that all the signals in the system are guaranteed to be bounded under a reasonable set of assumptions.

1.1 Model Reference Adaptive Control

In Model Reference Adaptive Control (MRAC), [65, 64, 72, 5, 52], the objective is to design an adaptive controller such that the system under control follows a reference model. There are two different approaches to MRAC termed Direct [54, 65, 5] and Indirect [64, 13, 9, 29] Adaptive Control. In Direct Adaptive control, the controller parameters are updated online such that the output of the closed loop system follows the reference model with bounded errors. In Indirect Adaptive control the parameters of the system are estimated using a parameter estimation algorithm. The estimated parameters are then used to design the controller such that the closed loop system follows the reference model. In this thesis a Direct Adaptive output feedback control in the presence of unmodeled dynamics is investigated.

MRAC in output feedback form is composed of three major subsystems as shown in Figure 1. The first component is the reference model which specifies the desired response of the system under control. For example, in an aircraft control problem the reference model is constructed such that it satisfies the flying qualities specification. It may itself be a closed loop model of the dynamics of an aircraft obtained from a gain scheduled linear control design performed at selected flight conditions. The most

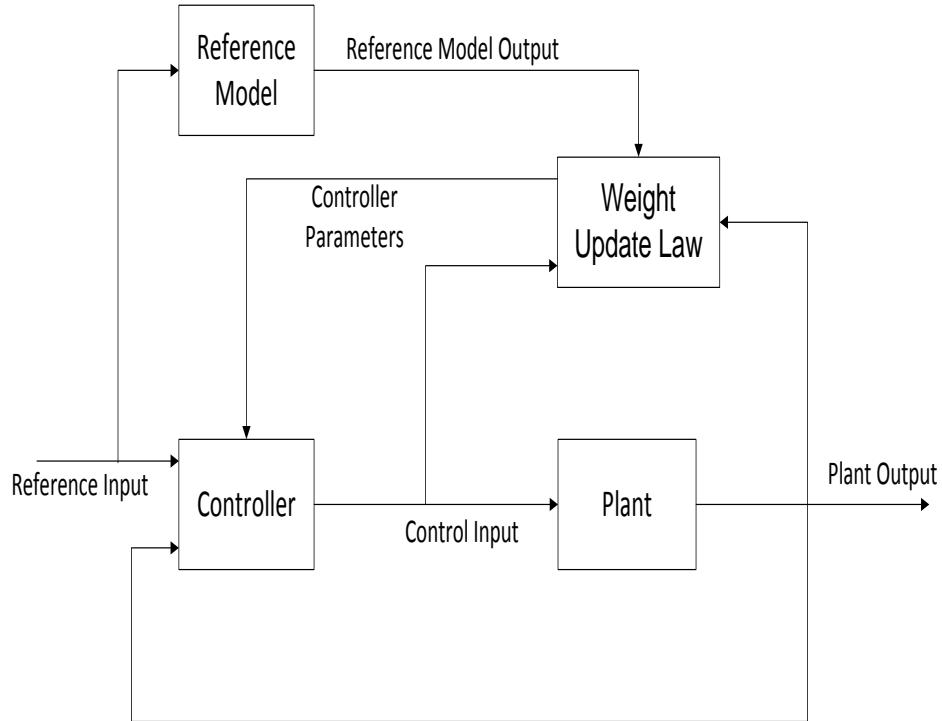


Figure 1: Model Reference Adaptive Control Architecture

important subsystem in MRAC architecture is the weight update law that specifies how the controller parameters vary with time. The weight update law has to be chosen such that the error between output of the actual system under consideration and the reference model output, together with all internal signals, remain bounded. Since adaptive control architectures result in closed loop systems that are nonlinear, the weight update law is chosen such that the time derivative of a candidate Lyapunov function is at least negative semi-definite. The third component of the MRAC scheme is the controller structure. For example one could design the controller with a fixed structure in which some or all of the parameters of the controller are updated online [39]. In this setting the design of the controller may be considered as a part of the overall MRAC design process. Another approach is to consider an existing controller with fixed parameters which is augmented with an adaptive element whose parameters are updated [83, 85, 40, 11, 10]. In this setting the controller is given, and not

a variable in the overall MRAC design process. This approach has found more acceptance since it is possible to retrofit legacy controllers designed using linear control theory with adaptive elements to improve robustness to parametric uncertainty.

The mathematical models of the system that need to be controlled are realized using one of two methods, physics based modeling or data fitting using experimental data. In physics based modeling, the mathematical model is obtained using Newton's laws of motion for mechanical systems and Kirchoff's current and voltage laws for systems involving electrical components. In either of these methods a number of simplifying assumptions are utilized to obtain the mathematical model of the system under consideration. Models obtained using this method produce models that are accurate at low frequency but deviate significantly from the actual model at higher frequencies. This is representative of models for systems modeled assuming rigid body dynamics wherein the flexible modes of the system are ignored. When fitting a model using experimental data, one loses the underlying physical insight of the system under investigation. This approach often results in an input/output model in which the states do not correspond to physical quantities. Therefore, systems that are modeled using either of these methods produce models in which all the states are not available for feedback. Thus one needs to design adaptive controllers for systems in which only the output is available for feedback (see Section 1.3). Research in adaptive output feedback control of uncertain nonlinear dynamic systems has seen renewed interest due to emerging applications in the area of flight control of extremely flexible aircraft and rotorcraft that cannot be modeled as a state feedback problem [75, 79]. In the recent past, peizo electric films and synthetic jets have been used for active control of flexible structures and fluid flows over airfoils [62, 37, 47, 61]. Synthetic jet actuators are highly nonlinear in nature and in addition they couple with the system that they are used to control and give to rise to higher order dynamics that have to be accounted for while designing the control system.

The use of adaptive control to overcome parametric uncertainty has been studied extensively. Most of these studies fall within the scope of state feedback adaptive control wherein the higher order dynamics have been ignored. Output feedback adaptive control to address both parametric and unmodeled dynamics is an area of active research. Two different approaches have been studied extensively in the design of output feedback adaptive control. One approach that has been proposed is the use of a fixed observer to estimate the state of the system under control [51, 23]. This requires that the dimension of the plant be known. This approach has also been extended in which the linear observer is replaced by an adaptive observer [30]. In the other approach the requirement that the dimension of the plant be known is relaxed by using an error observer in place of the state observer [81, 4]. The major drawback with this approach is the increased complexity associated with the design and implementation of the resulting adaptive controller. Recently Kostarigka et al [45] have developed a switching type dynamic adaptive output feedback neural network for uncertain systems with prescribed performance. The authors show that guaranteeing a boundedness property for the states of a specifically defined augmented closed loop system is sufficient and necessary to solve the problem under consideration.

1.2 Function Approximators

Model Reference Adaptive Control schemes necessitate approximation of unknown nonlinear uncertainty present in most physical system. This necessitates the use of function approximators in the design of MRAC architectures. Several different parametric structures can be used to approximate this uncertainty. Splines [3], wavelets [12], artificial neural networks [21] are some examples of parametric structures that have been studied in the context of MRAC. Each of these have their advantages and

disadvantages. Parametric structures of the form:

$$y = W^T \sigma(\bar{x}) \quad (1.1)$$

$$y = W^T \sigma(V^T \bar{x}), \quad (1.2)$$

are used to approximate uncertainties, where $\bar{x} \in R^{n+1}$:

$$\bar{x} = [x_1 \ x_2 \ x_3 \ \dots \ x_n \ 1]^T, \quad (1.3)$$

$$W = [w_1 \ w_2 \ w_3 \ \dots \ w_n \ w_b]^T, \quad (1.4)$$

$$V = \begin{bmatrix} v_{11} & v_{12} & v_{13} & \dots & v_{1n} & v_{1b} \\ v_{21} & v_{22} & v_{23} & \dots & v_{2n} & v_{2b} \\ v_{31} & v_{32} & v_{33} & \dots & v_{3n} & v_{3b} \\ \vdots & \vdots & \vdots & \ddots & \vdots & \vdots \\ v_{b1} & v_{b2} & v_{b3} & \dots & v_{bn} & v_{bb} \end{bmatrix}, \quad (1.5)$$

The important distinguishing feature of these structures is the nonlinear activation function $\sigma(\cdot)$, in Equations (1.1) and (1.2), that act on the inputs and are usually bounded in their output. Some of the commonly used activation functions are sigmoid, tanh, radial basis functions etc. Example outputs of nonlinear activation functions for sigmoid, tanh and radial basis functions are:

$$\sigma(z) = \frac{1 - e^{-z}}{1 + e^{-z}}, \quad (1.6)$$

$$\tanh(z) = \frac{e^{2z} - 1}{e^{2z} + 1}, \quad (1.7)$$

$$\phi(z) = e^{|z-c|^2/\mu} \quad (1.8)$$

Such parametric structures have been termed Neural Networks (NNs) [53, 6, 5, 60] and have been used extensively in adaptive control [88, 6]. These structures are classified as linear in the parameter neural network or as nonlinear in the parameter neural network structures based on whether the output y is a linear function of the weights, as in Equation (1.1), or a nonlinear function of the weights, as in Equation (1.2). These structures are diagrammed in Figures 2 and 3. In general, parameterizations of

the uncertainty where the weights appear nonlinearly provide a better approximation as opposed to that when the weights appear linearly. This thesis is limited to the use of parametric structure of the form in Figure 2.

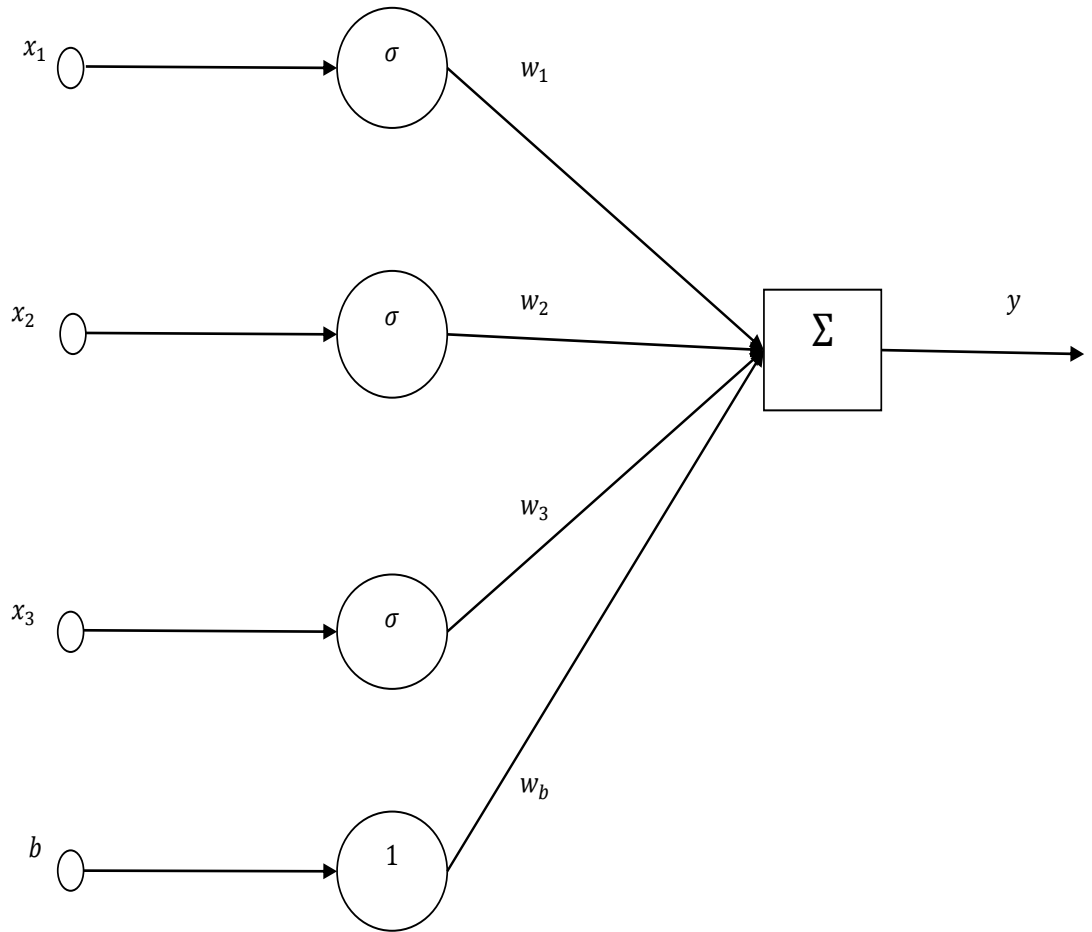


Figure 2: Linear in the parameter neural network with 3 inputs and a bias

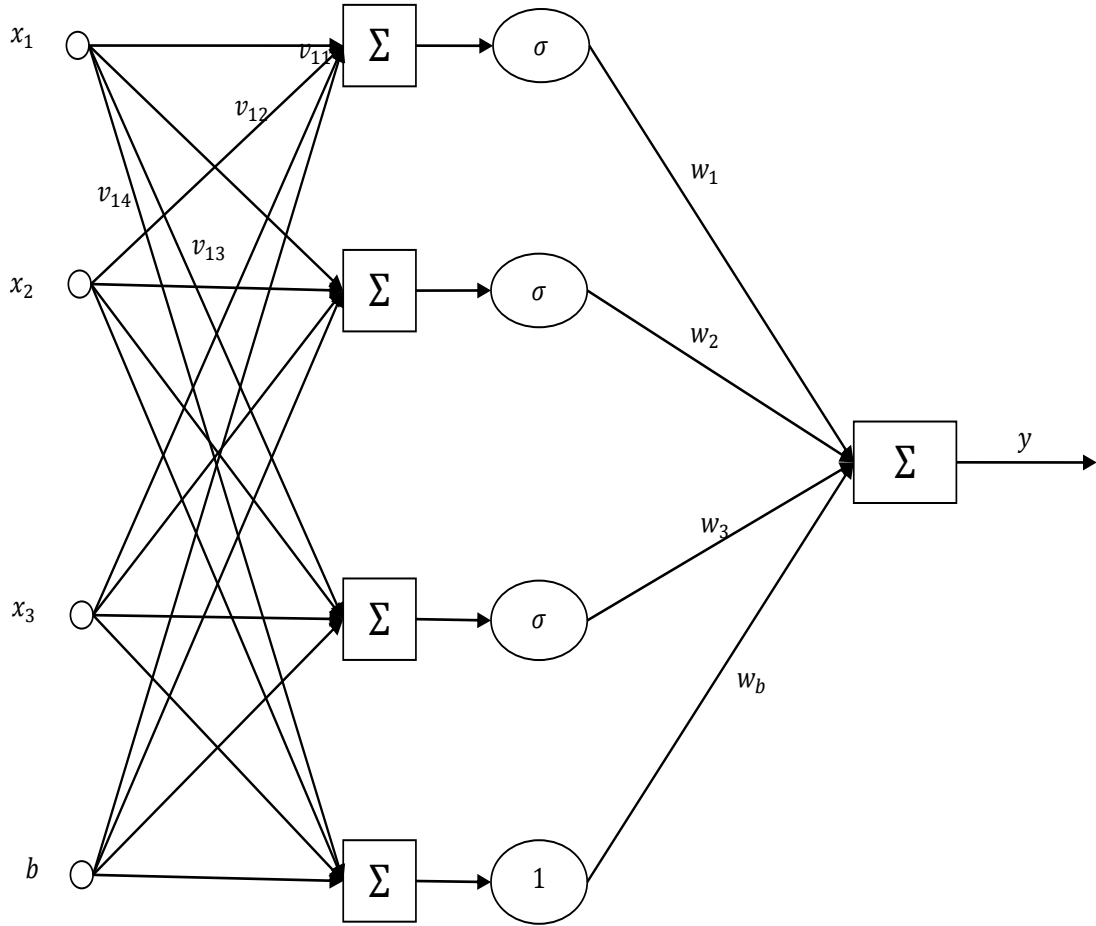


Figure 3: Neural Network with a single hidden layer

1.3 Research in Output Feedback Adaptive Control

There are two major approaches to Output feedback adaptive control. One method is based on state estimation whereas the other uses an error observer. Marino et al.[56] and Krstic et al.[46] have presented output feedback adaptive control with backstepping based architectures. One major drawback of such adaptive control architectures is their dependence on time derivatives of the inputs and outputs of the system making them unsuitable for designing controllers for noisy systems. Kim and Lewis[44] have proposed using neural network based observers in the design of output feedback adaptive designs.

Seshagiri et al.[71] have proposed an adaptive output feedback control architecture for output tracking for single input single output nonlinear systems that are input-output linearizable with full state feedback. They use a Radial Basis Function (RBF) to approximate the nonlinearities of the system under consideration. Their method utilizes a high gain observer, parameter projection and control saturation to achieve semi global uniform ultimate boundedness.

Calise et al[4] developed a direct adaptive output feedback control design procedure for highly uncertain nonlinear systems, which does not rely on state estimation. The authors considered single-input/single-output (SISO) nonlinear systems. The method employs feedback linearization, coupled with a neural network to compensate for modeling errors. A fixed dynamic compensator is used to stabilize the system. The neural network is adapted online using a linear combination of the tracking error signal and the compensator states. They further augment the controller with a low pass filter designed to satisfy a strictly positive real condition. The proposed method applies to systems with parametric uncertainties but does not address systems with unmodeled dynamics.

Hovakimyan et al.[32] consider SISO non-affine in control uncertain systems with the output having full relative degree. The authors use a linear error observer to design an output feedback adaptive control architecture. Using approximate feedback linearization the nonlinear dynamics are inverted and the authors then use an error signal derived from a linear error observer as inputs to the neural network as well as in the adaptation laws to account for modeling errors. The authors show ultimate boundedness using Lyapunov's direct method.

Lavretsky[49] has introduced an adaptive output feedback tracking controller for dynamical systems with matched uncertainties. In this method it is shown that approximately achieving a Strictly Positive Real (SPR) property with a state observer enables the design of a direct adaptive model reference output feedback controller in

the presence of matched uncertainties. The asymptotic properties of the Algebraic Riccati Equation of a standard LQG/LTR [17] controller are used to prove boundedness of all the signals within the closed loop system. The adaptive controller is implemented as an augmentation to a nominal controller that was designed using a LQG/LTR method.

Kim et al. [?, 42] have proposed a novel scheme for output feedback adaptive control. This approach is based on the use of a linear observer to estimate the states of the system. The observer in this control architecture is designed such that it replaces the reference model in standard MRAC architecture. The adaptive element consists of a parametric structure of the the form in Equation (1.1) with a novel weight update law. The new weight update law ensures that the estimated states of the observer track the reference model states as well as the actual states of the system with bounded errors. Though the formulation followed in this approach is in the setting of MRAC, the realization does not need the reference model to generate the error signal. This architecture is desirable since existing observer based controllers can be augmented solely by addition of the adaptive element. The authors have evaluated this architecture on a simple wing rock model and also on an aeroelastic aircraft model which demonstrated the performance benefits associated with this method. A similar approach based on a parameter dependent Riccatti equation in the context of derivative free MRAC is presented in [86, 82, 87]. However, a major deficiency of this method is that is not applicable to systems with unmodeled dynamics. In addition, the method developed does not account for systems with input uncertainty. Further they also do not address the effect of noisy sensor signals on adaptive control.

1.4 Research in Adaptive Control Of Systems with Unmodeled Dynamics

Rohrs et al.[70] were the first to study the effect of continuous time adaptive control algorithms subjected to unmodeled plant dynamics. In their study it was determined

that standard adaptive control algorithms can excite the unmodeled high frequency dynamics of the underlying nonlinear dynamics associated with the plant driving the system unstable. This was especially true in the presence of sinusoidal reference inputs and/or sinusoidal disturbances. As a result of this study they concluded that existing adaptive control algorithms circa 1985 cannot be used in practical designs where the plant contains unmodeled dynamics because the adaptive control may drive the system unstable. It was their conclusion that further study was necessary to study the effect of adaptive controllers for systems with unmodeled dynamics.

Taylor et al.[78] presented a feedback linearization based regulation control design that accounted for both unknown parameters and unmodeled dynamics. In this paper a new adaptive update law was developed to account for the effects of unknown parameters while maintaining robustness to unmodeled dynamics present in the system under control. Furthermore, they were able to provide conditions for the global stability of the adaptive control law for the reduced order model for a class of nonlinear systems. They were able to show that the proposed adaptive weight update law preserved the regulation property in a stability region in the presence of unmodeled dynamics. In addition an estimate of the size of the stability region was obtained.

Astrom,K.J,[2] evaluated the behavior of adaptive control systems in non ideal situations. The effect of the interaction between disturbance acting on the system and the presence of unmodeled dynamics and adaptive control is also explored. The paper establishes the importance of the persistency of excitation in adaptive control. Ways to ensure that difficulties do not occur in the presence of anomalies are also presented.

Spall, J.C. et al.[76] consider the use of neural networks (NN's) in controlling a nonlinear, stochastic system with unknown process equations. Their approach based on using the output error of the system to train the neural network controller without the need to assume or construct a separate model for the unknown process dynamics.

The paper uses a new stochastic approximation algorithm for the weight estimation, which is based on a simultaneous perturbation gradient approximation. It has been shown that this algorithm can greatly enhance the efficiency over more standard stochastic approximation algorithms based on finite-difference gradient approximations. The approach is illustrated on a simulated waste water treatment system with stochastic effects and non-stationary dynamics.

Jiang, J.P. et al[35] present a constructive robust adaptive nonlinear control scheme that improves the robustness of an adaptive back stepping algorithm. The method accounts for a class of uncertainties including nonlinearly appearing parametric uncertainty, uncertain nonlinearities, and unmeasured input-to-state stable dynamics. One major advantage of the proposed adaptive control laws is that they do not require a dynamic dominating signal to guarantee the robustness property of Lagrange stability.

Yang et al[81] describe an adaptive output feedback-based disturbance compensator design. Compared to the classical disturbance observer design, their approach can be applied to a class of systems that can be nonlinear and/or unstable. Their main assumptions are that the relative degree of the regulated output variable is known, and that the system is minimum phase. The proposed method is evaluated on a system with unstable, unmodeled dynamics, and with both matched and unmatched external disturbances.

In another work Calise et al[7] propose an approach for augmenting a linear controller design with a neural-network-based adaptive element. The basic approach presented in the paper involves formulating an architecture for which the associated error equations have a form suitable for applying existing results for adaptive output feedback control of nonlinear systems. The proposed approach has been shown to be particularly well suited for control of flexible systems subject to limits in control

authority. The proposed methods effectiveness was tested on a laboratory experiment consisting of a three-disk torsional pendulum system, including control voltage saturation and stiction.

Hovakimyan et al[30] address the problem of augmenting a linear observer with an adaptive element. The design of the adaptive element in the paper employs two nonlinearly parameterized neural networks, the input and output layer weights of both the networks are adapted on line. The goal was to improve the performance of the linear observer when applied to a nonlinear system. In this method the learning signal was generated using a second linear observer of the nominal system's error dynamics.

Kim et al.[43] consider adaptive output feedback control of uncertain nonlinear systems and in particular to the design of high-bandwidth flight control of unmanned rotorcraft. They extend the method developed in [32] to systems with unmodeled dynamics. A linear error observer is used as inputs to the neural network as well as in the weight update law. The authors show that under a set of mild restrictions the method can be extended to plants of arbitrary but bounded dimension. The proposed method is applied in the design of a high-bandwidth pitch attitude control of an unmanned rotor craft. Due to the use of feedback linearization in the design of the adaptive controller, this method cannot be used to augment an existing linear controller.

In another work Hovakimyan et al [33] developed an output feedback control for uncertain MIMO systems with unmodeled dynamics using linearly parameterized neural networks which operates over a tapped delay line of memory units comprised of the systems input/output signals. The proposed methodology is applicable to non-minimum phase systems and for systems with both matched and unmatched uncertainties. The architecture proposed by the authors can be used to augment an existing linear controller and thus lends itself to augment existing controller designs.

The proposed method does not estimate the states of the system, instead it uses an error observer the outputs of which are used in the weight update laws. Ultimate boundedness of all the signals in the system is shown through Lyapunov's direct method. Simulations of an inverted pendulum on a cart to illustrate the theoretical results.

Yucelen et al. [84] consider robustness to unmodeled dynamics in a state feedback setting. The authors examine the performance of a derivative free adaptive control law [83] in the presence of matched unmodeled dynamics. In this work, the authors show that robustness to unmodeled dynamics is improved by increased adaptation gain which is accomplished by including a bias term in the set of basis functions. The attitude control of a flexible spacecraft model are used to compare the sensitivity of the derivative-based and derivative free adaptive control law to unmodeled dynamics.

In this thesis an output feedback adaptive control in the presence of higher order unmodeled dynamics and to account for uncertain control effectiveness and actuator failures. The method utilizes a neural network that operates on a tapped delay line of inputs and outputs of the system to compensate for both structured parametric uncertainties as well as for unmodeled dynamics acting on the system . A new weight update law that is similar in to the one developed by Kim et al. [?] is obtained using a parameter dependent Riccati equation. The unique attributes of the proposed approach are that it can be used to augment an existing linear controller without modifying the parameters of that controller, it does not rely on the use of high gains either in the adaptation law or in the observer design, it also does not involve the use of an error observer in the weight update law and is adaptive to the presence of matched unmodeled dynamics acting on the system.

1.5 Thesis Contributions and Overview

The main goal of the thesis is to develop an output feedback adaptive control methodology that is applicable to systems with unmodeled dynamics by augmenting an existing observer based nominal control. A simple but effective approach for reducing the effect of noisy signals on the adaptive control law is developed. The method is extended to systems with unmodeled dynamics with input uncertainty. The aim of the thesis is to develop a weight update law that preserves the boundedness of all the signals in the system.

In Chapter 2, adaptive feedback control for systems with matched uncertainties and unmodeled dynamics is presented. The unique attributes of the method are that it can be used to augment an existing linear controller without modifying the parameters of that controller, it is applicable to systems with unmodeled dynamics, it does not rely on the use of high gains neither in the adaptation law nor in the observer design, it is applicable to non-minimum phase systems and it does not require realization of a reference model. The stability properties of the adaptive system are established using a Lyapunov like stability analysis that relies on the existence of a positive definite solution of a parameter dependent Riccati equation. The effectiveness of the approach is illustrated through simulations on a wing rock model appended with unmodeled dynamics and on an attitude control of a flexible spacecraft with attitude feedback.

In Chapter 3 the effect of sensor noise in output feedback adaptive control is considered. A simple but effective approach that filters the error signal used in the weight update law is used to reduce the effect that sensor noise has on the adaptive portion of the control. All the signals in the system are shown to be Uniformly Ultimately Bounded (UUB) by applying singular perturbation theory by treating the filter as a fast subsystem and the system dynamics together with weight update law being treated as the slow subsystem. Simulations on the flexible spacecraft model corrupted with sensor noise are used to demonstrate the effectiveness of the method.

In Chapter 4, the adaptive controller developed in Chapter 2 is extended to systems with uncertain control effectiveness. As in the previous chapters, boundedness of all the signals in the system is shown through a Lyapunov like stability analysis. This extension retains the attributes of the adaptive control developed in Chapter 2. Next the approach developed in Chapter 3 is utilized to reduce the effect of noisy sensor signals on adaptive control for systems with input uncertainty. Simulations on the flexible spacecraft model with uncertain control effectiveness and output signals corrupted with sensor noise are used to demonstrate the effectiveness of the method.

In Chapter 5, the theory developed in Chapters 2 to 4 is applied to the design of an altitude control employing a 44 state model of a highly flexible aircraft. The output feedback adaptive controller design that augments an observer based linear control design is shown to be robust to uncertainties, unmodeled dynamics as well uncertain control effectiveness. Effectiveness of adaptive control to suppress the presence of noisy sensor signals is also considered by introducing noise on the measured outputs.

CHAPTER II

ADAPTIVE OUTPUT FEEDBACK CONTROL FOR MATCHED UNMODELED DYNAMICS

2.1 Introduction

In this chapter an adaptive control methodology for output feedback adaptive control is formulated. The method is applicable for uncertain systems with matched parametric uncertainty and/or matched unmodeled dynamics. The method augments an existing observer based nominal control with an adaptive element such that the output tracks a smooth reference input with bounded error. The distinguishing feature of the method is neither a high gain observer nor a linear error observer is employed in its realization. Other attributes of the approach are that it can be used to augment an existing linear controller without modifying the parameters of that controller, it is applicable to systems with unmodeled dynamics, it is applicable to non-minimum phase systems and it does not require realization of a reference model.

2.2 Problem Formulation

Consider the following minimal realization of an uncertain system coupled with a nonlinear function of unmodeled states

$$\begin{aligned}\dot{x}(t) &= Ax(t) + B[u(t) + g(x(t), x_d(t))], \\ y(t) &= Cx(t), \\ y_r(t) &= C_r x(t),\end{aligned}\tag{2.1}$$

where $x(t) \in \mathbb{R}^{n_x}$, is the state vector, $u(t) \in \mathbb{R}^m$, is the control input, $y(t) \in \mathbb{R}^p$ $p \geq m$, is the output available for feedback and $y_r(t) \in \mathbb{R}^m$ is the regulated output.

$A \in \mathbb{R}^{n_x \times n_x}$, $B \in \mathbb{R}^{n_x \times m}$, $C \in \mathbb{R}^{p \times n_x}$ and $C_r \in \mathbb{R}^{m \times n_x}$ are known matrices, and $g(x(t), x_d(t)) : \mathbb{R}^{n_x + n_{x_d}} \rightarrow \mathbb{R}^m$ denotes the effect of matched modeling error that may depend on both $x(t)$ and unmodeled dynamics represented by the unmodeled states in $x_d(t) \in \mathbb{R}^{n_{x_d}}$. The unmodeled states are assumed to evolve over time with the following dynamics

$$\dot{x}_d(t) = f_d(x(t), x_d(t)), \quad (2.2)$$

where both the function $f_d(x(t), x_d(t)) : \mathbb{R}^{n_x} \times \mathbb{R}^{n_{x_d}} \rightarrow \mathbb{R}^{n_{x_d}}$ and n_{x_d} are unknown.

Further the following assumptions hold :

Assumption 2.1: The system given in Equation (2.1) and Equation (2.2) is observable over the compact set \mathbb{D} with $y(t)$ regarded as the output.

Assumption 2.2: The function $g(x(t), x_d(t))$ is n times continuously differentiable over the compact set \mathbb{D} .

Assumption 2.3: $x_d = 0$ is a globally exponentially stable equilibrium point for the nonlinear system

$$\dot{x}_d(t) = f_d(0, x_d(t)) \quad (2.3)$$

and $\|\tilde{f}_d\| \triangleq \|f_d(x, x_d) - f_d(0, x_d)\| \leq b_d \quad \forall (x, x_d) \in \mathbb{D}$.

Remark 2.2.1. *There is no loss of generality regarding the choice of the origin as the equilibrium point, because any equilibrium point can be shifted to the origin by a change of variables.*

Remark 2.2.2. *Assumption 2.3 implies that the system in (2.2) is input-to-state stable with $x(t)$ as its input. Then, from converse Lyapunov theory, there exists a Lyapunov function $V_{x_d}(x_d)$ for the system in (2.3) satisfying the following conditions*

[38]:

$$c_1|x_d|^2 \leq V_{x_d}(x_d) \leq c_2|x_d|^2 \quad (2.4)$$

$$\frac{\partial V_{x_d}}{\partial x_d} f_d(0, x_d) \leq -c_3|x_d|^2 \quad (2.5)$$

$$\left| \frac{\partial V_{x_d}}{\partial x_d} \right| \leq c_4|x_d| \quad (2.6)$$

Using Equations (2.4-2.6), an upper bound for the time derivative of $V_{x_d}(x_d)$ can be derived as follows :

$$\begin{aligned} \dot{V}_{x_d}(x_d) &= \frac{\partial V_{x_d}}{\partial x_d} f_d(x, x_d) \\ \dot{V}_{x_d}(x_d) &= \frac{\partial V_{x_d}}{\partial x_d} f_d(0, x_d) + \frac{\partial V_{x_d}}{\partial x_d} f_d(x, x_d) - \frac{\partial V_{x_d}}{\partial x_d} f_d(0, x_d) \\ \dot{V}_{x_d}(x_d) &\leq -c_3|x_d|^2 + c_4b_d|x_d| \end{aligned} \quad (2.7)$$

Next we state a key assumption needed to parameterize the uncertainty acting on the system.

Assumption 2.4: The function $g(x, x_d)$ acting on the system in (2.1) can be linearly parameterized as

$$g(x, x_d) = W^T \zeta(\xi) + \epsilon(x, x_d), \quad \forall (x, x_d) \in \mathbb{D} \quad (2.8)$$

where $W \in \mathbb{R}^{s \times m}$ is an unknown ideal weight matrix satisfying $\|W\| \leq \bar{W}$, $\zeta(\xi) \in \mathbb{R}^{s \times 1}$, is a known basis vector of the form $\zeta(\xi) = [\zeta_1(\xi_1), \zeta_2(\xi_2), \zeta_3(\xi_3), \dots, \zeta_s(\xi_s)]^T$ satisfying $|\zeta_i(\xi_i)| \leq \bar{\zeta}$, and $\epsilon(x, x_d)$ is the residual error between the uncertainty and the linear parametrization satisfying $|\epsilon(x, x_d)| < \bar{\epsilon}$ on \mathbb{D} . The input vector ξ is a vector composed of a sufficient number of delayed values of the output y and input u and is defined by :

$$\begin{aligned} \xi(t) &= [y^T(t) \quad y^T(t-d) \quad \dots \quad y^T(t - (n_y - 1)d) \\ &\quad u^T(t) \quad u^T(t-d) \quad \dots \quad u^T(t - (n_u - 1)d)]^T \end{aligned} \quad (2.9)$$

where, $d > 0$ is a time delay.

Remark 2.2.3. *For the case where the unmodeled dynamics are of the form*

$$\dot{x}_d = Fx_d + Hx \quad (2.10)$$

and the basis functions for the uncertainty are known, then the $\mathbb{D} = \mathbb{R}^n$.

Using the main results from [50] and [31], it can be shown that the residual error $\epsilon(x, x_d)$ in Equation (2.8) can be made arbitrarily small given a sufficient number of basis functions.

Remark 2.2.4. *For SISO systems, the minimum number of delayed values of the output and input needed to approximate the uncertainty are $n_y = n - 1$ and $n - \rho - 1$ respectively, where $n = n_x + n_{x_d}$ and ρ is the relative degree of the output. For MIMO systems the number of input-output delays required to approximate the uncertainty depends on the vector relative degree of the system and the observability indices of the system as stated in [31].*

For nonlinear systems, the matrices A , B , C and C_r in Equation (2.1) are usually obtained by linearizing the dynamics at selected equilibrium conditions, and the resulting set of linear models are used to design a linear controller at each operating point. It is assumed that such a nominal controller for the system in Equation (2.1) exists for a neighborhood of each equilibrium point, and can be written in the form

$$u_n(t) = -K_x \hat{x}(t) + K_r r(t), \quad (2.11)$$

where $r(t) \in \mathbb{R}^m$, $|r| \leq \bar{r}$, is the bounded reference command, $K_x \in \mathbb{R}^{m \times n_x}$ is the state gain, $K_r \in \mathbb{R}^{m \times m}$ is the input gain and $\hat{x}(t)$ is an estimate of the state $x(t)$ which is obtained by the use of a state observer operating only on $y(t)$ and $u_n(t)$.

$$\begin{aligned} \dot{\hat{x}}(t) &= A\hat{x}(t) + Bu_n(t) + L(y(t) - \hat{y}(t)), \\ \hat{y}(t) &= C\hat{x}(t), \end{aligned} \quad (2.12)$$

where L is the observer gain designed such that $A - LC$ is Hurwitz.

Given A, B, K_x and K_r , define a reference model for the desired response of the closed loop system

$$\begin{aligned}\dot{x}_m(t) &= A_m x_m(t) + B_m r(t), \\ y_m(t) &= C_r x_m(t)\end{aligned}\tag{2.13}$$

where $A_m = A - BK_x$ is Hurwitz by design and $B_m = BK_r$. The gains K_x and K_r are designed for the system given in Equation (2.1) assuming that $x(t)$ is available for feedback and that $g(x(t), x_d(t)) = 0$ so that the regulated output $y_r(t)$ tracks the reference input $r(t)$ with acceptable transient error.

The aim of the adaptive control is to design a control law $u(t)$ such that regulated output $y_r(t)$ in Equation (2.1) tracks the output of the reference model $y_m(t)$ with bounded error using only the output $y(t)$ and $u(t)$ and their delayed values for feedback. Towards this end the nominal control law given in Equation (2.11) is augmented with an adaptive element $u_{ad}(t)$

$$u(t) = u_n(t) - u_{ad}(t)\tag{2.14}$$

The adaptive element $u_{ad}(t)$ is given by

$$u_{ad}(t) = \hat{W}^T(t)\zeta(\xi(t))\tag{2.15}$$

where $\hat{W}(t)$ is regarded as an estimate of W defined in Equation (2.8).

Define the state estimation error, output tracking error and the weight estimation errors as follows :

$$\tilde{x}(t) \triangleq x(t) - \hat{x}(t)\tag{2.16}$$

$$\tilde{y}(t) \triangleq MC\tilde{x}(t) = C_e\tilde{x}(t)\tag{2.17}$$

$$\tilde{W}(t) \triangleq W - \hat{W}(t)\tag{2.18}$$

where $M \in \mathbb{R}^{m \times p}$ can be freely chosen. The manner in which M can be chosen is addressed later in Remark 2.2.4. Also denote the state and estimated state tracking

errors:

$$e(t) \triangleq x(t) - x_m(t) \quad (2.19)$$

$$\hat{e}(t) \triangleq \hat{x}(t) - x_m(t) \quad (2.20)$$

The dynamics for the state estimation error $\tilde{x}(t)$ and the estimated state tracking error $\hat{e}(t)$ are given by :

$$\dot{\tilde{x}}(t) = A_e \tilde{x}(t) + B \tilde{g}(t), \quad (2.21)$$

$$\dot{\hat{e}}(t) = A_m \hat{e}(t) + LC \tilde{x}(t), \quad (2.22)$$

where $A_e = A - LC$ and $\tilde{g}(t) = g(x(t), x_d(t)) - u_{ad}(t)$. Note that since A_m is Hurwitz by design, \hat{e} is bounded provided \tilde{x} is bounded. The estimate of the ideal weight, $\hat{W}(t)$ in Equation (2.15), is updated based on the following weight update law

$$\dot{\hat{W}}(t) = \gamma_w \left[\zeta(\xi(t)) \tilde{y}^T(t) - \sigma \hat{W}(t) - \frac{\zeta(\xi(t)) \zeta^T(\xi(t))}{2\mu} \hat{W}(t) \right] \quad (2.23)$$

where γ_w and σ are tunable positive adaptation gains. The weight update law given in Equation (2.23) is the same as that developed in [?] with the exception that the basis function inputs consist of the current and delayed values of outputs and control inputs as previously defined in Equation (2.9), whereas in Kim [?] the basis function inputs consist of the states of the observer. It will be demonstrated that this makes the approach applicable to systems with unmodeled dynamics. The adaptive control architecture is illustrated in Figure 4 wherein the blocks corresponding to the nominal controller are shown in green, the plant in blue and the adaptive control blocks in red. Note that because of the definition of \tilde{y} in Equation (2.17), the observer serves the role of a reference model, and the reference model dynamics in Equation (2.13) are not a part of the adaptive control architecture.

Stability analysis of the weight update law in Equation (2.23) employs a candidate Lyapunov function that is dependent on the solution of a parameter dependent Riccati

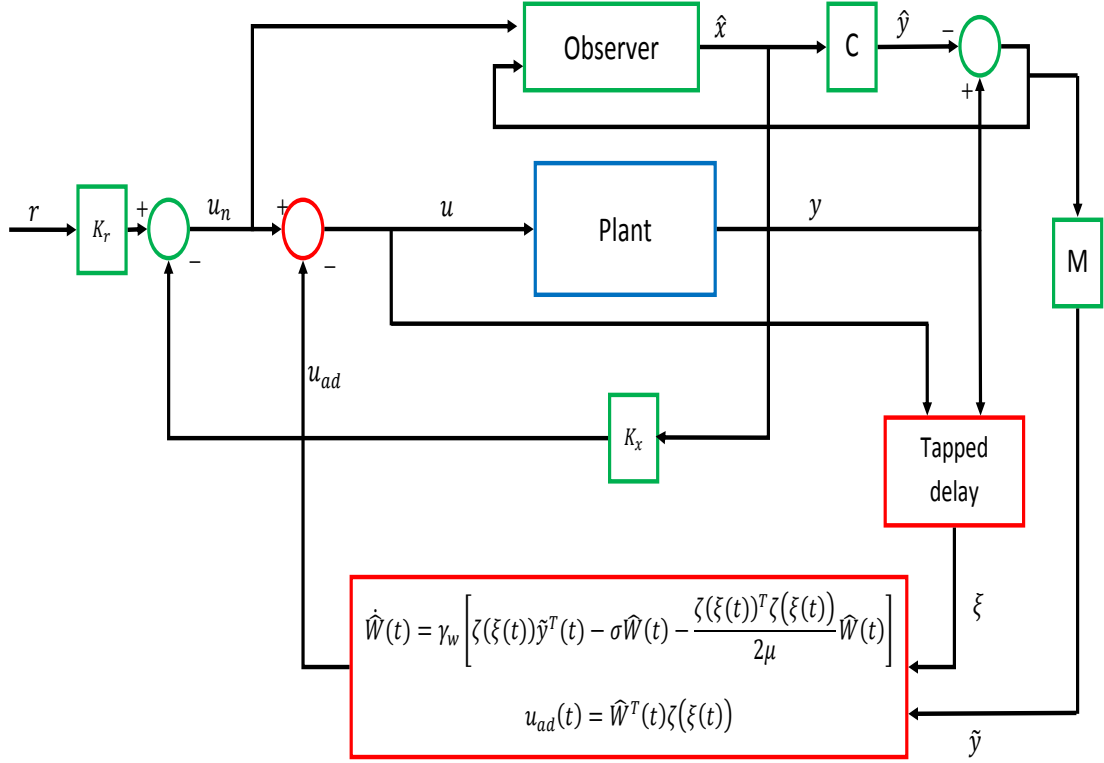


Figure 4: Adaptive Control Architecture for Systems With Unmodeled Dynamics

equation [?] given by :

$$0 = A_e^T P + P A_e + Q_0 + \mu N N^T \quad (2.24)$$

$$N = C_e^T - P B \quad (2.25)$$

where $Q_0 > 0$ for which there exists $\bar{\mu} > 0$ such that (2.24) possesses a unique positive definite solution for all $0 < \mu < \bar{\mu}$.

Remark 2.2.5. If $N = 0$ in Equation (2.25), it follows that:

$$0 = A_e^T P + P A_e + Q_0 \quad (2.26)$$

$$0 = C_e^T - P B \quad (2.27)$$

which implies that the transfer function associated with the system $G(s) = C_e(sI - A_e)^{-1}B$ is strictly positive definite. In this case Equation (2.24) reduces to a Lyapunov equation associated with the state estimation error dynamics in Equation (2.22), which is usually employed in the stability analysis of adaptive systems, and $\bar{\mu} = \infty$. This suggests that for the purpose of adaptive control design, it is advantageous to choose $M = M_o$, where M_o minimizes a norm measure of N_0 , where N_0

$$N_0 \triangleq (MC)^T - P_0B \quad (2.28)$$

with P_0 defined as the value of P that satisfies the Lyapunov equation in (2.26). Taking the Frobenius norm as a measurement, it can be shown that

$$M_0^T = [CC^T]^{-1}CP_0B \quad (2.29)$$

Remark 2.2.6. When $[CC^T]$ is positive semidefinite, The pseudo inverse of $[CC^T]$ can be used in (2.29) instead of the inverse.

The following lemma shows that a positive definite solution exists for the algebraic dependent Riccati equation (2.24) and can be obtained using Potter's method [68]. This also means that $\bar{\mu}$ can be determined by searching for the boundary values that result in a failure of the algorithm to converge. We employ the notation $\text{Ric}()$ and $\text{dom}(\text{Ric})$ as defined in Ref [16].

Lemma 2.2.1. : Define the Hamiltonian matrix H ,

$$H = \begin{bmatrix} A_e - \mu BC_e & \mu BB^T \\ -Q & -(A_e - \mu BC_e)^T \end{bmatrix} \quad (2.30)$$

where $Q = Q_0 + \mu C_e C_e^T$ and $R = BB^T$. Then for all $0 < \mu < \bar{\mu}$, $H \in \text{dom}(\text{Ric})$ and $P = \text{Ric}(H)$

Proof. The proof follows directly from Lemmas 3 and 4 in [16] □

2.3 Boundedness of Signals

In this section the boundedness of all signals in the system is shown via Lyapunov like analysis using the parameter dependent Riccati equation introduced in the previous section. The following theorem concerns the the state and weight estimation errors.

Theorem 2.3.1. *Consider the system in Equation (2.1) and Equation (2.2), along with the control law given in (2.14), composed of the nominal control in (2.11) and the adaptive control in (2.15) together with the observer in (2.12) and the weight update law in (2.23), where $\mu < \bar{\mu}$ as defined by Lemma 2.2.1. Under Assumptions 2.1, 2.2, 2.3 and 2.4 and, for a sufficiently large \mathbb{D} , \tilde{x} and \tilde{W} are UUB.*

Proof. Consider the candidate Lyapunov function

$$V(\tilde{x}, \tilde{W}, x_d) = \tilde{x}^T P \tilde{x} + \frac{1}{\gamma_w} \text{tr}[\tilde{W}^T \tilde{W}] + V_{x_d}(x_d) \quad (2.31)$$

The time derivative of Equation (2.31) along the closed loop solutions of Equation (2.1) is given by

$$\dot{V}(\tilde{x}, \tilde{W}, x_d, t) = 2\tilde{x}^T P \dot{\tilde{x}} - \frac{2}{\gamma_w} \text{tr}[\tilde{W}^T \dot{\tilde{W}}] + \dot{V}_{x_d}(x_d) \quad (2.32)$$

Substituting for $\dot{\tilde{x}}$ from Equation (2.21) along with the definition of \tilde{g} , Assumption 2.2, Equation (2.15), the weight update law in Equation (2.23), and Equation (2.18), Equation (2.32) can be written as

$$\begin{aligned} \dot{V}(\tilde{x}, \tilde{W}, x_d, t) &= \tilde{x}^T (A_e^T P + P A_e) \tilde{x} + 2\tilde{x}^T P B \left[\tilde{W}^T \zeta(\xi) + \epsilon \right] \\ &\quad - 2\text{tr} \left[\tilde{W}^T \zeta(\xi) \tilde{y}^T - \sigma \tilde{W}^T \hat{W} - \tilde{W}^T \frac{\zeta(\xi) \zeta^T(\xi)}{2\mu} \hat{W} \right] \\ &\quad + \dot{V}_{x_d}(x_d) \end{aligned} \quad (2.33)$$

Using Equation (2.17), Equation (2.18), Equation (2.24), Equation (2.25) and simplifying, Equation (2.33) can be written as

$$\begin{aligned}
\dot{V}(\tilde{x}, \tilde{W}, x_d, t) &= -\tilde{x}^T Q \tilde{x} + 2\tilde{x}^T P B \epsilon - 2\tilde{x}^T N \tilde{W}^T \zeta(\xi) \\
&+ 2\sigma \text{tr} [\tilde{W}^T W] - 2\sigma \text{tr} [\tilde{W}^T \tilde{W}] + \frac{\zeta^T(\xi) W \tilde{W}^T \zeta(\xi)}{\mu} \\
&- \frac{\zeta^T(\xi) \tilde{W} \tilde{W}^T \zeta(\xi)}{\mu} + \dot{V}_{x_d}(x_d)
\end{aligned} \tag{2.34}$$

where $Q \triangleq Q_0 + \mu N N^T$.

Young's inequality states that $2a^T b \leq v a^T a + \frac{b^T b}{v}$, $v > 0$. This can be generalized to compatible matrices as $2\text{tr}[A^T B] \leq v \text{tr}[A^T A] + \frac{1}{v} \text{tr}[B^T B]$. Applying the vector form to the third term in Equation (2.34) with $a = -N\tilde{x}$, $b = \tilde{W}^T \zeta(\xi)$ and $v = \mu$ produces

$$-2\tilde{x}^T N \tilde{W}^T \zeta(\xi) \leq \mu \tilde{x}^T N N^T \tilde{x} + \frac{1}{\mu} \zeta^T(\xi) \tilde{W} \tilde{W}^T \zeta(\xi) \tag{2.35}$$

Likewise, applying the matrix form of Young's inequality to the fourth term in Equation (2.34), with $v = 1$ produces

$$\begin{aligned}
2\sigma \text{tr} [\tilde{W}^T W] &\leq \sigma \text{tr} [\tilde{W}^T \tilde{W}] + \sigma \text{tr} [W^T W] \\
2\sigma \text{tr} [\tilde{W}^T W] &\leq \sigma \text{tr} [\tilde{W}^T \tilde{W}] + \sigma \bar{W}^2
\end{aligned} \tag{2.36}$$

Using *Assumption 2.2*, the second term in Equation (2.34) is bounded as follows:

$$2\tilde{x}^T P B \epsilon \leq 2\bar{\epsilon} \|P B\| |\tilde{x}| \tag{2.37}$$

Substituting all the above inequalities and the upper bound for \dot{V}_{x_d} from Equation (2.7). Equation (2.34) can be written as

$$\begin{aligned}
\dot{V}(\tilde{x}, \tilde{W}, x_d, t) &\leq -\tilde{x}^T Q_0 \tilde{x} \\
&+ 2\bar{\epsilon} \|P B\| |\tilde{x}| \\
&+ \frac{\zeta^T(\xi) W \tilde{W}^T \zeta(\xi)}{\mu} + \sigma \bar{W}^2 - \sigma \text{tr} [\tilde{W}^T \tilde{W}] \\
&- c_3 |x_d|^2 + c_4 b_d |x_d|
\end{aligned} \tag{2.38}$$

where we have made use of the definition of Q below Equation (2.34). Applying

$$\zeta^T(\xi)W\tilde{W}^T\zeta(\xi) \leq s^2\bar{\zeta}^2\bar{W}\|\tilde{W}\| \quad (2.39)$$

and using the following definitions:

$$c \triangleq \lambda_{\min}(Q_0) \quad (2.40)$$

$$d_1 \triangleq \bar{\epsilon}\|PB\| \quad (2.41)$$

$$d_2 \triangleq \frac{1}{\mu}s^2\bar{\zeta}^2\bar{W} \quad (2.42)$$

$$d_3 \triangleq c_4b_d \quad (2.43)$$

$$e^2 \triangleq \sigma\bar{W}^2 + \frac{d_1^2}{c} + \frac{d_2^2}{4\sigma} + \frac{d_3^2}{c_3} \quad (2.44)$$

the inequality in Equation (2.38) becomes

$$\begin{aligned} \dot{V}(\tilde{x}, \tilde{W}, x_d, t) &\leq -c \left[|\tilde{x}| - \frac{d_1}{c} \right]^2 \\ &\quad - \sigma \left[|\tilde{W}| - \frac{d_2}{2\sigma} \right]^2 - c_3 \left[|x_d| - \frac{d_3}{c_3} \right]^2 + e^2 \end{aligned} \quad (2.45)$$

Consequently, we can conclude that either

$$|\tilde{x}| > \Psi_1 \text{ or } |\tilde{W}| > \Psi_2 \text{ or } |x_d| > \Psi_3 \quad (2.46)$$

renders $\dot{V}(\tilde{x}, \tilde{W}, t) < 0$, where Ψ_1, Ψ_2 and Ψ_3 are given by:

$$\Psi_1 = \frac{d_1}{c} + \frac{e}{\sqrt{c}} \quad (2.47)$$

$$\Psi_2 = \frac{d_2}{2\sigma} + \frac{e}{\sqrt{\sigma}} \quad (2.48)$$

$$\Psi_3 = \frac{d_3}{c_3} + \frac{e}{\sqrt{c_3}} \quad (2.49)$$

and therefore both \tilde{x} and \tilde{W} are UUB. \square

Corollary 2.3.1. *Under the conditions stated in Theorem 2.3.1, An estimate for the ultimate bound for $\eta(t) \triangleq [\tilde{x}^T \tilde{W}^T x_d^T]$, is given by*

$$r_\eta = \sqrt{\frac{\lambda_{\max}(P)\Psi_1^2 + 1/\gamma_w\Psi_2^2 + c_2\Psi_3^2}{\vartheta}} \quad (2.50)$$

where $\vartheta = \min(\lambda_{\min}(P), \frac{1}{\gamma_w}, c_1)$. Further, an estimate for the ultimate bound on \tilde{x} is given by

$$r = \sqrt{\frac{\lambda_{\max}(P)\Psi_1^2 + 1/\gamma_w\Psi_2^2 + c_2\Psi_3^2}{\lambda_{\min}(P)}} \quad (2.51)$$

Proof. Define the sets:

$$B_{r_\eta} \triangleq \{\eta : |\eta| \leq r\} \quad (2.52)$$

$$\Omega_\alpha \triangleq \{\eta \in B_{r_\eta} : V(\tilde{x}, \tilde{W}, x_d) \leq \alpha\} \quad (2.53)$$

such that $B_{r_\eta} \subset D_\eta$ for a sufficiently large set D_η and $\alpha \triangleq \min_{|\eta|=r}(V(\tilde{x}, \tilde{W}, x_d)) = r^2\vartheta$. The geometric representation of the sets is given in Figure 5. From the definition of $V(\tilde{x}, \tilde{W}, x_d)$ in Equation (2.31) it follows that the set Ω_α is an invariant set if

$$\alpha \geq \lambda_{\max}(P)\Psi_1^2 + \frac{1}{\gamma_w}\Psi_2^2 + c_2\Psi_3^2 \quad (2.54)$$

Therefore the minimum size of B_{r_η} is given by Equation (2.50). Further, on the boundary of set Ω_α , the maximum value for $|\tilde{x}|$ occurs when $\|\tilde{W}\|$ and $|x_d|$ are zero, therefore an estimate for the ultimate bound on \tilde{x} is given by Equation (2.51) \square

Remark 2.3.1. *The proofs of Theorem 2.3.1 and Corollary 2.3.1 assume the sets \mathbb{D} and \mathbb{D}_η are sufficiently large. If we define B_{R_η} as the largest ball in \mathbb{D}_η , and assume the initial conditions are such that $\eta(0) \in B_{R_\eta}$, then from Figure 5 we have the added condition that $r_\eta < R_\eta$, which implies an upper bound on γ_w . It can be shown that in this case the upperbound must be such that $\vartheta = \gamma_w^{-1}$. With r_η defined by Equation (2.50) and $\vartheta = \gamma_w^{-1}$, the condition $r_\eta < R_\eta$ implies*

$$\gamma_w < \frac{R_\eta^2 - \Psi_2^2}{\lambda_{\max}(P)\Psi_1^2 + c_2\Psi_3^2} \quad (2.55)$$

Therefore, it follows that the meaning of \mathbb{D}_η sufficiently large implies

$$R > \sqrt{\gamma_w\lambda_{\max}(P)\Psi_1^2 + \Psi_2^2 + \gamma_w c_2\Psi_3^2} \quad (2.56)$$

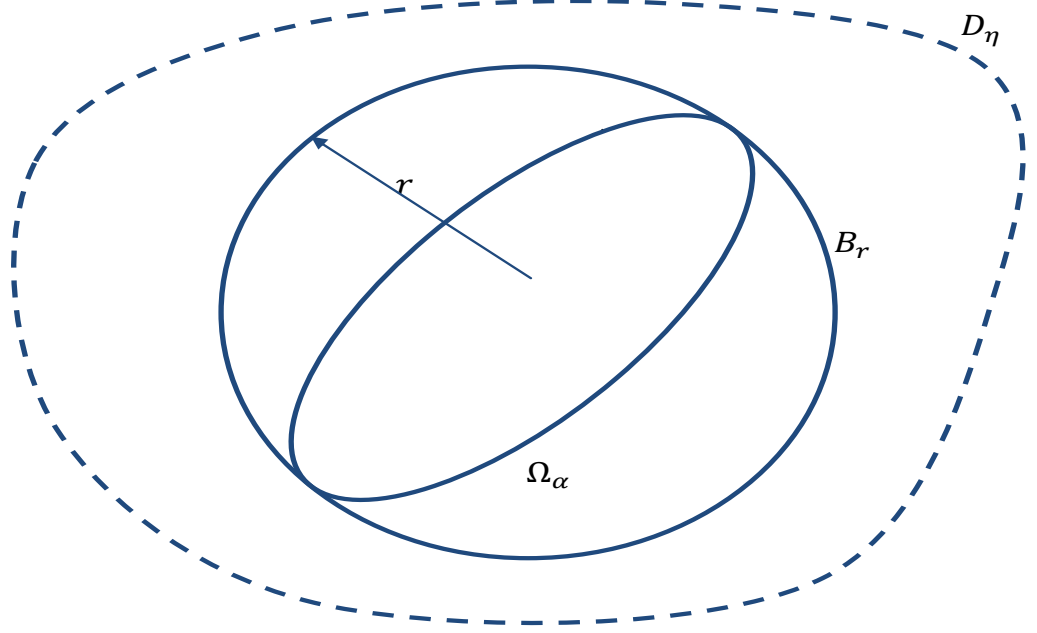


Figure 5: Geometric representation of sets

and $\eta(0) \subset B_{R_\eta}$. The meaning of \mathbb{D} sufficiently large is difficult to characterize since $x(t)$ depends on the initial condition $x(0)$. See also [?]

Corollary 2.3.2. *If the state estimation error \tilde{x} is bounded, then the state tracking error $e = x - x_m$ is bounded.*

Proof. see also [?]

$$\begin{aligned}
 |e| &= |x - x_m| \\
 &= |x - \hat{x} - (x_m - \hat{x})| \\
 &\leq |x - \hat{x}| + |x_m - \hat{x}| \\
 &\leq |\tilde{x}| + |\hat{e}|
 \end{aligned} \tag{2.57}$$

From Theorem 2.3.1, \tilde{x} is bounded. The estimated state tracking error, \hat{e} , is bounded from Equation (2.22). Hence the state tracking error, e , is bounded. \square

Since $x_m(t)$ is bounded, it follows from Corollary 2.3.2 that $x(t)$ is bounded. Further *Assumption 2.1* ensures that x_d is bounded since it is input-to-state stable [38].

Corollary 2.3.3. *If the state estimation error \tilde{x} is UUB by r in Equation (2.51), then the state tracking error e is UUB by $r(1 + v)$. where*

$$v \triangleq \frac{2\|P_m LC\|}{\lambda_{\min}(Q_m)} \quad (2.58)$$

Proof. Consider the following positive definite function

$$V(\hat{e}) = \hat{e}^T P_m \hat{e} \quad (2.59)$$

where P_m satisfies

$$0 = A_m^T P_m + P_m A_m + Q_m, \quad Q_m > 0 \quad (2.60)$$

The time derivative of Equation (2.59) along the closed loop solutions of Equation (2.22) is given by

$$\dot{V}(\hat{e}, \tilde{x}) = -\hat{e}^T Q_m \hat{e} + 2\hat{e}^T P_m LC \tilde{x} \quad (2.61)$$

$$\dot{V}(\hat{e}, \tilde{x}) \leq -\lambda_{\min}(Q_m)|\hat{e}| \left[|\hat{e}| - \frac{2\|P_m LC\|\|\tilde{x}\|}{\lambda_{\min}(Q_m)} \right] \quad (2.62)$$

From Equation (2.22) \hat{e} is bounded as long as \tilde{x} is bounded. It therefore follows that once \tilde{x} reaches its ultimate bound, r , $\dot{V}(\hat{e}, \tilde{x}) < 0$ for all $|\hat{e}| > rv$, and from Equation (2.57), $|e|$ is UUB by $r(1 + v)$. \square

Remark 2.3.2. *The effect of actuator saturation and rate limits on the boundedness of all the signals in the system has not been addressed as part of this thesis. In all the examples that follow it has been assumed that the actuator rate limits and or saturations are not active. It may be possible include actuator limits by extending the method of 'hedging' described in Ref [36] to the output feedback case.*

Remark 2.3.3. While the system considered in this thesis is of the form given in Equation (2.1) there is no direct coupling of the control input to the measurements. The method developed in this section can be easily extended for systems of the form :

$$\begin{aligned}
\dot{x}(t) &= Ax(t) + B[u(t) + g(x(t), x_d(t))], \\
y(t) &= Cx(t) + Du(t), \\
y_r(t) &= C_r x(t),
\end{aligned} \tag{2.63}$$

when there is no uncertainty associated with the D matrix with the following observer

$$\begin{aligned}
\dot{\hat{x}}(t) &= A\hat{x}(t) + Bu_n(t) + L(y(t) - \hat{y}(t)), \\
\hat{y}(t) &= C\hat{x}(t) + Du(t),
\end{aligned} \tag{2.64}$$

However the adaptive control cannot be easily extended for systems with uncertain D matrix without the use of an adaptive observer.

Remark 2.3.4. By introducing the parameter $\mu < \bar{\mu}$ the boundedness of all the signals in the system under the adaptive control developed in this section is shown using the parameter dependent Riccatti equation instead of a Lyapunov equation. The use of the Riccatti equation instead of the Lyapunov equation obviates the need to use large gains in the observer based nominal control design. Using the method developed in this thesis the need to approximate the SPR condition on the system $G(s) = C_e(sI - A_e)^{-1}B$ through high gain design of the nominal controller is eliminated such as was done in Ref's. [49] and [51]. Furthermore the SPR condition is not applicable to non-minimum phase systems. The last term in the weight adaptive also depends on the parameter μ . The form of the last term in the weight update law is similar to that of the sigma modification term but with a varying gain due to the presence of the matrix $\zeta(\xi(t))\zeta^T(\xi(t))$ which is dependent on the basis function.

2.4 Wing Rock Dynamics

Modern fighter aircraft are designed to meet enhanced performance criteria for air superiority missions. This may require that they operate in nonlinear regimes of flight envelope associated with complex flight dynamics phenomenon. The nonlinear regimes of the flight envelope that include flight at high angles of attack that induce undesirable phenomena such as yaw departure, pitching oscillations and pitch roll coupling. The phenomena of wing rock is associated with flight at moderate to large angles of attack and involves sustained lateral oscillations dominated by a rolling oscillation. The severity of the wing rock phenomena is determined mainly by the amplitude of the oscillation and to a lesser extent by the frequency of the oscillation. This oscillation in roll is a major concern for high performance aircraft as it restricts their ability to perform enhanced agility maneuvers at high angle of attack tasks such as maneuvering, and point and shoot aiming.

Ngyuen et al. [66] conducted both static and dynamic wind tunnel tests to study the aerodynamic factors which caused the low speed wing rock of a free to roll flat plate delta wing with 80 degrees of leading edge sweep. Their investigations indicate that the wing rock phenomenon is caused by the dependence of aerodynamic damping in the roll axis on the side slip angle such that unstable damping is obtained for small side slip angles which becomes stable at increased angles of attack. The development of a wing rock model and its control have been studied in Ref's. [20, 34, 55, 19, 73, 77]. The differential equation describing the wing rock motion is given by [55, 19, 73]

$$\ddot{\phi} = \frac{\rho U_{\infty}^2 S b}{2 I_{xx}} C_l + d_0 u \quad (2.65)$$

where ϕ is the roll angle, ρ is density of air, U_{∞} is free-stream velocity, b is wing span, I_{xx} is the wing mass moment of inertia, the control input u is aileron deflection in radians and d_0 is the control effectiveness. The roll-moment coefficient is expressed

as

$$C_l = a_0 + a_1\phi + a_2\dot{\phi} + a_3|\phi|\dot{\phi} + a_4|\dot{\phi}|\dot{\phi} + a_5\phi^3 \quad (2.66)$$

where the aerodynamic parameters a_i are nonlinear functions of the angle of attack of the aircraft. The above model can be represented by the following state space model

$$\begin{aligned} \dot{x}_1 &= x_2 \\ \dot{x}_2 &= \Delta(x) + d_0u \end{aligned} \quad (2.67)$$

where $x = (x_1, x_2)^T = (\phi, \dot{\phi})^T$ and $\Delta(x)$ is given by

$$\Delta(x) = b_0 + b_1\phi + b_2\dot{\phi} + b_3|\phi|\dot{\phi} + b_4|\dot{\phi}|\dot{\phi} + b_5\phi^3 \quad (2.68)$$

where $b_0 = 0$, $b_1 = -0.2789$, $b_2 = 0.2274$, $b_3 = -0.9368$, $b_4 = 0.1432$, and $b_5 = 0.3218$ are aerodynamic coefficients. In order to evaluate the adaptive control methodology developed in the previous section, the wing rock model is augmented with the following matched unmodeled dynamics, given by

$$\dot{x}_d = Fx_d + Gx \quad (2.69)$$

where the matrices F, G are given by:

$$F = \begin{bmatrix} 0 & 1 \\ -0.0004 & -0.0320 \end{bmatrix}, G = \begin{bmatrix} 0 & 0 \\ 0 & 1 \end{bmatrix}, \quad (2.70)$$

With the addition of the above unmodeled dynamics, the state space model in Equation (2.67) changes to

$$\begin{aligned} \dot{x}_1 &= x_2 \\ \dot{x}_2 &= \Delta(x) + d_0u + \begin{bmatrix} 0 & 1 \end{bmatrix} x_d \\ y &= x_1 \end{aligned} \quad (2.71)$$

We now design a nominal controller for the system given in Equation (2.71) with $\phi(t)$ as the output, assuming $\Delta(x) = 0$ and $x_d = [0 \ 0]^T$. The objective of the

controller is to design the input $u(t)$ such that $\phi(t)$ follows the reference input $r(t)$. The state feedback gain K_x is obtained assuming both the states are available using Linear Quadratic Regulator theory with $\bar{Q} = \text{diag}(20, 2)$ and $R = 5$, This results in a feedback gain of $K_x = [2.0000, 2.0976]^T$. Once the feedback gain has been calculated the feed forward gain $K_r = 2$ is computed to obtain a zero steady state error for a step reference input.

The next step is to design the linear observer to estimate both the states x_1 and x_2 . The estimates are then used instead of the actual states for feedback in the nominal control design. We will assume that the nominal observer is designed such that the poles of the observer are κ times faster than the closed loop model/reference model. Note that A_e appears in Equation (2.21). Therefore, the choice of κ is an important design parameter that influences the maximum allowable value for the parameter μ such that the parameter dependent algebraic Riccati equation has a positive definite solution. Figure 6 shows the $\bar{\mu}$ boundary versus κ for $Q_0 = I_2$. For $\kappa = 8$, and using pole placement to assign the poles of A_e in Equation (2.21), an observer gain $L = [20.9762, 200.0000]^T$ is obtained and the maximum allowable value for μ is $\bar{\mu} = 87.59$.

The reference model dynamics for adaptive control design are defined by setting $A_m = A - BK_x$ resulting in a second order model with a natural frequency of 1.41 rad/s and a damping ratio of 0.74. The reference model input matrix is then given by $B_m = BK_r$. In the adaptive design, a bias term and six sigmoidal basis functions $\zeta_i(\xi_i)$ are used to form the basis vector, so $\zeta_1 = 1$ and

$$\zeta_i(\xi) = \frac{1 - e^{-a_i \xi_i}}{1 + e^{-a_i \xi_i}}, \quad i = 2, 3, 4, 5, 6, 7 \quad (2.72)$$

with $a = [0.82 \ 0.82 \ 0.82 \ 0.82 \ 5 \ 5]$, $\xi = [\phi_n(t) \ \phi_n(t - d) \ \phi_n(t - 2d) \ \phi_n(t - 3d) \ u(t - dt) \ u(t - d - dt)]^T$, where the normalized output is $\phi_n(t) = \phi(t)/(\pi/2)$, and time delay, $d = 0.15$ seconds. The activation potentials for the sigmoidal activation function are chosen such that their outputs are linear when the signals are within their nominal

range and are saturated beyond the nominal range. For this system $n = n_x + n_{x_d} = 4$, and the relative degree for this system is $\rho = n_x = 2$. Therefore, the minimum number of delayed values are employed in Equation (2.72). Further to avoid having to implement a fixed point iteration, $u(t - dt)$ and $u(t - d - dt)$ are used as inputs to the basis function instead of $u(t)$ and $u(t - d)$ respectively, where $dt = 0.005$ is the sampling time of the controller implemented in the discrete domain. The remaining choices for the parameters in the adaptive law are $\gamma = 1000$, this was chosen to provide adequate tracking of commanded input, The sigma modification gain, σ was set to be equal to $0.05/\gamma$ and μ was chosen to be 70 which is less than $\bar{\mu}$.

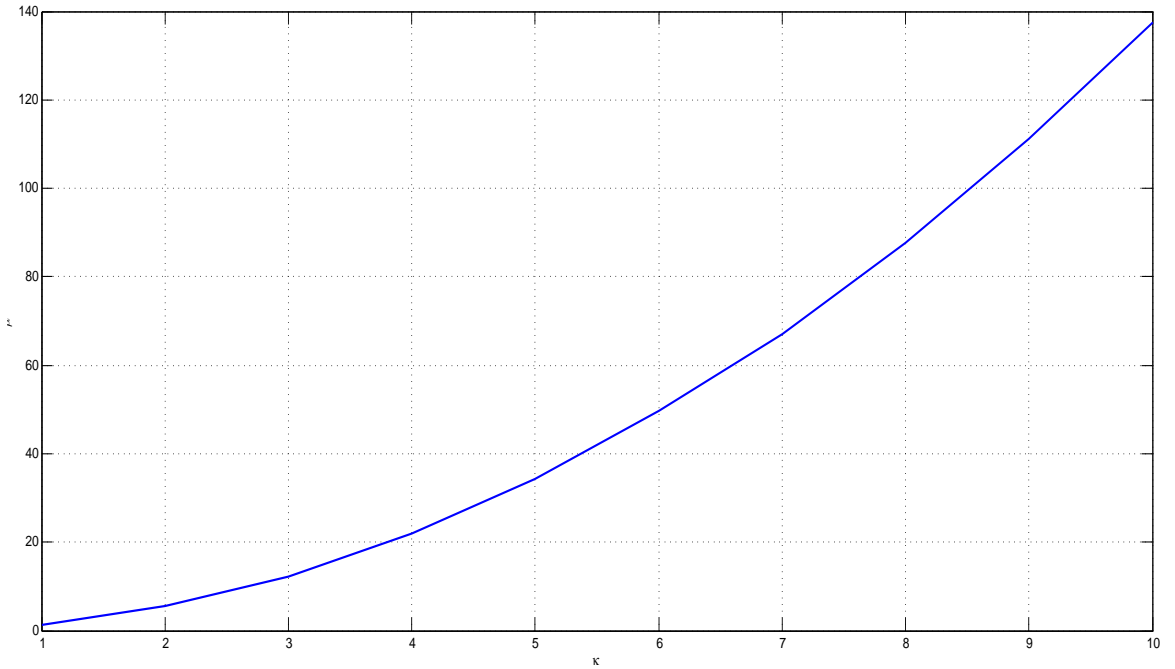


Figure 6: Limit value of $\bar{\mu}$ for $Q_0 = I_2$

A simulation is first carried out without uncertainty ($\Delta x = 0$) and without unmodeled dynamics ($x_d = [0 \ 0]^T$) to determine the performance of the nominal control design. The results of the simulation for a step input of $r_0 = 60$ degrees is given in Figure 7 and the corresponding control input is shown in Figure 8

The same simulation is repeated with both the uncertainty and the effect of unmodeled dynamics acting on the system. As observed from Figure 9, response with

nominal control goes unstable. The simulation is then repeated with the adaptive control enabled. As observed from Figure 9, the adaptive control stabilizes the closed loop system in the presence of both the uncertainty and unmodeled dynamics. A comparison of the corresponding control inputs for this case is given in Figure 10.

The next example compares the adaptive control law developed in [?] for the wing rock model with both parametric uncertainties and unmodeled dynamics acting on the system with the extension developed in this proposal. As mentioned previously, Reference [?] uses the observer estimates of the modeled states to form the basis vector. So for illustrative purposes the basis vector is made of a bias term ($\zeta_1 = 1$) and two sigmoidal basis functions of the form

$$\zeta_i(\xi) = \frac{1 - e^{-a\xi_i}}{1 + e^{-a\xi_i}}, \quad i = 2, 3 \quad (2.73)$$

with $a=0.82$ and $\xi = [\hat{\phi}_n \ \hat{\dot{\phi}}_n]$, where $\hat{\phi}_n = \hat{\phi}/(\pi/2)$ and $\hat{\dot{\phi}}_n = \hat{\dot{\phi}}/(\pi/2)$. The remaining choices for the parameters in the adaptive law are $\gamma = 1000$, $\sigma = 0.005$ and $\mu = 70$, the same values used in the previous example. The results of this comparison are given in Figure 11. As observed from this figure, the Reference [?] based design goes unstable while the design that employs a tapped delay line results in a stable response. A comparison of the corresponding control inputs is shown in Figure 12

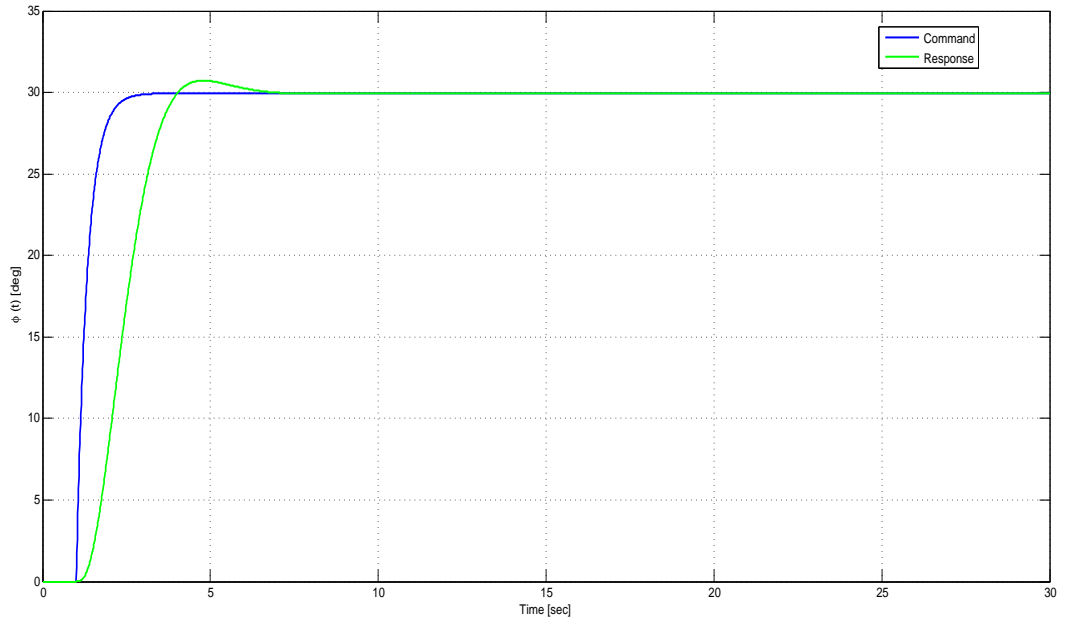


Figure 7: Bank angle response of the nominal controller without uncertainty and unmodeled dynamics.

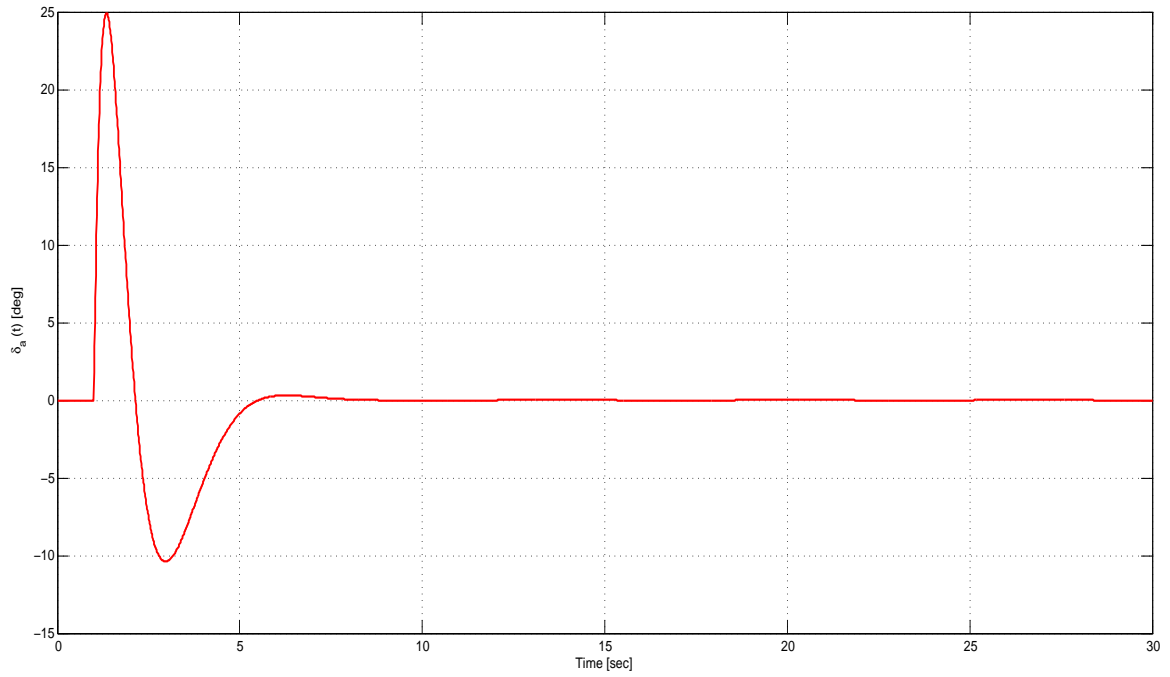


Figure 8: Nominal control input without uncertainty and unmodeled dynamics.

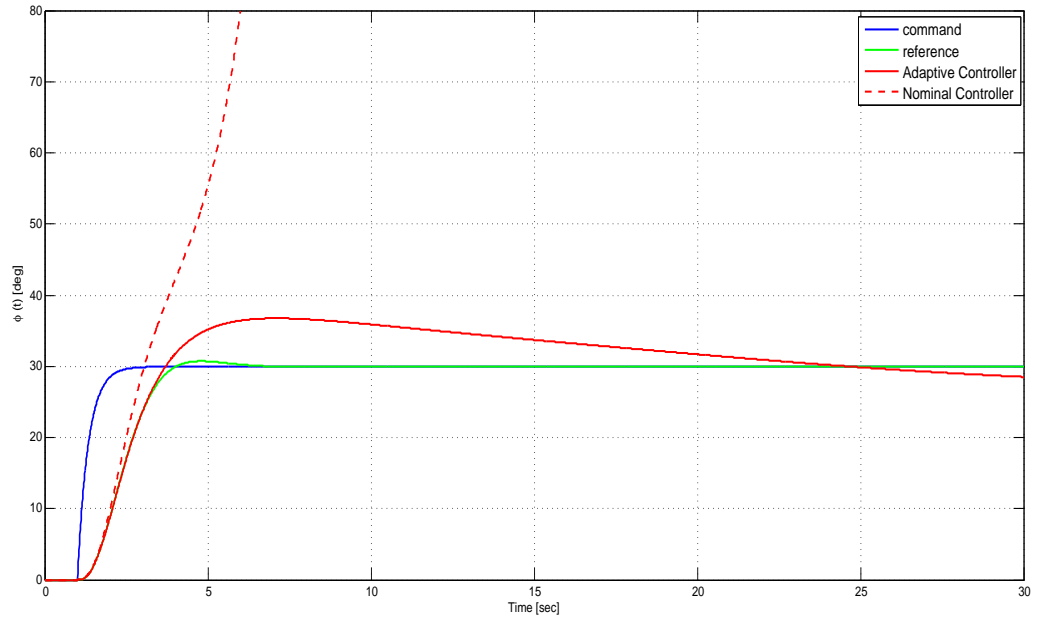


Figure 9: Comparison of bank angle responses with uncertainty and unmodeled dynamics.

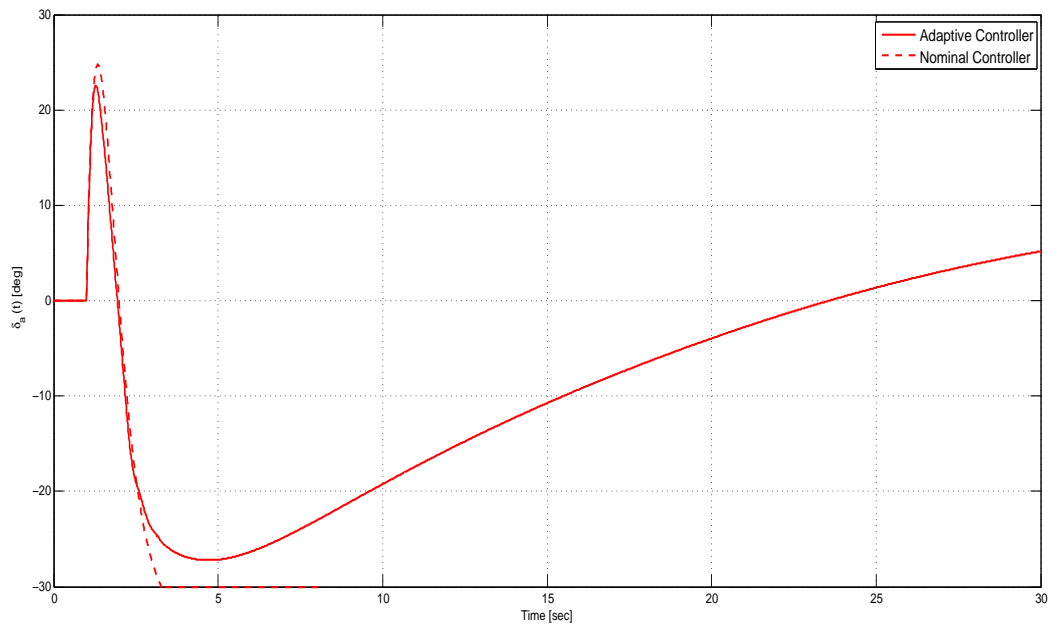


Figure 10: Comparison of control inputs with uncertainty and unmodeled dynamics.

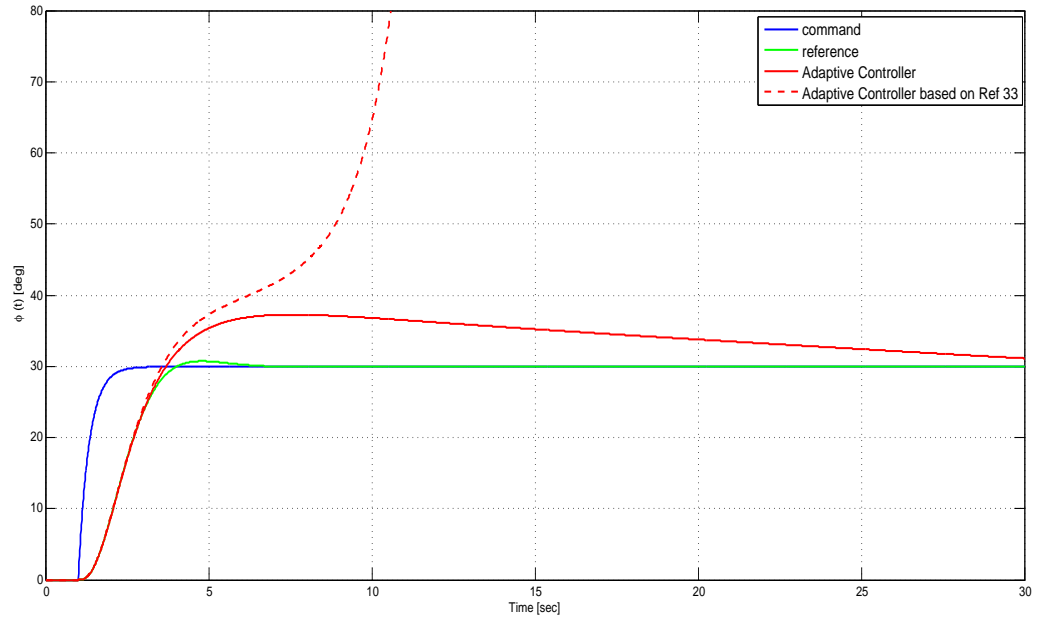


Figure 11: Comparison of bank angle responses for two different adaptive laws.

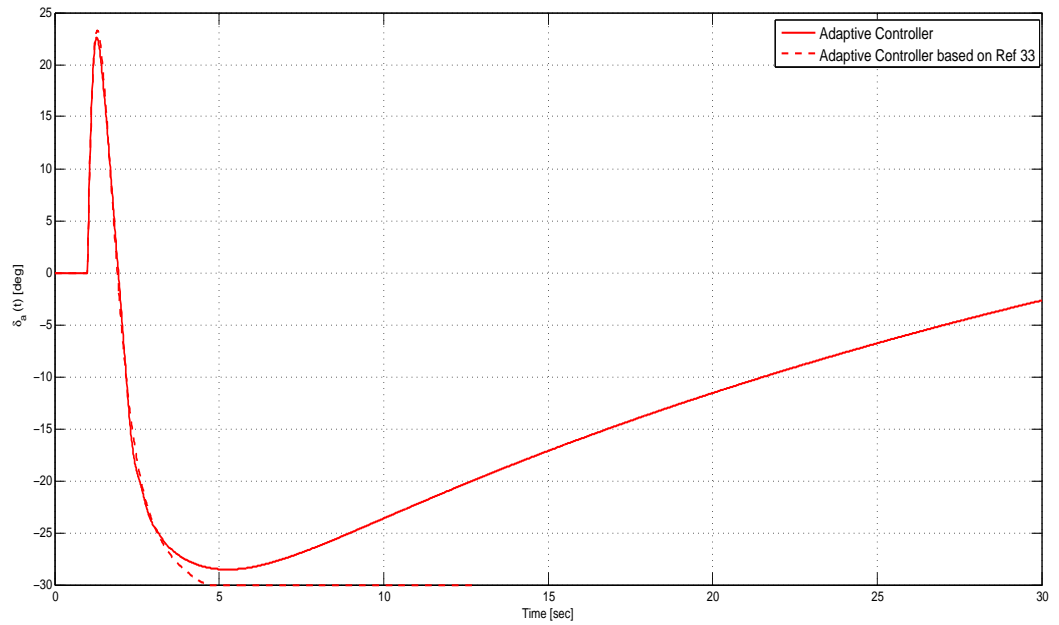


Figure 12: Comparison of control inputs for two different adaptive laws.

2.5 Control of Flexible Spacecraft

In this section, the attitude control of a flexible spacecraft with attitude feedback is considered [80]. The attitude kinematics are given by:

$$\dot{q} = \frac{1}{2}(q \times \omega + q_0\omega) \quad (2.74)$$

where $q \in \mathbb{R}^3$, $[q_0 \ q^T]^T \in \mathbb{R}^4$ denotes the unit quaternion vector, therefore $q_0^2 + |q|^2 = 1$, and $\omega \in \mathbb{R}^3$ is the angular rate vector. The dynamic equations of a spacecraft with flexible appendages can be expressed as:

$$J\dot{\omega} + \omega \times (J\omega + \delta\dot{\eta}) + \delta^T\ddot{\eta} = u \quad (2.75)$$

$$\ddot{\eta} + C\dot{\eta} + K\eta + \delta\dot{\omega} = 0 \quad (2.76)$$

where $J \in \mathbb{R}^{3 \times 3}$ is the total moment of inertia of the spacecraft, $u \in \mathbb{R}^3$ is the control torque vector, and $\eta \in \mathbb{R}^N$ is the modal coordinate vector relative to the main body. $\delta \in \mathbb{R}^{N \times 3}$ is the coupling matrix between the rigid body and flexible dynamics, $K = \text{diag}[\Lambda_1^2, \Lambda_2^2, \dots, \Lambda_N^2]$ and $C = \text{diag}[2\zeta_1\Lambda_1, 2\zeta_2\Lambda_2, \dots, 2\zeta_N\Lambda_N]$ are the stiffness and damping matrices with N the number of elastic modes considered, ζ_i is the associated damping and Λ_i the natural frequency of the flexible modes. In order to test the effectiveness of the adaptive control, the following values for the flexible spacecraft are used :

$$J = \begin{bmatrix} 350 & 3 & 4 \\ 3 & 270 & 10 \\ 4 & 10 & 190 \end{bmatrix} \text{Kg}m^2 \quad (2.77)$$

$$\delta = \begin{bmatrix} 6.46 & 1.28 & 2.16 \\ -1.25 & 0.91 & -1.67 \\ 1.11 & 2.48 & -0.83 \end{bmatrix} \quad (2.78)$$

For $N = 3$, the natural frequencies and damping ratios of the decoupled flexible modes, are $\Lambda_1 = 0.768$, $\Lambda_2 = 1.104$ and $\Lambda_3 = 1.873$ rad/s and $\zeta_1 = 0.0056$, $\zeta_2 = 0.0086$ and $\zeta_3 = 0.013$ respectively.

By defining $z_1 \triangleq q$ and $z_2 \triangleq 2\dot{q}$, $\eta_1 \triangleq \eta$ and $\eta_2 \triangleq \dot{\eta} + \delta\omega$, Equation (2.74) and Equation (2.75) can be rewritten in the form Equation (2.1) as:

$$\dot{z}_1 = \frac{1}{2}z_2 \quad (2.79)$$

$$\dot{z}_2 = \bar{Q}J^{-1}u + g_0(q, \omega, \eta_1, \eta_2, u) \quad (2.80)$$

$$\dot{\eta}_1 = \eta_2 \quad (2.81)$$

$$\dot{\eta}_2 = \eta_1 + \delta\omega \quad (2.82)$$

Where

$$\bar{Q} \triangleq \begin{bmatrix} q_0 & -q_3 & q_2 \\ q_3 & q_0 & -q_1 \\ -q_2 & q_1 & q_0 \end{bmatrix} \quad (2.83)$$

η_1 and η_2 are treated as the unmodeled dynamics acting on the system. The use of η_1 and η_2 instead of ω and η as the unmodeled states allows the dynamics of the unmodeled states to be of the form given in Equation (2.2). If the system is linearized about the equilibrium attitude, $q_0 = 1$ and $q = [0 \ 0 \ 0]^T$, then in equilibrium $\bar{Q}_e = I_3$, and A, B, C in Equation (2.1) become:

$$A = \begin{bmatrix} 0 & 0 & 0 & 0.5 & 0 & 0 \\ 0 & 0 & 0 & 0 & 0.5 & 0 \\ 0 & 0 & 0 & 0 & 0 & 0.5 \\ 0 & 0 & 0 & 0 & 0 & 0 \\ 0 & 0 & 0 & 0 & 0 & 0 \\ 0 & 0 & 0 & 0 & 0 & 0 \end{bmatrix} \quad (2.84)$$

$$B = \begin{bmatrix} 0_3 \\ J^{-1} \end{bmatrix} \quad (2.85)$$

$$C = C_r = \begin{bmatrix} I_3 & 0_3 \end{bmatrix} \quad (2.86)$$

The state feedback gain K_x is obtained using LQR theory with $Q = I_6$ and $R = 0.001I_3$. The nominal observer is a Kalman filter designed for the process:

$$\dot{x} = Ax + Bu + \Gamma w \quad (2.87)$$

$$y = Cx + v \quad (2.88)$$

where $\Gamma = [0_3; I_3]$ and the process and measurement noise matrices are $Q_w = I_6$ and $R_v = 0.001I_3$ respectively. The expression used for the feed forward gain is $K_r = -(C_r A_m B)^{-1}$. This provides zero steady state error for step changes in attitude command. The reference model dynamics for adaptive control design are defined by setting $A_m = A - BK_x$ and $B_m = BK_r$. For $M = I_3$ in Equation (2.17), the resulting maximum allowable value for the parameter μ from Lemma 2.1 is $\bar{\mu} = 14160$. In this case $n = n_x + n_{x_d} = 12$. For this particular problem, 11 delayed values of y and 3 delayed value of u along with a bias term are used to form the basis vector with sigmoidal activation function having activation potentials of 3 for y and its delayed values and 0.2 for u and its delayed values such that the output is linear for the nominal range and is saturated outside their nominal ranges respectively. Further, to avoid implementing a fixed point iteration $u(t-dt)$ is used in place of $u(t)$, where $dt = 0.005$ is the controller update rate.

A simulation is first carried out with the nominal control acting on the nonlinear spacecraft model without flexible modes ($g(q, \omega, \eta, \dot{\eta}) = 0$). As observed from the Figure 13, it is seen that even without the effect of the flexible modes, the system goes unstable for a command input $r = [-0.5 \ -0.2 \ 0.8]^T$. The response of the reference model ($qr1, qr2, qr3$) is also plotted in the Figure 13. The instability is primarily due to the $q \times \omega$ term in Equation (2.74). Note that the nominal controller was designed by linearizing the spacecraft model about the equilibrium condition $q_0 = 1$ and $\dot{q} = [0; 0; 0]^T$. The new equilibrium condition $r = [-0.5 \ -0.2 \ 0.8]^T$ is "far"

from the initial set point condition. This means that the nominal controller can be considered a "poor" design with respect to the commanded equilibrium point. Figure 14 shows that the system with adaptive augmentation using the weight update law given in Equation (2.23), with the adaptive control designed using $\gamma = 1000$, $\mu = 2000$, $\sigma = 0.0005$ and a delay of 0.015 seconds, in the presence of nonlinearity provides adequate tracking of the reference response. Next the simulation is repeated with the effect of the flexible modes coupling with the rigid body dynamics. Figure 15 shows that, the adaptive control developed in accordance with Ref [?], using the same values of γ , μ and σ , is unable to track the reference input and ultimately goes unstable in the presence of the flexible modes. Figure 16 shows that the adaptive control designed using the delayed values of y and u as inputs to the basis functions with the weight update law given in Equation (2.23) provides adequate tracking performance with respect to the reference response, without destabilizing the flexible modes.

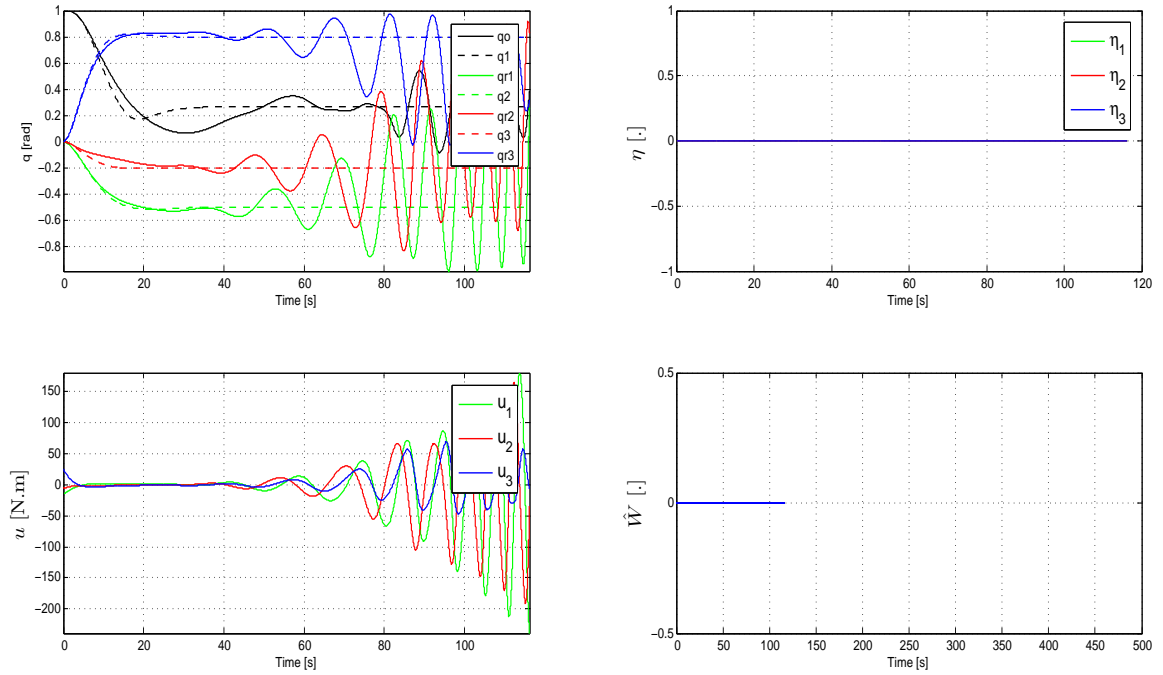


Figure 13: Response of the rigid spacecraft model under nominal control.

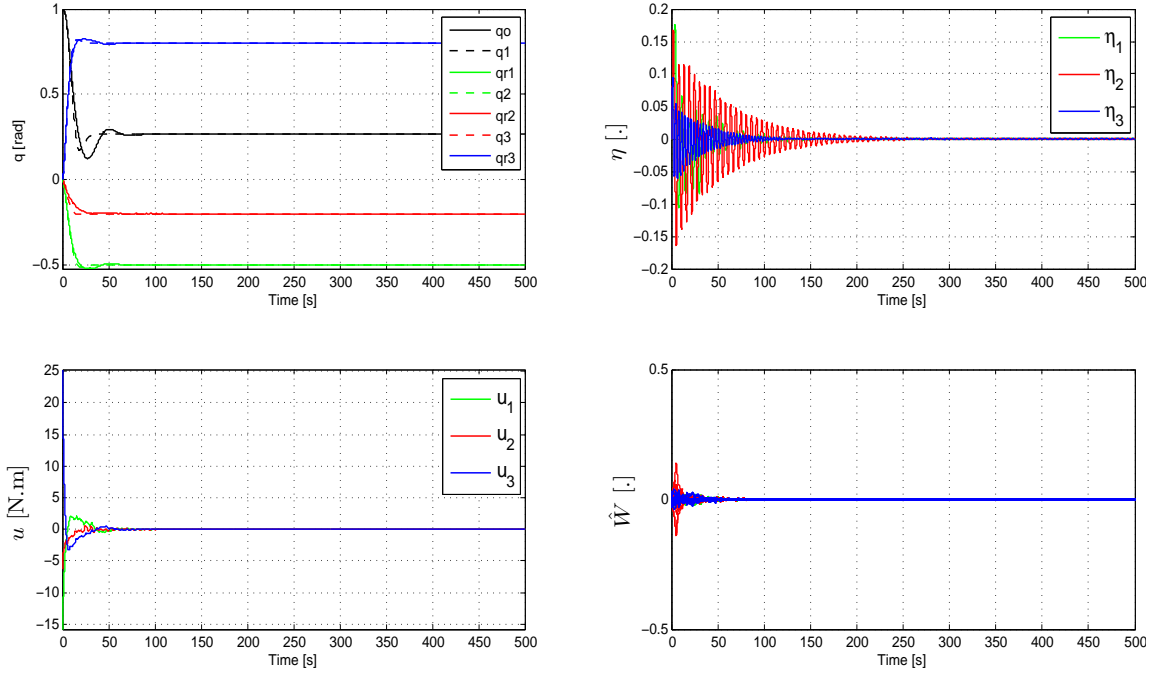


Figure 14: Response of the rigid spacecraft model under adaptive controller that employs delayed inputs and outputs.

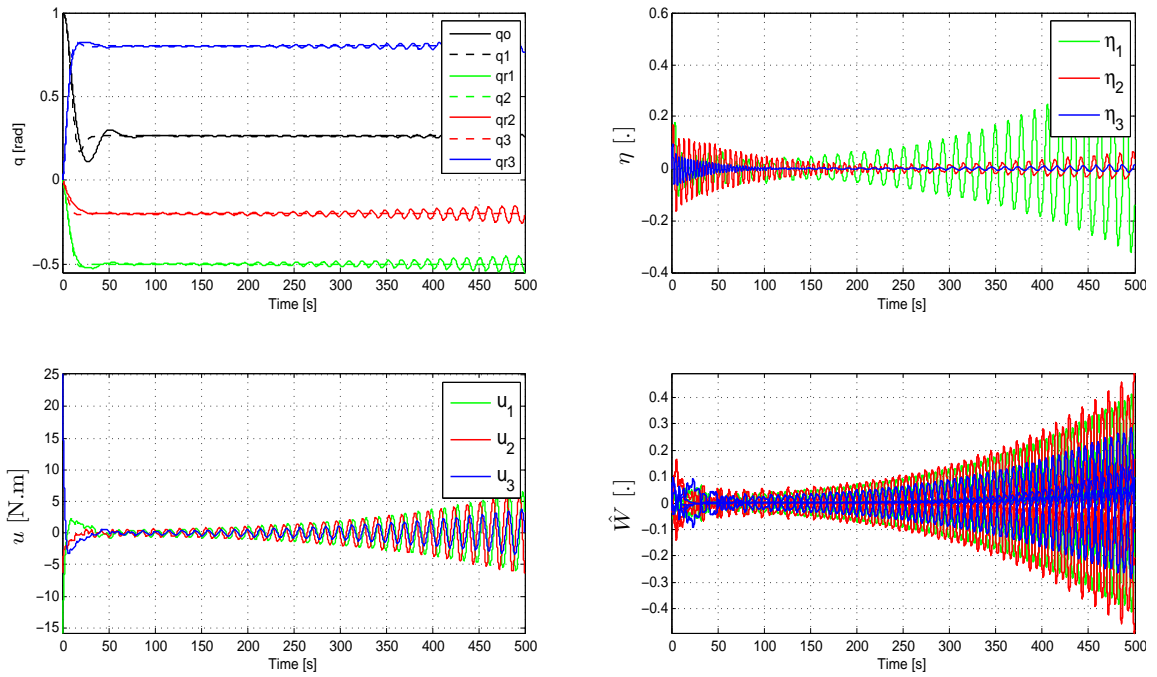


Figure 15: Response of the flexible spacecraft model under Ref.[41] adaptive control.

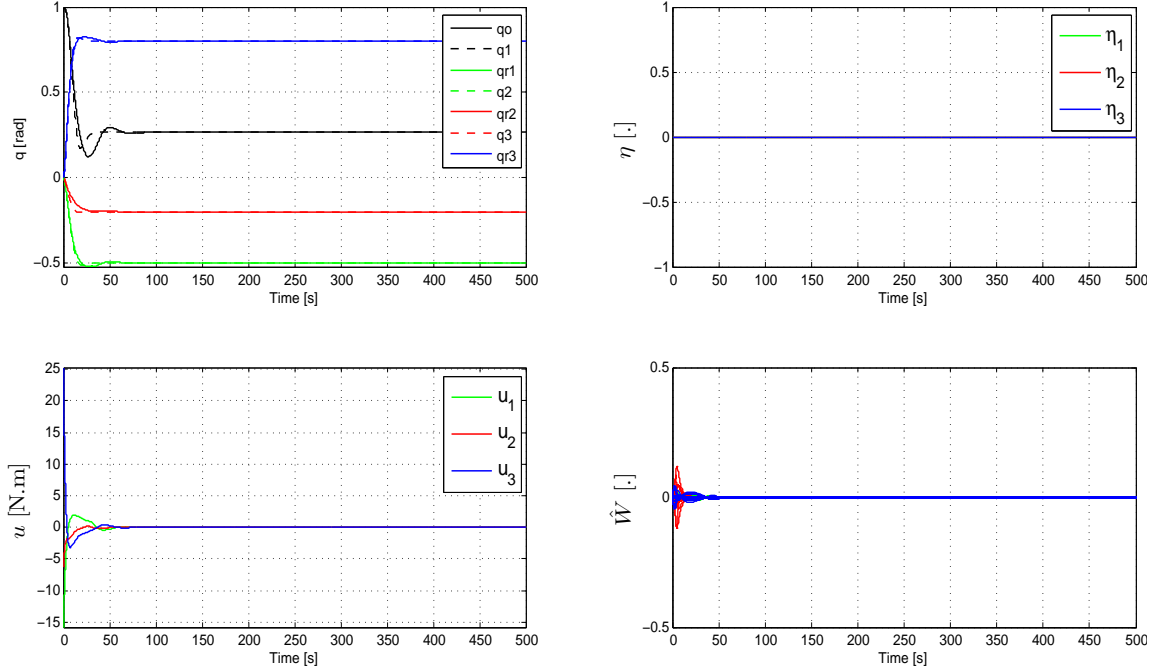


Figure 16: Response of the flexible spacecraft model under adaptive controller that employs delayed inputs and outputs.

2.6 Summary

This Chapter presents an output feedback adaptive controller design approach applicable to systems with unmodeled dynamics. The unique attributes of the approach are that it can be used to augment an existing linear controller without modifying the parameters of that controller, it is applicable to systems with unmodeled dynamics, it does not rely on the use of high gains neither in the adaptation law nor in the observer design, it is applicable to non-minimum phase systems and it does not require realization of a reference model. The stability properties of the adaptive system are established using a Lyapunov like stability analysis that relies on the existence of a positive definite solution of a parameter dependent Riccati equation.

CHAPTER III

REDUCING THE EFFECT OF NOISE IN ADAPTIVE CONTROL

3.1 Introduction

In this chapter the adaptive control methodology developed in Chapter 2 is extended for systems with noisy measurements. While adaptive control theory provides a means for reducing the effects of modeling error, this comes at the cost of introducing a new pathway for sensor noise to enter the actuators, and therefore problems may arise with regard to actuator rate limits, energy consumption, and ultimately actuator failure. This is particularly an issue when attempting to improve transient performance of an adaptive law through the use of high adaptation gain.

3.2 The effect of noise on adaptive control

Kutay [47], address the sensitivity of noise on the error observer based adaptive output feedback control approach of [33]. For the adaptive laws developed using the error observer method it was observed experimentally that the adaptive control architecture is susceptible to sensor noise. In Kutay [47] a reduced order observer has been proposed that eliminates the redundancy in estimating the available compensator states. The author presents a Lyapunov-like stability analysis to show the ultimate boundedness of all the signals in the system. Numerical and experimental results are presented that shows the reduction in the effect of sensor noise on the adaptive control process.

In Singla et al. [74], An output feedback structured model reference adaptive control law has been developed for spacecraft rendezvous and docking problems. The

authors study the effect of bounded output measurement errors on the performance of an adaptive controller. Their method relies on estimating the relative velocities between the spacecraft using a filter based on the passivity properties of the spacecraft translational and attitude dynamics to generate the pseudo-velocity-like signals. A Lyapunov like stability analysis is presented to show ultimate boundedness of all the signals in the system in the presence of sensor noise and errors. Numerical simulations of spacecraft rendezvous and docking show the efficacy of the proposed method in the presence of noise.

Calise et al. [8] consider the effect of sensor noise on adaptive control laws. The authors have developed a new modification term called adaptive loop recovery (ALR) that tries to preserve the loop transfer properties of a reference model associated with a non-adaptive control design. It has been shown that the ALR modification gain has to be chosen sufficiently large to preserve the loop transfer properties. The authors show that the use of a large gain for the ALR modification term does not make the adaptive control law more susceptible to sensor noise compared to standard adaptive control law. The authors do not explicitly consider the effect of sensor noise on the adaptive control law without the ALR modification term.

In this Chapter we adopt a simple approach to address the effect of noise on output feedback adaptive control, and provide a theoretical justification based on singular perturbation theory [38]. The adaptive control is similar to that developed in Chapter 2 except that it uses the filtered version of the output error in order to reduce the effect of noise which could potentially drive the actuators to their rate limits. An advantage to this approach is that it does not require modification of the observer portion of the nominal control law, which is used in place of the usual reference model to generate an error signal for the adaptive law. The benefits of this approach are illustrated by numerical simulations of the flexible space craft example used in Chapter 2 with the addition of sensor noise.

3.3 Reducing the effect of sensor noise

In order to reduce the amount of sensor noise on the control signal due to the augmentation of adaptive control, the weight update law developed in Equation (2.23) is replaced with the following

$$\dot{\hat{W}}(t) = \gamma_w \left[\zeta(\xi(t)) \tilde{y}_f^T(t) - \sigma \hat{W}(t) - \frac{\zeta(\xi(t)) \zeta^T(\xi(t))}{2\mu} \hat{W}(t) \right], \quad (3.1)$$

where the filtered version of $\tilde{y}(t)$, $\tilde{y}_f(t)$, is used to suppress the effect of noisy sensor signals. For simplicity of presentation in this Chapter, the filtered error signal is obtained using a first order filter which is given by:

$$\tau \dot{\tilde{y}}_f(t) = -\tilde{y}_f(t) + \tilde{y}(t), \quad (3.2)$$

although a higher order filter could also be used. Also, we have assumed in Equation (3.2) that the same first order filter is applied to each element of \tilde{y} . The arguments that follow apply equally well when the order and/or the bandwidths of the filters that are applied to each element are different. We are concerned here with the properties of the adaptive controller for sufficiently large bandwidth (sufficiently small τ in the case of a first order filter).

Remark 3.3.1. *The addition of the filter introduces a delay that can affect the performance of the adaptive control in the presence of noisy measurements. Therefore the choice of the filter frequency has to be balanced between reducing the effect of noisy measurements on the control input and the performance of the adaptive controller.*

3.4 Boundedness Analysis

In this section arguments from singular perturbation theory [38, 63] are used to show that boundedness of all error signals is preserved when the weight update law in Equation (3.1) is employed with τ sufficiently small.

Theorem 3.4.1. *Consider the system in Equation (2.1) and Equation (2.2), along with the control law given in Equation (2.14), composed of the nominal control in Equation (2.11) and the adaptive control in Equation (2.15) together with the observer in Equation (2.12) and the weight update law in Equation (3.1), where $\mu < \bar{\mu}$ as defined by Lemma 2.2.1. Under Assumptions 2.1, 2.2, 2.3 and 2.4 and for $n \geq n_x + n_{x_d}$ defined below (2.9), then $\exists \tau^* > 0 : \forall 0 < \tau < \tau^*$, \tilde{x} and \tilde{W} defined in Equation (2.16) and (2.18) are UUB, for a sufficiently large \mathbb{D} .*

Proof. Equations (2.1), (2.2) along with Equations (3.1) and (3.2) above have the form of a singularly perturbed system with τ viewed as a small parameter. According to Tikhonovs theorem [38], an approximation for the solutions for $\tilde{x}(t, \tau)$ and $\tilde{W}(t, \tau)$ can be constructed from the solution of the reduced system obtained by setting $\tau = 0$ in Equation (3.2), in which case the filtered signal $\tilde{y}_f(t)$ is equal to $\tilde{y}(t)$ and *Theorem 2.3.1* applies to the reduced system. A requirement for the application of Tikhonovs theorem is that the equilibrium point of the boundary layer system is exponentially stable uniformly in $\tilde{y}(t) \forall t \geq 0$. The boundary layer system is obtained by applying the time transformation $t_{bl} = t/\tau$ to Equation (3.2), which results in

$$\frac{d\tilde{y}_f(t_{bl})}{dt_{bl}} = -\tilde{y}_f(t_{bl}) + \tilde{y}(t) \quad (3.3)$$

From Equation (3.3) it is evident that the exponential stability requirement is satisfied with $\tilde{y}(t)$ viewed as the equilibrium point $\forall t \geq 0$. The main result of Tikhonovs theorem is that $\exists \tau \forall 0 < \tau < \tau^*$

$$\tilde{x}(t, \tau) = \tilde{x}_r(t) + O(\tau) \quad (3.4)$$

$$\tilde{W}(t, \tau) = \tilde{W}_r(t) + O(\tau) \quad (3.5)$$

where $O(\tau)$ signifies a term of the order of τ and subscript 'r' denotes the reduced solution. Therefore $\tilde{x}(t, \tau)$ and $\tilde{W}(t, \tau)$ are UUB. \square

Corollary 3.4.1. *Under the conditions stated in Theorem 3.3.1, An estimate for the*

ultimate bound for $\eta(t) \triangleq [\tilde{x}^T \tilde{W}^T x_d]$, is given by

$$r_\eta = \sqrt{\frac{\lambda_{max}(P)\Psi_1^2 + 1/\gamma_w\Psi_2^2 + c_2\Psi_3^2}{\underline{\lambda}}} \quad (3.6)$$

Further an estimate for the ultimate bound on \tilde{x} is given by

$$r = \sqrt{\frac{\lambda_{max}(P)\Psi_1^2 + 1/\gamma_w\Psi_2^2 + c_2\Psi_3^2}{\lambda_{min}(P)}} \quad (3.7)$$

Proof. Proof follows directly from *Corollary 2.3.1* □

The following corollary shows that if \tilde{x} is bounded then the state tracking error e , is also bounded.

Corollary 3.4.2. *If the state estimation error \tilde{x} is bounded, then the state tracking error $e = x - x_m$ is bounded.*

Proof. Proof follows directly from *Corollary 2.3.2* □

Since $x_m(t)$ is bounded, it follows from Corollary 2.3.2 that $x(t)$ is bounded. Further *Assumption 2.1* ensures that x_d is bounded since it is input-to-state stable [38].

Corollary 3.4.3. *If the state estimation error \tilde{x} is UUB by r in Equation (3.7), then the state tracking error e is UUB by $r(1 + v)$. where*

$$v \triangleq \frac{2\|P_m LC\|}{\lambda_{min}(Q_m)} \quad (3.8)$$

Proof. Proof follows directly from *Corollary 2.3.3* □

3.5 Control of Flexible Spacecraft

In this section, the attitude control of a flexible spacecraft previously treated in Section 2.5 in Chapter 2 is reexamined, but this time with additive sensor noise. The

attitude measurements are corrupted with band limited white noise with a power spectral density of spectral density of 2×10^{-4} . A simulation is first carried out with the adaptive control law developed in Chapter 2 with the same gains K_x, K_r . In addition the parameters of the weight update law are kept the same as the example in Chapter 2, i.e. $\gamma = 1000, \mu = 2000, \sigma = 0.0005$. Figure 17 shows that the control signal is extremely noisy. Also shown in Figure 17 are the adaptive weights which are also extremely noisy and is the primary mechanism by which noise enters the control.

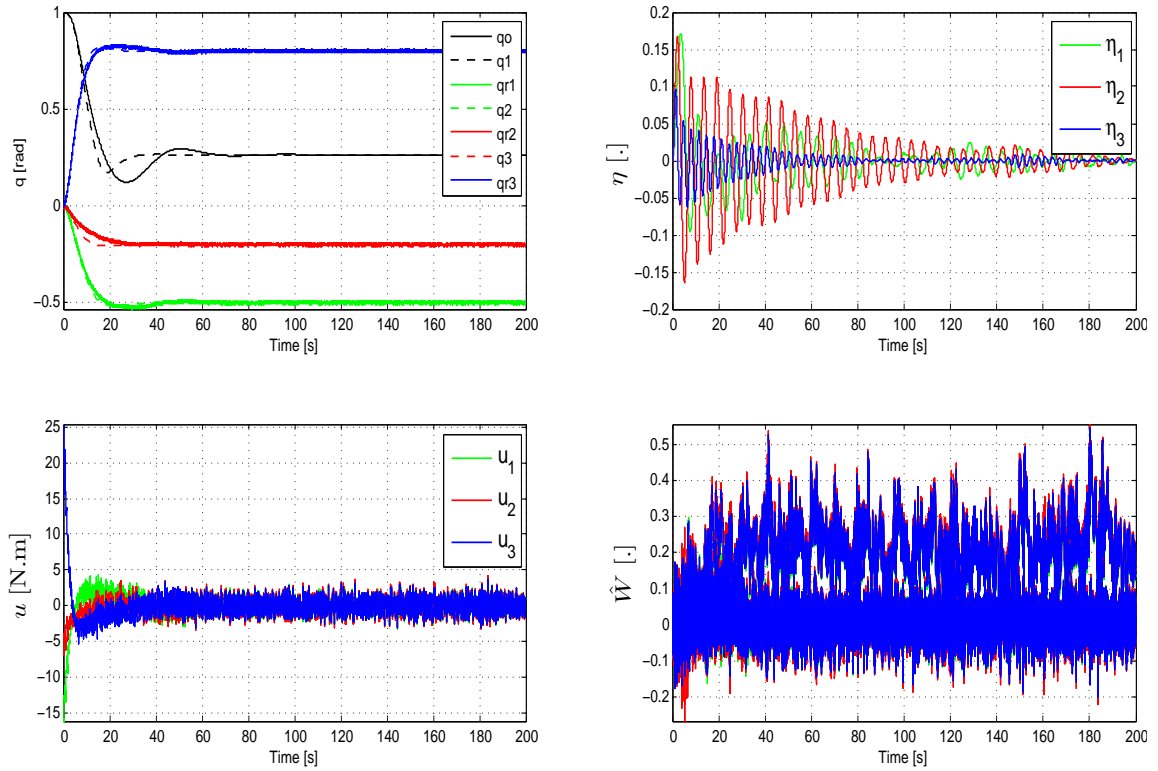


Figure 17: Adaptive control response of the spacecraft model in the presence of noise with the weight update developed in Chapter 2.

For the next simulation, a first order filter with a time constant of $\tau = 0.5$ is applied to each of the error signals between y and \hat{y} . The filtered output is used in the weight update law given in Equation (3.1). The performance of the adaptive control law is similar to that developed in Chapter 2, however the effect of sensor noise in the control has been greatly reduced. This is particularly evident in the

weights shown in Figure 18.

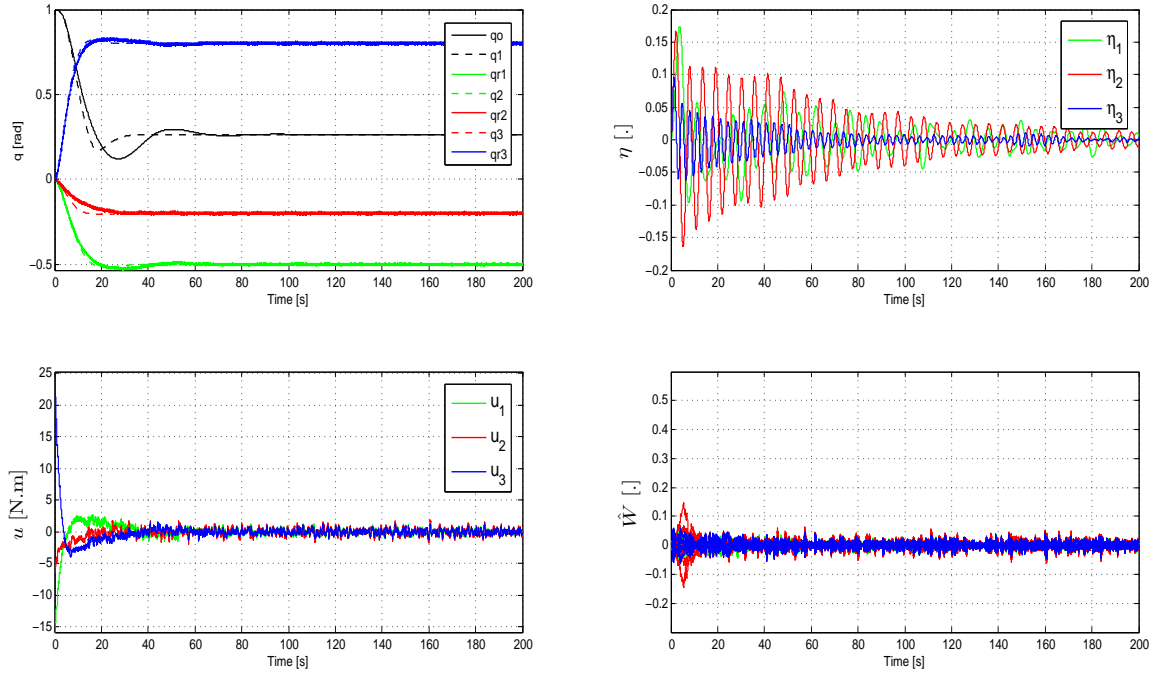


Figure 18: Adaptive control response of the spacecraft model in the presence of noise with filtered error signal.

3.6 Summary

This Chapter considers the effect of sensor noise in adaptive control, and presents a simple but effective approach for reducing its effect in the adaptive control law. The proposed approach filters the error signal used in the weight adaptation law. All the signals in the system are shown to be UUB using arguments from singular perturbation theory by treating the filter as a fast subsystem and the system dynamics together with weight update as a slow subsystem.

CHAPTER IV

ADAPTIVE OUTPUT FEEDBACK CONTROL FOR SYSTEMS WITH INPUT UNCERTAINTY

4.1 Introduction

In this chapter the adaptive control methodology developed in Chapter 2 is extended to systems with uncertainty in control effectiveness, which is referred to here as 'input uncertainty'. Lavertsky has addressed the effect of input uncertainty on adaptive control both in the context of both state feedback [48] and output feedback[49]. Tansel et al. [84] account for input uncertainty within the setting adaptive control with state feedback. In this Thesis, an approach similar to that of [84] is used to account for input uncertainty. The Chapter is organized as follows, First the problem formulation that defines the class of systems with input uncertainty and the form of the adaptation law to be applied is presented. The next section uses a Lyapunov like analysis to establish boundedness of all the signals in the closed loop system. This approach is then applied to the attitude control of a flexible spacecraft model introduced in Chapter 2. Section 4.3 extends the adaptive control methodology to systems with input uncertainty in the presence of noisy measurements. The efficacy of the method is presented through simulations on the attitude control of a flexible spacecraft with noisy measurements.

4.2 Problem Formulation

Consider the following minimal realization of a linear system coupled with a nonlinear function of unmodeled states

$$\begin{aligned}\dot{x}(t) &= Ax(t) + B\Lambda [u(t) + g(x(t), x_d(t))], \\ y(t) &= Cx(t), \\ y_r(t) &= C_r x(t)\end{aligned}\tag{4.1}$$

Equation (4.1) has the same form as Equation (2.1) in Chapter 2 except for the introduction of $\Lambda \in \mathbb{R}^{m \times m}$ which is regarded as an unknown diagonal matrix with diagonal elements, $0 < \underline{\lambda} < \lambda_i < \bar{\lambda}$ that represent an uncertainty in gain associated with the columns of input matrix B

The unmodeled states $x_d(t)$ satisfy Equation (2.2) and Assumptions 2.1, 2.2 and 2.3 hold. All the other definitions from Chapter 2 apply with regard to the other variables that appear in Equation (4.1).

Similar to what was done in Chapter 2, define the state estimation error as

$$\tilde{x}(t) \triangleq x(t) - \hat{x}(t)\tag{4.2}$$

substituting for $u(t)$ from Equation(2.11) in Equation (4.1) and employing the following definitions :

$$g_1(x, x_d, u_x) \triangleq g(x, x_d) - Du_x\tag{4.3}$$

$$D \triangleq I - \Lambda^{-1} = \text{diag} \left(\frac{\lambda_i - 1}{\lambda_i} \right) \quad i = 1, 2..m\tag{4.4}$$

$$u_x \triangleq K_x \hat{x}\tag{4.5}$$

$$u_r \triangleq K_r r,\tag{4.6}$$

the state estimation error dynamics can be written as

$$\dot{\tilde{x}}(t) = A_e \tilde{x}(t) + B\Lambda [Du_r(t) - u_{ad}(t) + g_1(x, x_d, u_x)],\tag{4.7}$$

where $A_e \triangleq A - LC$. Next we state a key assumption regarding the parameterizations of the uncertainty $g_1(x, x_d, u_x)$

Assumption 4.2: The function $g_1(x, x_d, u_x)$ can be linearly parameterized as

$$\begin{aligned} g_1(x, x_d, u_x) &= \begin{bmatrix} W_1^T & 0 \\ 0 & W_2^T \end{bmatrix} \begin{bmatrix} \zeta(\xi) \\ \zeta(u_x) \end{bmatrix} + \begin{bmatrix} \epsilon_1(x, x_d) \\ \epsilon_2(u_x) \end{bmatrix} \\ g_1(x, x_d, u_x) &= W^T \zeta(\delta) + \epsilon(x, x_d, u_x), \quad \forall \delta \triangleq [\xi^T u_x^T]^T \in \mathbb{D}. \end{aligned} \quad (4.8)$$

where $W \triangleq \text{diag}(W_1^T, W_2^T) \in \mathbb{R}^{(s+m) \times m}$ is an unknown ideal weight matrix satisfying $\|W\| \leq \bar{W}$, $\zeta(\delta(t)) \in \mathbb{R}^{(s+m) \times 1}$, is a known basis vector of the form

$$\zeta(\delta(t)) = [\zeta_1(\xi_1), \zeta_2(\xi_2), \dots, \zeta_s(\xi_s), \zeta_{s+1}(u_{x_1}), \dots, \zeta_{s+m}(u_{x_m})]^T \quad (4.9)$$

satisfying $|\zeta_i(\xi_i/u_{x_i})| \leq \bar{\zeta}$, and $\epsilon(x, x_d, u_x)$ is the residual error between the uncertainty and the linear parametrization satisfying $|\epsilon(x, x_d, u_x)| < \bar{\epsilon}$ on $\bar{\mathbb{D}}$, where $\bar{\mathbb{D}}$ is a subset of \mathbb{D} . The input vector ξ is a vector composed of tapped delays of the output y and input u and is given by Equation (2.9).

The adaptive element, u_{ad} , is given by

$$u_{ad}(t) = \hat{W}^T(t) \zeta(\delta(t)) + \hat{D}^T(t) u_r(t) \quad (4.10)$$

where \hat{W}, \hat{D} are the estimates of Z and D respectively. Define the output tracking error and the weight estimation errors as follows :

$$\tilde{y}(t) \triangleq MC\tilde{x}(t) = C_e\tilde{x}(t) \quad (4.11)$$

$$\tilde{W}(t) \triangleq W - \hat{W}(t) \quad (4.12)$$

$$\tilde{D}(t) \triangleq D - \hat{D}(t) \quad (4.13)$$

where $M \in \mathbb{R}^{m \times p}$ can be freely chosen. The manner in which M can be chosen has previously been addressed in Remark 2.2.3. Also denote the state and estimated state tracking errors:

$$e(t) \triangleq x(t) - x_m(t) \quad (4.14)$$

$$\hat{e}(t) \triangleq \hat{x}(t) - x_m(t) \quad (4.15)$$

Using Equation (4.10), Equation (4.12), Equation (4.13), and *Assumption 4.2* the state estimation error dynamics and the estimated state tracking error $\hat{e}(t)$ can be written as :

$$\dot{\tilde{x}}(t) = A_e \tilde{x}(t) + B\Lambda \left[\tilde{D}^T(t)u_r(t) + \tilde{W}^T(t)\zeta(\delta(t)) + \epsilon \right], \quad (4.16)$$

$$\dot{\hat{e}}(t) = A_m \hat{e}(t) + LC\tilde{x}(t). \quad (4.17)$$

Note that since A_m is Hurwitz by design, \hat{e} is bounded provided \tilde{x} is bounded. The estimate of the ideal weights, $\hat{W}(t)$ and $\hat{D}(t)$ in Equation (4.10), are updated based on the following update laws :

$$\dot{\hat{W}}_1(t) = \gamma_{W_1} \left[\zeta(\xi(t))\tilde{y}^T(t) - \sigma_{W_1}\hat{W}_1(t) - \frac{\zeta(\xi(t))\zeta^T(\xi(t))}{\mu}\hat{W}_1(t) \right], \quad (4.18)$$

$$\dot{\hat{W}}_2(t) = \gamma_{W_2} \left[\zeta(u_x(t))\tilde{y}^T(t) - \sigma_{W_2}\hat{W}_2(t) - \frac{\zeta(u_x(t))\zeta^T(u_x(t))}{\mu}\hat{W}_2(t) \right], \quad (4.19)$$

$$\dot{\hat{d}}_i(t) = \gamma_d \left[u_{r_i}(t)\tilde{y}_i(t) - \sigma_{d_i}\hat{d}_i(t) - \frac{u_{r_i}^2(t)\hat{d}_i(t)}{\mu} \right] \quad (4.20)$$

where γ_{W_1} , γ_{W_2} , γ_d , σ_{W_1} , σ_{W_2} , σ_{d_i} are tunable positive adaptation gains and d_i is the i th diagonal element of \hat{D} . The stability analysis of the weight update law in Equations (4.18), (4.19) and (4.20) employs a Lyapunov candidate function that is dependent on the solution of the parameter dependent Riccati equation introduced in Chapter 2 which is given by :

$$0 = A_e^T P + P A_e + Q_0 + \mu N N^T \quad (4.21)$$

$$N = C_e^T - P B \quad (4.22)$$

4.3 Boundedness of signals

In this section the boundedness of all signals in the system is shown via Lyapunov like analysis using the parameter dependent Riccati equation. The following theorem concerns the state and weight estimation errors.

Theorem 4.3.1. *Consider the system in Equation (4.1) and Equation (2.2), along with the control law given in Equation (2.14), composed of the nominal control in*

Equation (2.11) and the adaptive control in Equation (4.10) together with the observer in Equation (2.12) and the weight update laws in Equations (4.18), (4.19) and (4.20), where $\mu < \bar{\mu}$ as defined by Lemma 2.2.1. Under Assumptions 4.1 and 4.2, for a sufficiently large $\bar{\mathbb{D}}$, \tilde{x} , \tilde{W} and \tilde{D} are UUB if $\lambda_{\min}(Q_0) > \mu \|N(I - \Lambda)N^T\|$

Proof. Consider the following Lyapunov candidate function

$$V(\tilde{x}, \tilde{W}, \tilde{d}_i, x_d, t) = \tilde{x}^T P \tilde{x} + tr \left[\Lambda \tilde{W}^T \Gamma_W^{-1} \tilde{W} \right] + \sum_{i=1}^m \lambda_i \frac{\tilde{d}_i^2}{\gamma_d} + V_{x_d} \quad (4.23)$$

where $\Gamma_W^{-1} = diag(1/\gamma_{W_1}, 1/\gamma_{W_2})$ and $\Sigma_W = diag(\sigma_{W_1}, \sigma_{W_2})$. The time derivative of (4.23) along the closed loop solutions of Equation (4.1) is given by

$$\dot{V}(\tilde{x}, \tilde{W}, \tilde{d}_i, x_d, t) = 2\tilde{x}^T P \dot{\tilde{x}} - 2tr \left[\Lambda \tilde{W}^T \Gamma_W^{-1} \dot{\tilde{W}} \right] - 2 \sum_{i=1}^m \lambda_i \frac{\tilde{d}_i \dot{\tilde{d}}_i}{\gamma_d} + \dot{V}_{x_d} \quad (4.24)$$

Substituting for $\dot{\tilde{x}}$ from Equation (4.16) and the weight update laws from Equations (4.18), (4.19) and (4.20), Equation (4.24) can be written as

$$\begin{aligned} \dot{V}(\tilde{x}, \tilde{W}, \tilde{d}_i, x_d, t) &= \tilde{x}^T (A_e^T P + P A_e) \tilde{x} + 2\tilde{x}^T P B \Lambda \epsilon + 2\tilde{x}^T P B \Lambda \tilde{D}^T u_r + 2\tilde{x}^T P B \Lambda \tilde{W}^T \zeta(\delta) \\ &\quad - 2tr \left[\Lambda \tilde{W}^T \zeta(\delta) \tilde{y}^T - \Lambda \tilde{W}^T \Sigma_W \dot{\tilde{W}} - \Lambda \tilde{W}^T \frac{\zeta^T(\delta) \zeta(\delta)}{\mu} \dot{\tilde{W}} \right] \\ &\quad - 2 \left(\sum_{i=1}^m \lambda_i \tilde{d}_i \left(u_{r_i} \tilde{y}_i + \sigma_{d_i} \hat{d}_i + \frac{u_{r_i}^2 \hat{d}_i}{\mu} \right) \right) \\ &\quad + \dot{V}_{x_d} \end{aligned} \quad (4.25)$$

Using Equation (4.21), Equation (4.22), Equation (4.12) and Equation (4.13) and simplifying, Equation (4.25) can be written as

$$\begin{aligned} \dot{V}(\tilde{x}, \tilde{W}, \tilde{d}_i, x_d, t) &= -\tilde{x}^T Q \tilde{x} + 2\tilde{x}^T P B \Lambda \epsilon - 2\tilde{x}^T N \Lambda \tilde{D}^T u_r - 2\tilde{x}^T N \Lambda \tilde{W}^T \zeta(\delta) \\ &\quad + 2tr \left[\Lambda \tilde{W}^T \Sigma_W W \right] - 2tr \left[\Lambda \tilde{W}^T \Sigma_W \dot{\tilde{W}} \right] \\ &\quad + 2tr \left[\Lambda \tilde{W}^T \frac{\zeta^T(\delta) \zeta(\delta)}{\mu} W \right] - 2tr \left[\Lambda \tilde{W}^T \frac{\zeta^T(\delta) \zeta(\delta)}{\mu} \dot{\tilde{W}} \right] \\ &\quad + 2 \sum_{i=1}^m \lambda_i \tilde{d}_i \sigma_{d_i} d_i - 2 \sum_{i=1}^m \lambda_i \tilde{d}_i \sigma_{d_i} \tilde{d}_i \\ &\quad + \frac{2}{\mu} \sum_{i=1}^m \lambda_i \tilde{d}_i u_{r_i}^2 d_i - \frac{2}{\mu} \sum_{i=1}^m \lambda_i \tilde{d}_i u_{r_i}^2 \tilde{d}_i \\ &\quad + \dot{V}_{x_d} \end{aligned} \quad (4.26)$$

where $Q = Q_0 + \mu NN^T$.

Applying the vector form of Young's Inequality the 3rd and 4th terms of Equation (4.26) can be written as:

$$-2\tilde{x}^T N \Lambda \tilde{W}^T \zeta(\delta) \leq \frac{\mu}{2} \tilde{x}^T N \Lambda N^T \tilde{x} + \frac{\zeta^T(\delta) \tilde{W} \Lambda \tilde{W}^T \zeta(\delta)}{\mu/2} \quad (4.27)$$

$$-2\tilde{x}^T N \Lambda \tilde{D}^T u_r \leq \frac{\mu}{2} \tilde{x}^T N \Lambda N^T \tilde{x} + \frac{(u_r)^T \tilde{D} \Lambda \tilde{D}^T (u_r)}{\mu/2} \quad (4.28)$$

Similarly, using the matrix form of young's inequality

$$2tr[\Lambda \tilde{W}^T W] \leq tr[\Lambda \tilde{W}^T \Sigma_W \tilde{W}] + tr[\Lambda W^T \Sigma_W W] \quad (4.29)$$

$$2 \sum_{i=1}^m \lambda_i \tilde{d}_i \sigma_{d_i} d_i \leq \sum_{i=1}^m \lambda_i \sigma_{d_i} \tilde{d}_i^2 + \sum_{i=1}^m \lambda_i \sigma_{d_i} d_i^2 \quad (4.30)$$

Substituting the above inequalities and \dot{V}_{x_d} from Equation (2.7), Equation (4.30) can be written as

$$\begin{aligned} \dot{V}(\tilde{x}, \tilde{W}, \tilde{d}_i, x_d, t) &\leq -(\lambda_{\min}(Q) - \mu \|N \Lambda N\|) |\tilde{x}|^2 + 2\bar{\epsilon} m \bar{\lambda} \|PB\| |\tilde{x}| \\ &\quad - \|\Sigma_W\| m \bar{\lambda} \|\tilde{W}\|^2 + \|\Sigma_W\| m \bar{\lambda} \bar{W}^2 + 2 \frac{m \bar{\lambda} \bar{\zeta}^2 \bar{W} \|\tilde{W}\|}{\mu} \\ &\quad - \sum_{i=1}^m \sigma_{d_i} \bar{\lambda}_i |\tilde{d}_i|^2 + \sum_{i=1}^m \sigma_{d_i} \bar{\lambda}_i \bar{d}_i^2 + \frac{2}{\mu} \sum_{i=1}^m \bar{\lambda}_i u_{r_i}^2 \bar{d}_i |\tilde{d}_i| \\ &\quad - c_3 |x_d|^2 + c_4 b_d |x_d| \end{aligned} \quad (4.31)$$

Using the following definitions :

$$c = \lambda_{\min}(Q_0) + \mu \|N(I - \Lambda)N^T\| > 0 \quad (4.32)$$

$$c_5 = \bar{\epsilon} \|PB\| m \bar{\lambda} \quad (4.33)$$

$$c_6 = m \bar{\lambda} \bar{W} \frac{(s+m)^2 \bar{\zeta}^2}{\mu} \quad (4.34)$$

$$c_7 = \|\Sigma_W\| m \bar{\lambda} \quad (4.35)$$

$$c_8 = c_4 b_d \quad (4.36)$$

$$c_{9_i} = \bar{\lambda}_i \bar{d}_i \frac{u_{r_i}^2}{\mu} \quad (4.37)$$

$$c_{10_i} = \sigma_{d_i} \bar{\lambda}_i \quad (4.38)$$

$$e^2 = \|\Sigma_W\| m \bar{\lambda} \bar{W}^2 + \frac{c_5^2}{c} + \frac{c_6^2}{c_7} + \sum_{i=1}^m \sigma_{d_i} \bar{\lambda}_i \bar{d}_i^2 + \sum_{i=1}^m \frac{c_{9_i}^2}{c_{10_i}} + \frac{c_8^2}{c_3} \quad (4.39)$$

the inequality in Equation (4.31) can be written as

$$\begin{aligned}
\dot{V}(\tilde{x}, \tilde{W}, \tilde{d}_i, x_d, t) &\leq -c \left[|\tilde{x}| - \frac{c_5}{c} \right]^2 \\
&\quad - c_7 \left[\|\tilde{W}\| - \frac{c_6}{c_7} \right]^2 \\
&\quad - c_3 \left[|x_d| - \frac{c_8}{c_3} \right]^2 \\
&\quad - \sum_{i=1}^m c_{10_i} \left(|\tilde{d}_i|^2 - \frac{c_{9_i}}{c_{10_i}} \right)^2 + e^2
\end{aligned} \tag{4.40}$$

Consequently we can conclude that either of the following conditions :

$$|\tilde{x}| > \Psi_1 \text{ or } \|\tilde{W}\| > \Psi_2 \text{ or } |\tilde{d}_i| > \Psi_{3_i} \text{ or } |x_d| > \Psi_4 \tag{4.41}$$

renders $\dot{V}(\tilde{x}, \tilde{W}, \tilde{d}_i, x_d, t) < 0$, where Ψ_1, Ψ_2, Ψ_3 and Ψ_4 are given by :

$$\Psi_1 \triangleq \frac{c_5}{c} + \frac{e}{\sqrt{c}} \tag{4.42}$$

$$\Psi_2 \triangleq \frac{c_6}{c_7} + \frac{e}{\sqrt{c_6}} \tag{4.43}$$

$$\Psi_{3_i} \triangleq \frac{c_{9_i}}{c_{10_i}} + \frac{e}{\sqrt{c_{10_i}}} \tag{4.44}$$

$$\Psi_4 \triangleq \frac{c_8}{c_3} + \frac{e}{\sqrt{c_3}} \tag{4.45}$$

and therefore $\tilde{x}, \tilde{W}, \tilde{d}_i, x_d$ are UUB. \square

Corollary 4.3.1. *Under the conditions stated in Theorem 4.3.1, An estimate for the ultimate bound for $\eta(t) \triangleq [\tilde{x}^T \text{vec}(\tilde{W}^T) \tilde{d}_1 \dots \tilde{d}_m x_d]^T$, is given by*

$$r_\eta = \sqrt{\frac{\lambda_{\max}(P)\Psi_1^2 + \lambda_{\max}(\Gamma_W^{-1})\bar{\lambda}\Psi_2^2 + \frac{\bar{\lambda}}{\gamma_d} \sum_{i=1}^m \Psi_{3_i}^2 + c_2\Psi_4^2}{\vartheta}} \tag{4.46}$$

Further an estimate for \tilde{x} is given by

$$r = \sqrt{\frac{\lambda_{\max}(P)\Psi_1^2 + \frac{\bar{\lambda}}{\gamma_w} \Psi_2^2 + \frac{\bar{\lambda}}{\gamma_d} \sum_{i=1}^m \Psi_{3_i}^2 + c_2\Psi_4^2}{\lambda_{\min}(P)}} \tag{4.47}$$

where $\vartheta = \min(\lambda_{\min}(P), \lambda_{\min}(\Gamma_W^{-1})\underline{\lambda}, \underline{\lambda}/\gamma_d I, c_1)$

Proof. The proof follows directly from 2.3.1, with the corresponding set D_η now defined to include the elements of \tilde{d}_i . \square

The following corollary shows that if \tilde{x} is bounded then the state tracking error e , is also bounded.

Corollary 4.3.2. *If the state estimation error \tilde{x} is bounded, then the state tracking error $e = x - x_m$ is bounded.*

Proof. Proof follows from Corollary 2.3.2 □

Since $x_m(t)$ is bounded, it follows from Corollary 4.3.1 that $x(t)$ is bounded. Further *Assumption* 4.1 ensures that x_d is bounded since it is input-to-state stable [38]. Therefore all the signals in the system are UUB.

Remark 4.3.1. *The proofs of Theorem 4.3.1 and Corollary 4.3.1 assume the sets \mathbb{D} and \mathbb{D}_η are sufficiently large. If we define B_R as the largest ball in \mathbb{D}_η , and assume the initial conditions are such that $\eta(0) \in B_R$, then from Figure 5 in Chapter 2, we have the added condition that $r_\eta < R_\eta$, which implies an upper bound on $\gamma \triangleq \max(\gamma_{W_1}, \gamma_{W_2}, \gamma_d)$. It can be shown that in this case the upper bound must be such that $\vartheta = \underline{\lambda}/\gamma$. With r_η defined by Equation (4.46) and $\vartheta = \underline{\lambda}/\gamma$, the condition $r_\eta < R_\eta$ implies*

$$\gamma < \frac{R^2 \underline{\lambda} - \bar{\lambda}(\Psi_2^2 + \sum_{i=1}^m \Psi_{3_i}^2)}{\lambda_{\max}(P)\Psi_1^2} \quad (4.48)$$

Therefore, it follows that the meaning of \mathbb{D}_η sufficiently large implies

$$R_\eta > \sqrt{\frac{\gamma \lambda_{\max}(P)\Psi_1^2 + \bar{\lambda}(\Psi_2^2 + \sum_{i=1}^m \Psi_{3_i}^2)}{\underline{\lambda}}} \quad (4.49)$$

and $\eta(0) \in B_R$. The meaning of \mathbb{D} sufficiently large is difficult to characterize since $x(t)$ depends on the initial condition $x(0)$.

Remark 4.3.2. *When $\Lambda = I_m$, $d_i = 0$ and Equation (4.32) reduces to Equation (2.40). Equation (4.33) is similar to Equation (2.41) except for the multiplication*

factor m . Equation (4.34) is similar to that of Equation (2.42) with s being replaced by $s + m$ and the presence of the same multiplication factor m in Equation (4.33). Furthermore the first two terms of Equation (4.39) are similar to Equation (2.44)

4.4 Control of Flexible Spacecraft in the presence of Input Uncertainties

In this section, the attitude control of the flexible aircraft introduced in Chapter 2 is considered in the presence of input uncertainties. The nominal controller in this section differs from Chapter 2 in that it is redesigned by defining the following pseudo control $u_1 \triangleq \bar{Q}J^{-1}u$. Using model inversion Equations (2.79) and (2.80) can be written as:

$$\dot{z}_1 = \frac{1}{2}z_2 \quad (4.50)$$

$$\dot{z}_2 = u_1 + g_0(q, \omega, \eta_1, \eta_2, u) \quad (4.51)$$

At the equilibrium attitude, $q_0 = 1$ and $q = [0 \ 0 \ 0]^T$, therefore $\bar{Q}_e = I_3$, and A, B, C in (4.1) become:

$$A = \begin{bmatrix} 0 & 0 & 0 & 0.5 & 0 & 0 \\ 0 & 0 & 0 & 0 & 0.5 & 0 \\ 0 & 0 & 0 & 0 & 0 & 0.5 \\ 0 & 0 & 0 & 0 & 0 & 0 \\ 0 & 0 & 0 & 0 & 0 & 0 \\ 0 & 0 & 0 & 0 & 0 & 0 \end{bmatrix} \quad (4.52)$$

$$B = \begin{bmatrix} 0_3 \\ I_3 \end{bmatrix} \quad (4.53)$$

$$C = \begin{bmatrix} I_3 & 0_3 \end{bmatrix} \quad (4.54)$$

$$\Lambda = \begin{bmatrix} \lambda_1 & 0 & 0 \\ 0 & \lambda_2 & 0 \\ 0 & 0 & \lambda_3 \end{bmatrix} \quad (4.55)$$

where we have introduced the effect of uncertain control effectiveness through the matrix Λ . Further the uncertainty matrix δ is given by:

$$\delta = \begin{bmatrix} 14.2040 & 2.8119 & 4.7438 \\ -2.7680 & 2.0186 & -3.6798 \\ 2.4571 & 5.4758 & -1.8408 \end{bmatrix} \quad (4.56)$$

The nominal controller gain K_x is obtained using LQR theory with $Q = I_6$, $\Lambda = I_3$ and $R = 0.001I_3$. The nominal observer is a Kalman filter designed for the process:

$$\dot{x} = Ax + B\Lambda u + \Gamma w \quad (4.57)$$

$$y = Cx \quad (4.58)$$

where $\Gamma = [0_3; I_3]$, $\Lambda = I_3$ and the process and measurement noise matrices are $Q_w = I_6$ and $R_v = 0.001I_3$ respectively. The expression used for the feedforward gain is $K_r = -(CA_m B)^{-1}$. This provides zero steady state error in the reference model response for step changes in attitude command. The reference model dynamics for adaptive control design are defined by setting $A_m = A - BK_x$ and $B_m = BK_r$.

A simulation is carried out with the nominal control acting on the rigid spacecraft model to evaluate nominal performance without nonlinearities ($g(q, \omega, \eta, \dot{\eta}, u) = 0$) and without input uncertainty ($\Lambda = I_3$) in Equation (4.1). As observed from Figure 19, nominal control provides adequate tracking of the reference input in the absence of uncertainty. The simulation is repeated with the nonlinear spacecraft model with the flexible modes and without input uncertainty. Figure 20 shows that even without the effect of the flexible modes and without input uncertainty, the system goes unstable for a reference input $r = [-0.5 \ -0.2 \ 0.8]^T$.

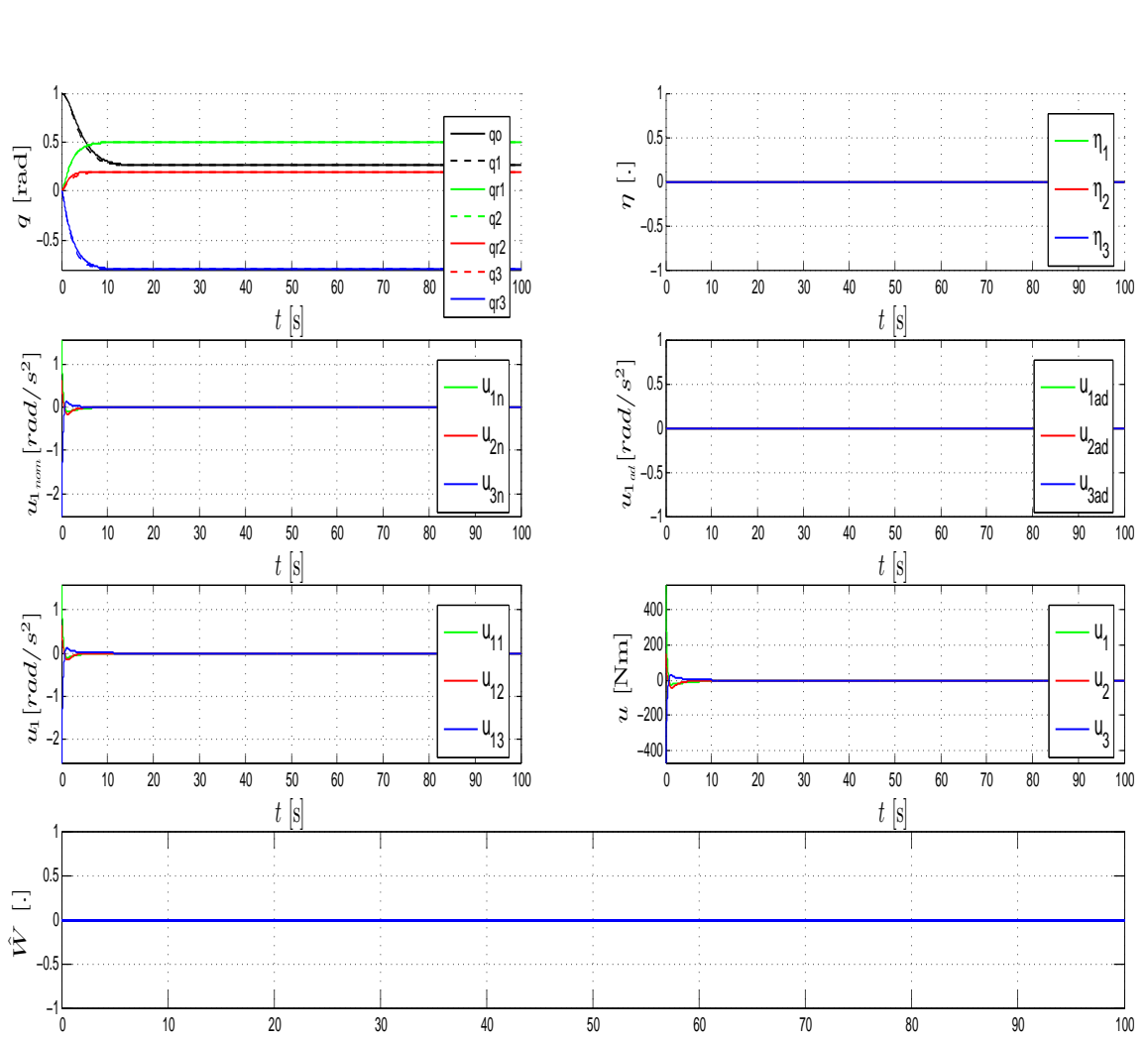


Figure 19: Response of the rigid spacecraft model under nominal control.

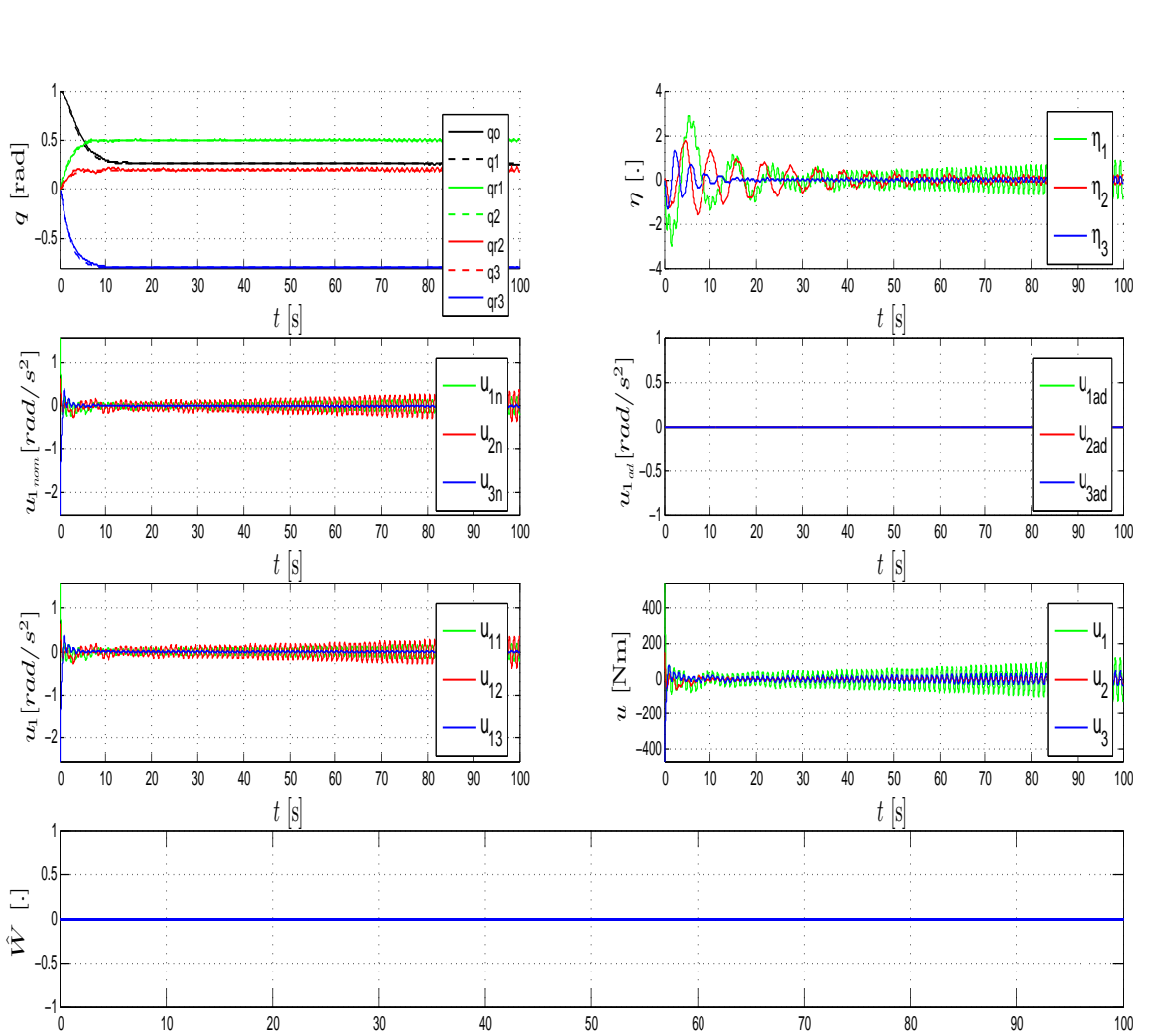


Figure 20: Response of the flexible nonlinear spacecraft model under nominal control.

As in Chapter 2, the reference model dynamics for adaptive control design are defined by setting $A_m = A - BK_x$ and $B_m = BK_r$. Using Equation (2.29), M is obtained as $-0.9659 * I_3$, the maximum allowable value for the parameter μ from Lemma 2.1 is $\bar{\mu} = 5.42$. Using $\mu = 3$, with $\bar{\lambda} = 1.5$ the value of c in (4.32) is 0.6991 as required in Theorem 4.3.1. As before $n_y = 11$ delayed values of y and $n_u = 5$ delayed values of u and $\bar{u}_x = u_x/150$ together with a bias term are used to form the basis vector in Equation (4.9) with sigmoidal basis function. The activation potentials of the sigmoidal activation functions for y and u were chosen as in *Chapter 2* while 25 is chosen for \bar{u}_x . The result in Figures 21 and 22 were obtained with $\gamma_{W_1} = 10$, $\mu = 3.2$, $\sigma_{W_1} = 0.005$, $\gamma_{W_2} = 0$, $\sigma_{W_2} = 0.005$, $\gamma_d = 0$, $\sigma_{d_i} = 0.005$, and

$d = 0.005$ for the parameters in the weight adaptation laws defined by Equations (4.18), (4.19) and (4.20). Figure 21 shows the performance that results with the adaptive controller acting on the flexible nonlinear spacecraft model without input uncertainty. Figure 22 shows the resulting performance with an input uncertainty corresponding to $\Lambda = \text{diag}(1.2, 0.6, 1.2)$. Comparing these figures with the nominal tracking performance in Figure 19, it is evident that with $\gamma_{W_2} = 0$ and $\gamma_d = 0$ the adaptive controller is adaptive to uncertainty due to nonlinearity and robust to unmodeled flexible dynamics, but it is not robust to input uncertainty. Figure 23 shows the adaptive control result obtained for the same parameter settings and uncertainty set as in Figure 5, except that γ_d and γ_{W_2} are set to 10 and 5 respectively. The response of $q(t)$ is nearly the same as the ideal response of the nominal control design in the absence of uncertainty in Figure 19. This shows that nominal performance is preserved by this design for all 3 sources of uncertainty. Therefore we can state that this design is adaptive to both nonlinearity and input uncertainty, and is robust to unmodeled dynamics.

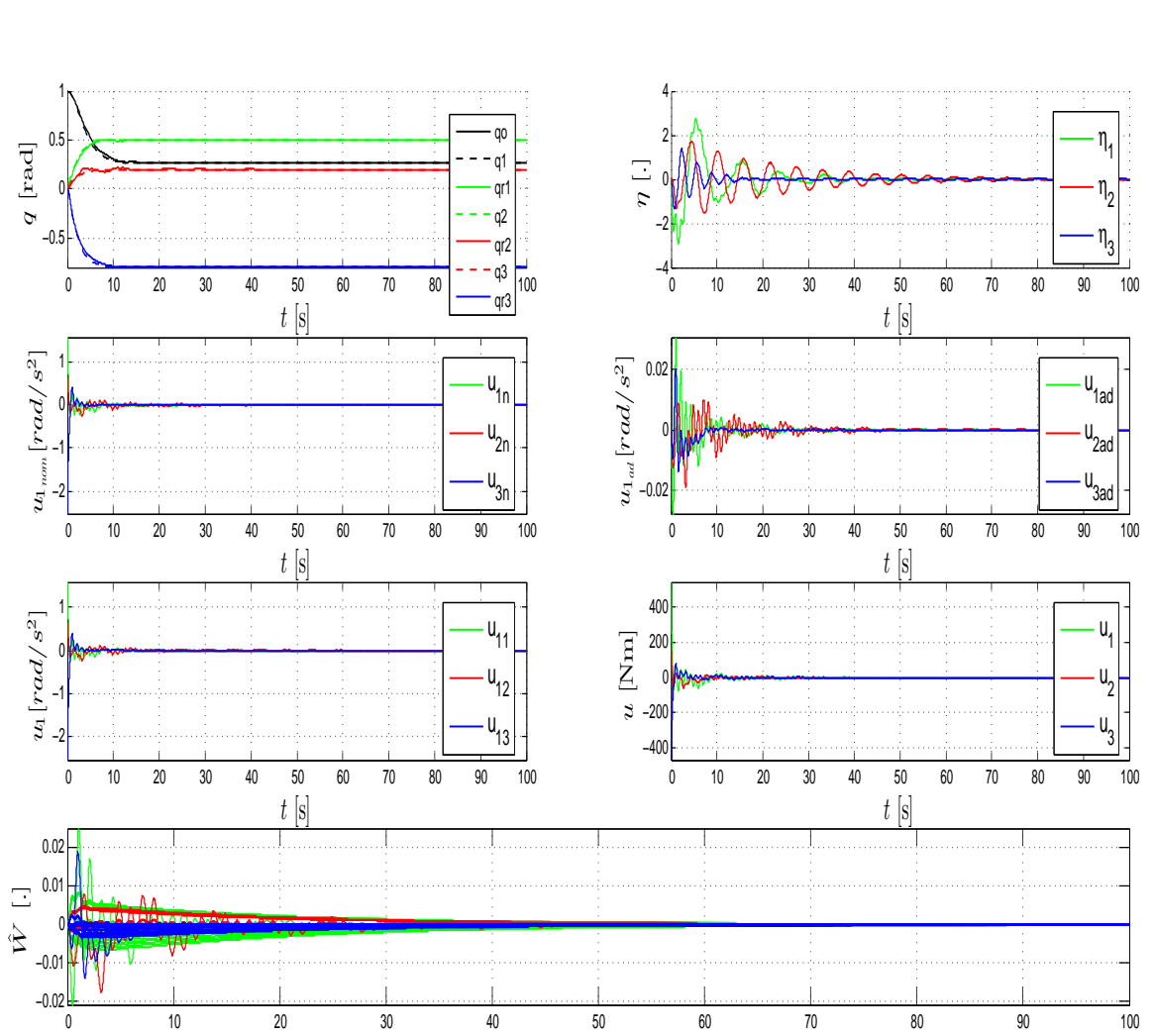


Figure 21: Response of the nonlinear flexible spacecraft model without input uncertainty for the adaptive design with $\gamma_d = 0$, $\Gamma_{W_2} = 0$

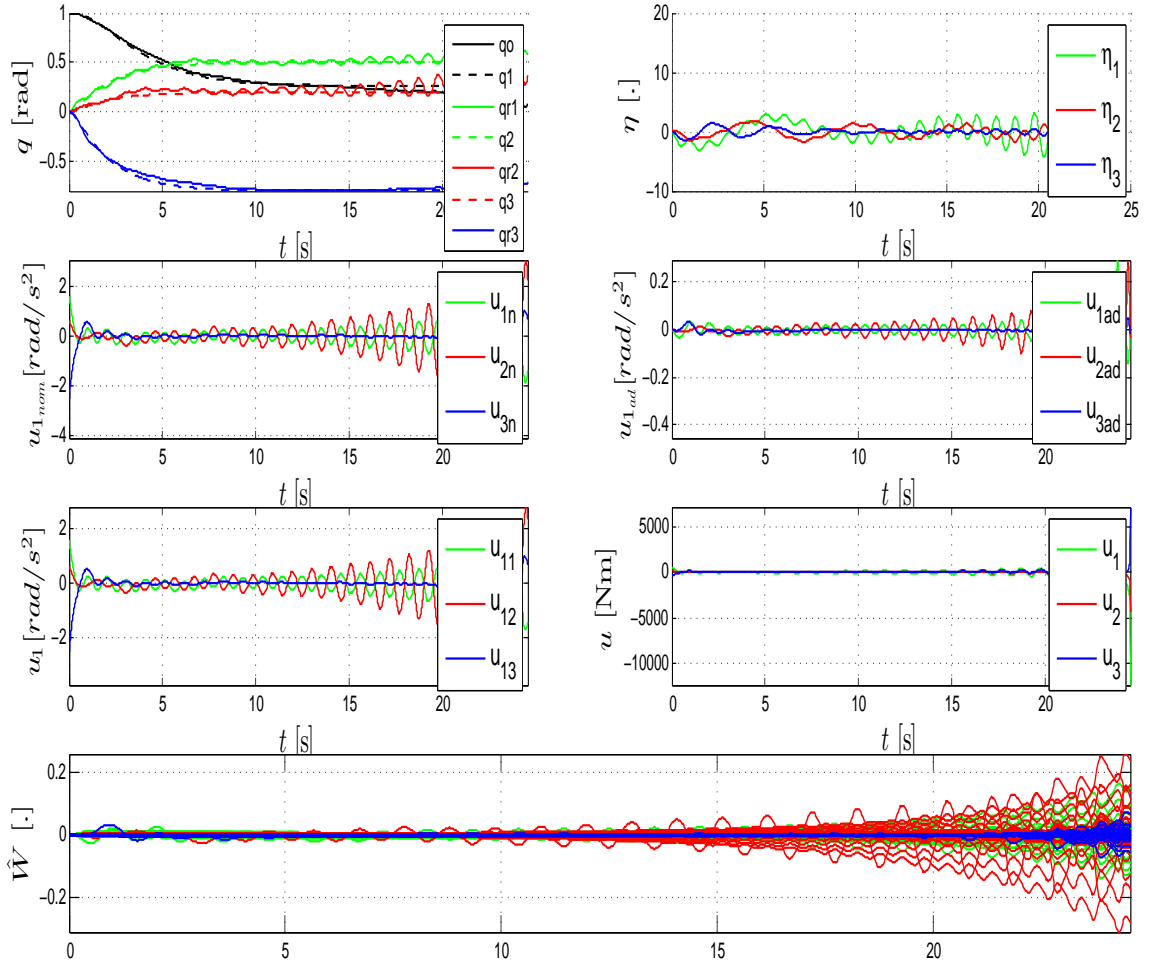


Figure 22: Response of the nonlinear flexible spacecraft model with input uncertainty for the adaptive design with $\gamma_d = 0$, $\Gamma_{W_2} = 0$

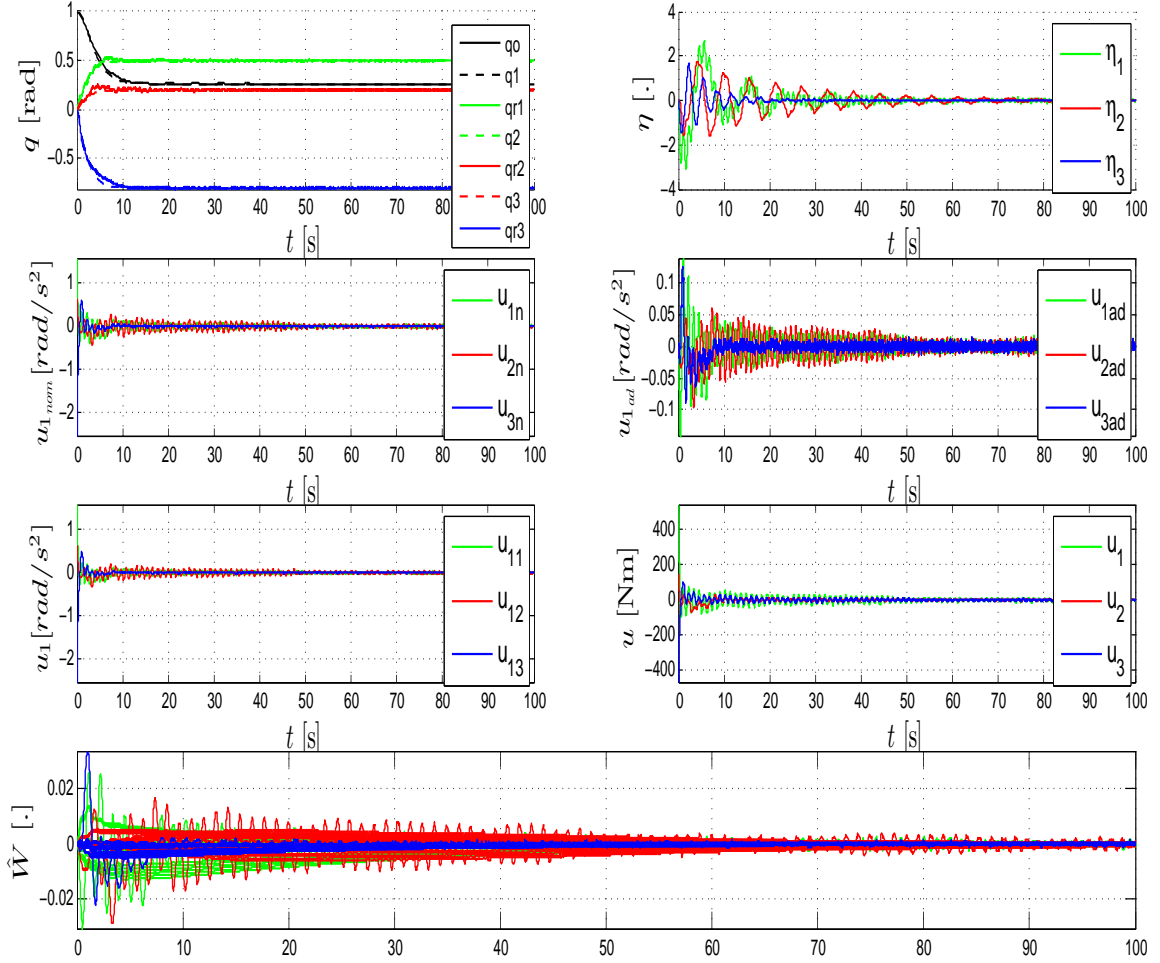


Figure 23: Response of the nonlinear flexible spacecraft model with input uncertainty for the adaptive design with $\gamma_d = 10$, $\Gamma_{W_2} = 5$

4.5 Reducing the effect of sensor noise for systems with input uncertainty

In this Section we adopt the approach in Chapter 3 to address the effect of sensor noise. The adaptive control is similar to that developed in the previous section except

that it uses filtered versions of the output error to reduce the effect of noise:

$$\dot{\hat{W}}_1(t) = \gamma_{W_1} \left[\zeta(\xi(t)) \tilde{y}_f^T(t) - \sigma_{W_1} \hat{W}_1(t) - \frac{\zeta(\xi(t)) \zeta^T(\xi(t))}{2\mu} \hat{W}_1(t) \right] \quad (4.59)$$

$$\dot{\hat{W}}_2(t) = \gamma_{W_2} \left[\zeta(u_x(t)) \tilde{y}_f^T(t) - \sigma_{W_2} \hat{W}_2(t) - \frac{\zeta(u_x(t)) \zeta^T(u_x(t))}{2\mu} \hat{W}_2(t) \right] \quad (4.60)$$

$$\dot{\hat{d}}_i(t) = \gamma_d \left[u_{r_i}(t) \tilde{y}_{f_i}(t) - \sigma_{d_i} \hat{d}_i(t) - \frac{u_{r_i}^2(t) \hat{d}_i(t)}{\mu} \right] \quad (4.61)$$

where $\gamma_{W_1}, \gamma_{W_2}, \gamma_d, \sigma_{d_i}, \sigma_{W_1}$ and σ_{W_2} are tunable positive adaptation gains and \tilde{y}_f^T satisfies

$$\tau \dot{\tilde{y}}_f(t) = -\tilde{y}_f(t) + \tilde{y}(t) \quad (4.62)$$

As before, we have assumed in Equation (4.62) that the same first order filter is applied to each element of \tilde{y}_f , since we are concerned here with the properties of the adaptive controller for sufficiently large bandwidth filter (sufficiently small τ in the case of a first order filter).

Theorem 4.5.1. *Consider the system in Equation (4.1) and Equation (4.2), along with the control law given in Equation (2.14), composed of the nominal control in Equation (2.11) and the adaptive control in Equation (4.10) together with the observer in Equation (2.12) and the weight update laws in Equations (4.58), (4.59) and (4.60), where $\mu < \bar{\mu}$ as defined by Lemma 2.1. Under Assumptions 2.1, 2.2, 2.3 and 2.4 and for $n \geq n_x + n_{x_d}$, $\exists \tau : \forall 0 < \tau < \tau^*$, such that \tilde{x} and \tilde{W} are UUB, for a sufficiently large \mathbb{D} .*

Proof. Proof follows directly from Theorem 3.4.1 □

4.6 Attitude control of flexible spacecraft with input uncertainty in the presence of noise

Attitude control of the spacecraft is evaluated in the presence of noisy measurements. A simulation is first carried out with the weight update law given in (4.18), (4.19) and

(4.20) with the same values for the tuning parameters used in Figure 23 but with the addition of band limited white sensor noise with power spectral density of 2×10^{-4} . Figure 24 shows that the adaptive control developed using the weight update laws in Equations (4.18), (4.19) and (4.20) provides adequate tracking performance, however the control signal is extremely noisy. Also shown in Figure 24 are the adaptive weights which are also extremely noisy. This once again illustrates the point that there is a direct path for the sensor noise to influence the adaptive component of the control signal. For the next simulation, a first order filter with a time constant of $\tau = 0.3$ is applied to each component of \tilde{y} , using the weight update laws in Equations (4.59), (4.60) and (4.61). Figure 25 shows that the effect of sensor noise on the control signal is significantly reduced. Also note the the level of noise in the adaptive weights is much smaller than the weights shown in Figure 24.

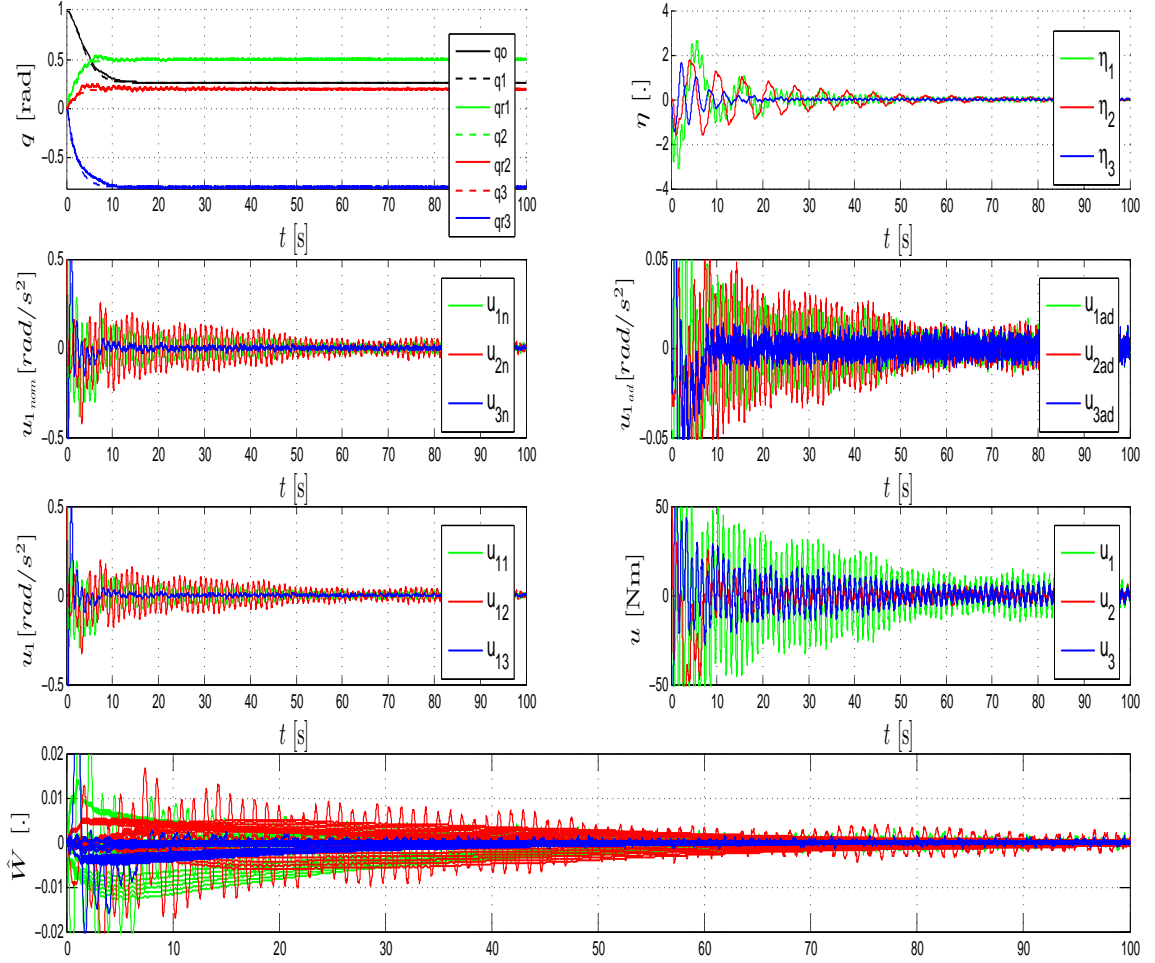


Figure 24: Response of the flexible spacecraft model with sensor noise using the weight update law in Equations (4.18), (4.19) and (4.20) and the same adaptation parameter values as in Figure 23.

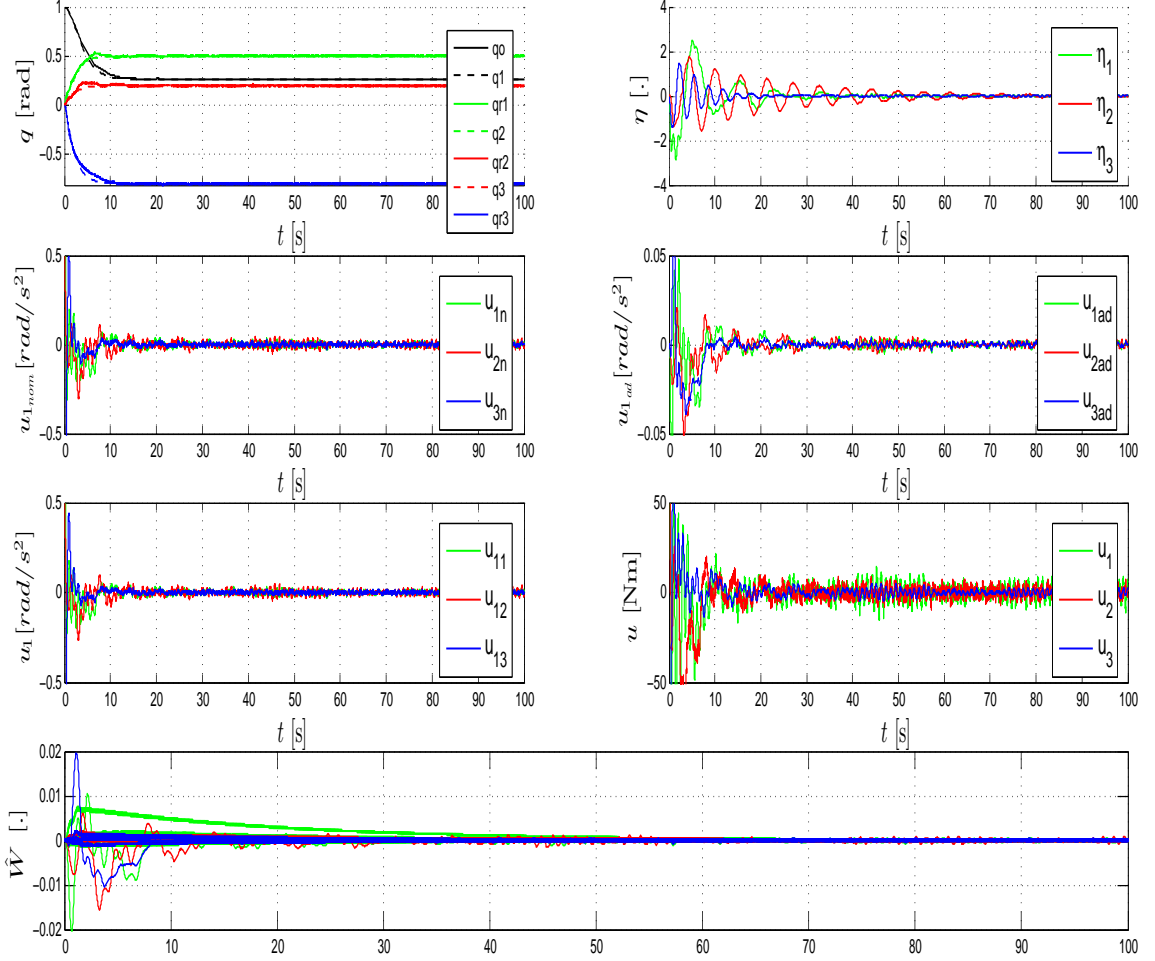


Figure 25: Response of the flexible spacecraft model with sensor noise using the weight update law in Equations (4.59), (4.60) and (4.61) and the same adaptation parameter values as in Figure 23.

4.7 Summary

In this Chapter, the adaptive controller developed in Chapter 2 is extended to systems with both input uncertainty and in the presence of noisy measurements. As in the previous Chapter's, boundedness of all the signals in the system is shown through a Lyapunov like stability analysis. The effectiveness of the proposed adaptive control law is demonstrated through simulations on the attitude control of a flexible spacecraft.

CHAPTER V

ADAPTIVE CONTROL OF A FLEXIBLE UNMANNED AERIAL VEHICLE

5.1 Introduction

The need for designing aircraft to meet stringent efficiency requirements are driving the use of lighter materials in modern airframes. The use of lighter materials results in aircraft that are flexible thus reducing the frequency separation between the rigid body and structural modes. In addition flexible aircraft are being evaluated for numerous applications ranging from long term surveillance and loitering for use as pseudo satellites. Classical flight control design relies on frequency separation between rigid modes and structural modes which no longer hold for flexible aircraft. This has driven extensive research in the use of adaptive control for designing control system for such airframes [24, 69, 22, 67]. In this chapter the adaptive control methodology developed in the previous chapters are used to augment an observer based altitude controller for a flexible Unmanned Aerial Vehicle (UAV). First, an observer based nominal controller is designed using a 4 state longitudinal model constructed using stability derivative data obtained from the rigidized flexible model of the UAV (see Appendix A.1). The performance of the nominal controller is evaluated on two different models of the UAV, an eight state model that only includes the rigid body modes (both longitudinal and lateral modes) and a forty four state model that includes aero lag modes and several flexible modes (see Appendix A.2 and Appendix A.3). Both the eight state and forty four state model were first obtained in modal form using ASWing [18], and then converted to real Jordan form for design and simulation purposes. This detail is further explained in Appendix B. An output feedback adaptive controller is

first developed based on Chapter 2 and is shown to improve the performance of the nominal controller in the presence of flexible modes. Next it is shown that the effect of uncertain control effectiveness on this design renders the system unstable, while the method developed in Chapter 4 is shown to provide adequate tracking to a step command input. Finally it is shown that filtering the error signal in the adaptive law improves the control response to sensor noise.

5.2 *Flexible UAV Model*

A flexible UAV model is used to demonstrate the effectiveness of the adaptive control theory developed in this thesis. Three different models of the UAV are available for design and evaluation purposes. The first model is obtained using stability derivative data by considering only the rigid body modes of the UAV. Using the stability derivatives and mass moments of inertia data from the UAV, a rigid body longitudinal dynamic model of the UAV is obtained in the form (See Appendix A.1):

$$\begin{aligned}\dot{x} &= Ax + Bu \\ y &= Cx\end{aligned}\tag{5.1}$$

where the state vector $x(t)$, control input $u(t)$ are given by

$$x(t) = [\bar{u}(t) \alpha(t) q(t) \theta(t)]^T\tag{5.2}$$

$$u(t) = [\delta_e(t) \delta_T(t) \delta_f(t)]^T\tag{5.3}$$

$$y(t) = [\bar{u}(t) q(t)]^T\tag{5.4}$$

where $\bar{u}(t) = u(t)/U_0$ is the normalized airspeed, $\alpha(t)$ is the angle of attack, $q(t)$ the pitch rate, and $\theta(t)$ the pitch attitude angle. $\delta_e(t)$ denotes the elevator deflection, $\delta_T(t)$ denotes throttle and $\delta_f(t)$ the full span flaps. The Eigenvalues obtained using the stability derivative model in Equation (5.1) are given in Table 1.

Table 1: Eigenvalues derived from stability derivative model

| Eigenvalue | Damping | Frequency(rad/s) |
|----------------|---------|------------------|
| -2.8100+0.142i | 0.99 | 2.810 |
| -2.8100-0.142i | 0.99 | 2.810 |
| -0.0455+0.300i | 0.15 | 0.303 |
| -0.0455-0.300i | 0.15 | 0.303 |

As seen from the modal analysis above, the rigid body longitudinal dynamic model has a highly damped mode at 2.81 rad/s and a lightly damped mode at 0.303 rad/s. These are representative of the short period and Phugoid modes of a conventional fixed wing aircraft. The eight state model of the UAV contains both the longitudinal and lateral-directional modes and also models the coupling between them. The Eigenvalues of the eight state model of the UAV are given in Table 2.

Table 2: Eigenvalues derived from eight state model

| Eigenvalue | Damping | Frequency(rad/s) |
|----------------|---------|------------------|
| -0.1210+0.059i | 0.90 | 0.135 |
| -0.1210-0.059i | 0.90 | 0.135 |
| -0.0576+0.298i | 0.19 | 0.304 |
| -0.0576+0.298i | 0.19 | 0.304 |
| -1.1500 | 1.00 | 1.150 |
| -2.7600+0.740i | 0.97 | 2.850 |
| -2.7600-0.740i | 0.97 | 2.850 |
| -9.6400 | 1.00 | 9.640 |

The eight state model has the short period mode at 2.85 rad/s with a damping

of 0.97 and the Phugoid mode at 0.304 rad/s with a damping of 0.19. This compares well with the longitudinal modes obtained from the four state model. In addition to the longitudinal modes, the eight state model contains a Dutch roll mode at 0.135 rad/s with a damping of 0.9, a roll mode at 9.64 rad/s and a stable spiral mode at 1.15 rad/s. Finally the Eigenvalues of the forty four state model of the UAV are given in Table 3.

The forty four state model has the short period mode at 2.59 rad/s with a damping of 0.97 and the Phugoid mode at 0.297 rad/s with a damping of 0.20. In addition to the longitudinal modes, the forty four state model contains a Dutch roll mode at 0.138 rad/s with a damping of 0.83, a roll mode at 9.41 rad/s and a stable spiral mode at 1.30 rad/s as well as several aero lag and flexible modes. As observed from the Eigenvalues of the rigid body model in Table 1 and Table 2, there is very little separation between the rigid body modes and the flexible modes of the UAV. Thus this model is ideal for evaluating the adaptive control designs developed in the previous chapters of this thesis. In the next section an altitude hold controller will be designed using the longitudinal stability derivative model given in Equation (5.1) and the resulting controller evaluated on both the eight state model and the forty four state model to determine the effect of unmodeled dynamics on the nominal controller.

Table 3: Eigenvalues derived from forty four state model

| Eigenvalue | Damping | Freq.(rad/s) | Eigenvalue | Damping | Freq.(rad/s) |
|----------------|---------|--------------|-----------------|---------|--------------|
| -0.115+0.0767i | 0.832 | 0.138e-001 | -8.1500 | 1.0000 | 8.1500 |
| -0.115+0.0767i | 0.832 | 0.138e-001 | -0.7970-8.610i | 0.0922 | 8.6400 |
| -0.0617+0.291i | 0.208 | 0.297 | -0.7970+8.610i | 0.0922 | 8.6400 |
| -0.0617+0.291i | 0.208 | 0.297 | -8.7200 | 1.0000 | 8.7200 |
| -1.30 | 1.000 | 1.300 | -6.3300- 6.060i | 0.7220 | 8.7600 |
| -1.9400-1.690i | 0.756 | 2.570 | -6.3300+ 6.060i | 0.7220 | 8.7600 |
| -1.9400-1.690i | 0.756 | 2.570 | -7.2000- 5.500i | 0.7940 | 9.0600 |
| -2.5200-0.557i | 0.977 | 2.590 | -7.2000+ 5.500i | 0.7940 | 9.0600 |
| -2.5200-0.557i | 0.977 | 2.590 | -9.0600 | 1.0000 | 9.0600 |
| -3.3400 | 1.000 | 3.340 | -9.4100 | 1.0000 | 9.4100 |
| -3.9900 | 1.0000 | 3.9900 | -9.9000 | 1.0000 | 9.9000 |
| -4.5200 | 1.0000 | 4.5200 | -10.100 | 1.0000 | 10.100 |
| -5.1900 | 1.0000 | 5.1900 | -10.400 | 1.0000 | 10.400 |
| -5.5600 | 1.0000 | 5.5600 | -10.500 | 1.0000 | 10.500 |
| -5.8900 | 1.0000 | 5.8900 | -10.800 | 1.0000 | 10.800 |
| -6.3700 | 1.0000 | 6.3700 | -0.3340-10.90i | 0.0308 | 10.900 |
| -6.5300 | 1.0000 | 6.5300 | -0.3340+10.90i | 0.0308 | 10.900 |
| -4.5900-4.720i | 0.6970 | 6.5800 | -11.100 | 1.0000 | 11.100 |
| -4.5900+4.720i | 0.6970 | 6.5800 | -11.200 | 1.0000 | 11.200 |
| -6.8800 | 1.0000 | 6.8800 | -11.400 | 1.0000 | 11.400 |
| -7.4600 | 1.0000 | 7.4600 | -3.9900-10.80i | 0.347 | 11.500 |
| -7.8700 | 1.0000 | 7.8700 | -3.9900+10.80i | 0.347 | 11.500 |

5.3 Nominal Control Design

The objective of the observer based nominal control design is to track commanded altitude. Towards this end we augment the four state model in Equation (5.1) with the altitude state given by:

$$\begin{aligned}\dot{h} &= U_0 \sin(\gamma) \\ \dot{h} &\approx U_0 \theta - U_0 \alpha\end{aligned}\tag{5.5}$$

Therefore Equation (5.1) becomes

$$\begin{aligned}\dot{x}_a &= \tilde{A}x_a + \tilde{B}u \\ y_a &= \tilde{C}x_a \\ y_r &= C_r x_a\end{aligned}\tag{5.6}$$

where y_a is the augmented output vector, y_r is the reference command, and

$$\begin{aligned}\tilde{A} &= \begin{bmatrix} A & 0 \\ C_h & 0 \end{bmatrix} \\ \tilde{B} &= \begin{bmatrix} B \\ 0 \end{bmatrix} \\ \tilde{C} &= \begin{bmatrix} C & 0 \\ 0 & 1 \end{bmatrix} \\ C_r &= \begin{bmatrix} 0 & 0 & 0 & 0 & 1 \end{bmatrix}\end{aligned}\tag{5.7}$$

with $C_h = [0 \ -U_0 \ 0 \ U_0]$ and the augmented state $x_a \triangleq [x \ h]^T$. The nominal controller design includes integral action to provide zero steady state error for step changes in altitude command. The integral state, x_{int} , given by:

$$\dot{x}_{int} = h_c(t) - h(t)\tag{5.8}$$

Where h_c is the commanded altitude and h the altitude state. The resulting augmented system matrix is formed by combining Equations (5.7) and (5.8) to obtain:

$$\begin{aligned}
\dot{x}_* &= \underbrace{\begin{bmatrix} \tilde{A} & 0 \\ -\tilde{C}_r & 0 \end{bmatrix}}_{A^*} \underbrace{\begin{bmatrix} x_a \\ x_{int} \end{bmatrix}}_{x^*} + \underbrace{\begin{bmatrix} \tilde{B} \\ 0 \end{bmatrix}}_{B^*} u(t) + \underbrace{\begin{bmatrix} 0 \\ I \end{bmatrix}}_{B_r^*} h_c(t) \\
y_s &= \underbrace{\begin{bmatrix} \tilde{C} & 0 \\ 0 & 1 \end{bmatrix}}_{C_s^*} \begin{bmatrix} x_a \\ x_{int} \end{bmatrix} \\
y_r &= \underbrace{\begin{bmatrix} C_r & 0 \end{bmatrix}}_{C_r^*} \begin{bmatrix} x_a \\ x_{int} \end{bmatrix}
\end{aligned} \tag{5.9}$$

where $y_s \triangleq [\bar{u} \ q \ h \ x_{int}]^T$ is the sensed output available for feedback. Since only $y_s(t)$ is available for feedback, first a state feedback controller is designed using LQR theory. The state feedback gain K_{x^*} is obtained with $\bar{Q} = \text{diag}(0, 0, 0, 1, 1, 0.01)$ and $R = 1e02 * \text{diag}([1/20, 1/100, 1/20])$.

$$K_{x^*} = \begin{bmatrix} -32.08 & 12.14 & -21.29 & -57.79 & -0.48 & 0.03 \\ -53.72 & 2.70 & -4.79 & -5.98 & -0.53 & 0.01 \\ 10.58 & -7.51 & 9.27 & 28.32 & 0.32 & -0.03 \end{bmatrix} \tag{5.10}$$

The nominal control design does not include a feedforward component, i.e $K_r = 0$. Therefore the nominal control input is given by:

$$u_n(t) = K_{x^*} \hat{x}^*(t) \tag{5.11}$$

The next step is to design an observer to estimate the states that are not available for feedback. The nominal observer is a Kalman filter designed using the loop transfer recovery (LTR) method [17] for the process given by

$$\begin{aligned}
\dot{x}_* &= A^* x^* + B^* u + B_r^* h_c + \Gamma_w \\
y_s &= C_s^* x^* + v
\end{aligned} \tag{5.12}$$

where Γ_w is given by

$$\Gamma_w = \rho^2(B^* + B^{*T}) \quad (5.13)$$

With the measurement noise matrix $R_v = \text{diag}([1, 1, .1, 1]) * 0.001$ and for $\rho = 0.01$, the resulting Kalman gain is:

$$L = \begin{bmatrix} 0.0131 & 0.0019 & -0.0440 & 0.0008 \\ 0.0019 & 0.0601 & -1.2634 & -0.0001 \\ 0.0033 & 0.0111 & 0.1104 & 0.0000 \\ 0.0024 & 0.0226 & 0.4786 & -0.0005 \\ -0.0044 & -0.1263 & 14.2060 & -0.0996 \\ 0.0008 & -0.0001 & -0.9960 & 0.3162 \end{bmatrix} \quad (5.14)$$

The observer dynamics for the system given in Equation (5.12) with PI control is given by

$$\dot{\hat{x}}^*(t) = A^* \hat{x}^*(t) + B^* u_n(t) + B_r^* r(t) + L(y_s(t) - \hat{y}_s(t)) \quad (5.15)$$

$$\hat{y}_s(t) = C_s^* \hat{x}^*(t) \quad (5.16)$$

A simulation is now carried out with the nominal controller using the stability derivative longitudinal model of the UAV. As observed from the Figure 26, the nominal controller provides adequate tracking with zero steady state error. Next the nominal controller is evaluated on the eight state model of the UAV. As observed from Figure 27, it is seen that the nominal control provides adequate tracking of commanded altitude. The transfer function of the elevator to altitude from the eight state model is given in Equations (5.17), (5.18) and (5.19) shows that the lateral directional modes are nearly canceled by zeros, this implies that there is little to no coupling between the longitudinal and lateral directional modes while tracking altitude commands.

$$\frac{H(s)}{\delta_e(s)} = \frac{N_{lon}(s)}{D_{lon}(s)} \times \frac{N_{lat}(s)}{D_{lat}(s)} \quad (5.17)$$

where

$$\frac{N_{lon}(s)}{D_{lon}(s)} = \frac{-0.32(s + 10.26)(s^2 + 0.47s + 0.08)}{s(s^2 + 0.11s + 0.09)(s^2 + 5.53s + 8.14)} \quad (5.18)$$

$$\frac{N_{lat}(s)}{D_{lat}(s)} = \frac{(s + 9.64)(s + 1.15)(s^2 + 0.24s + 0.02)}{(s + 9.64)(s + 1.15)(s^2 + 0.24s + 0.02)} \quad (5.19)$$

Finally, the performance of the nominal controller is evaluated on the forty four state UAV model. As observed from Figure 28, the nominal controller is unable to track the commanded altitude and actually goes unstable. This implies that the nominal controller is not robust to the unmodeled dynamics, i.e. the aero lag modes and flexible modes present in the forty four state model. The next step is to augment the nominal controller with the adaptive controller developed in Chapter 2 to improve the performance of the nominal controller in the presence of these unmodeled dynamics.

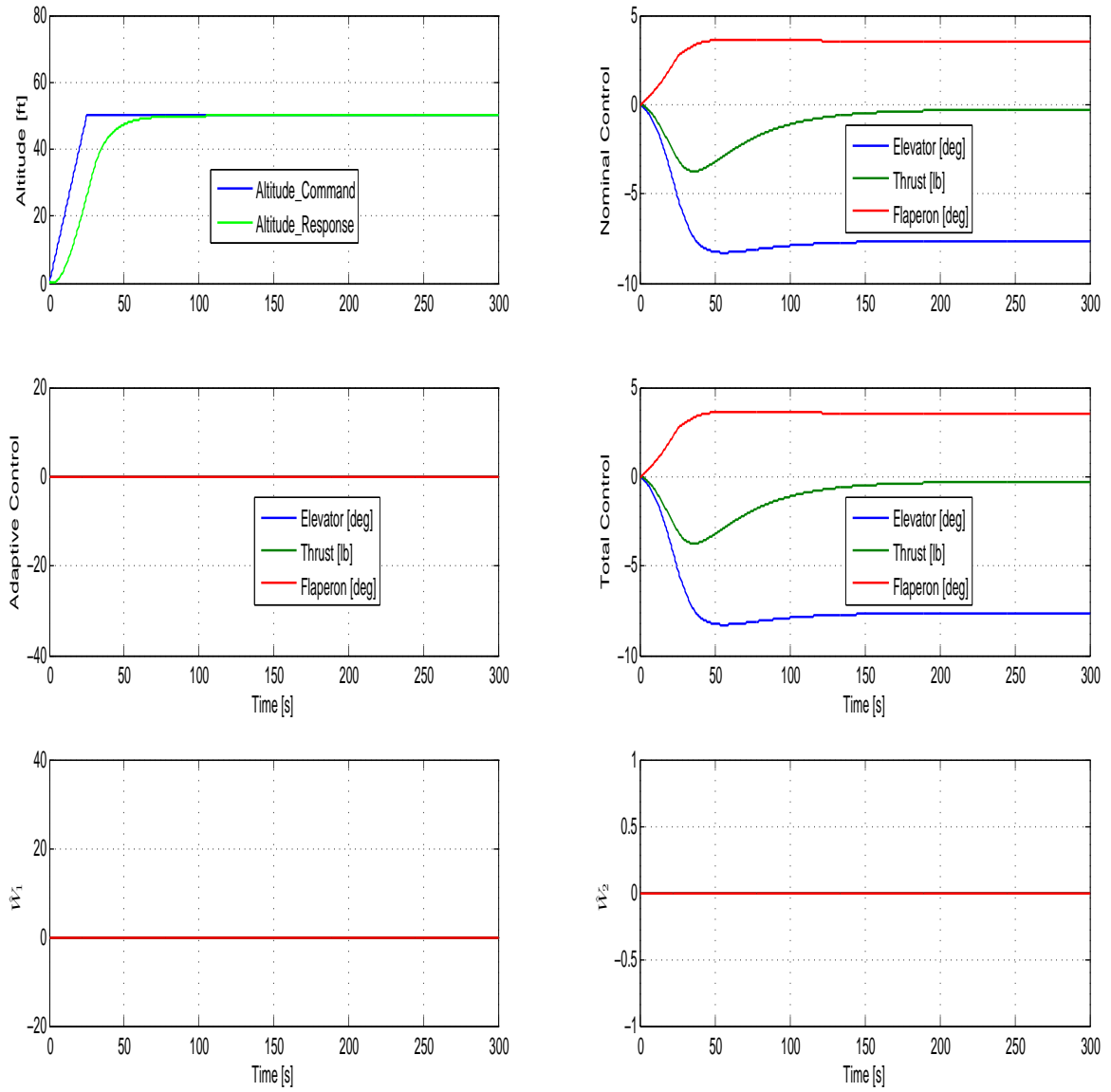


Figure 26: Response of the rigid stability derivative UAV model under nominal control.

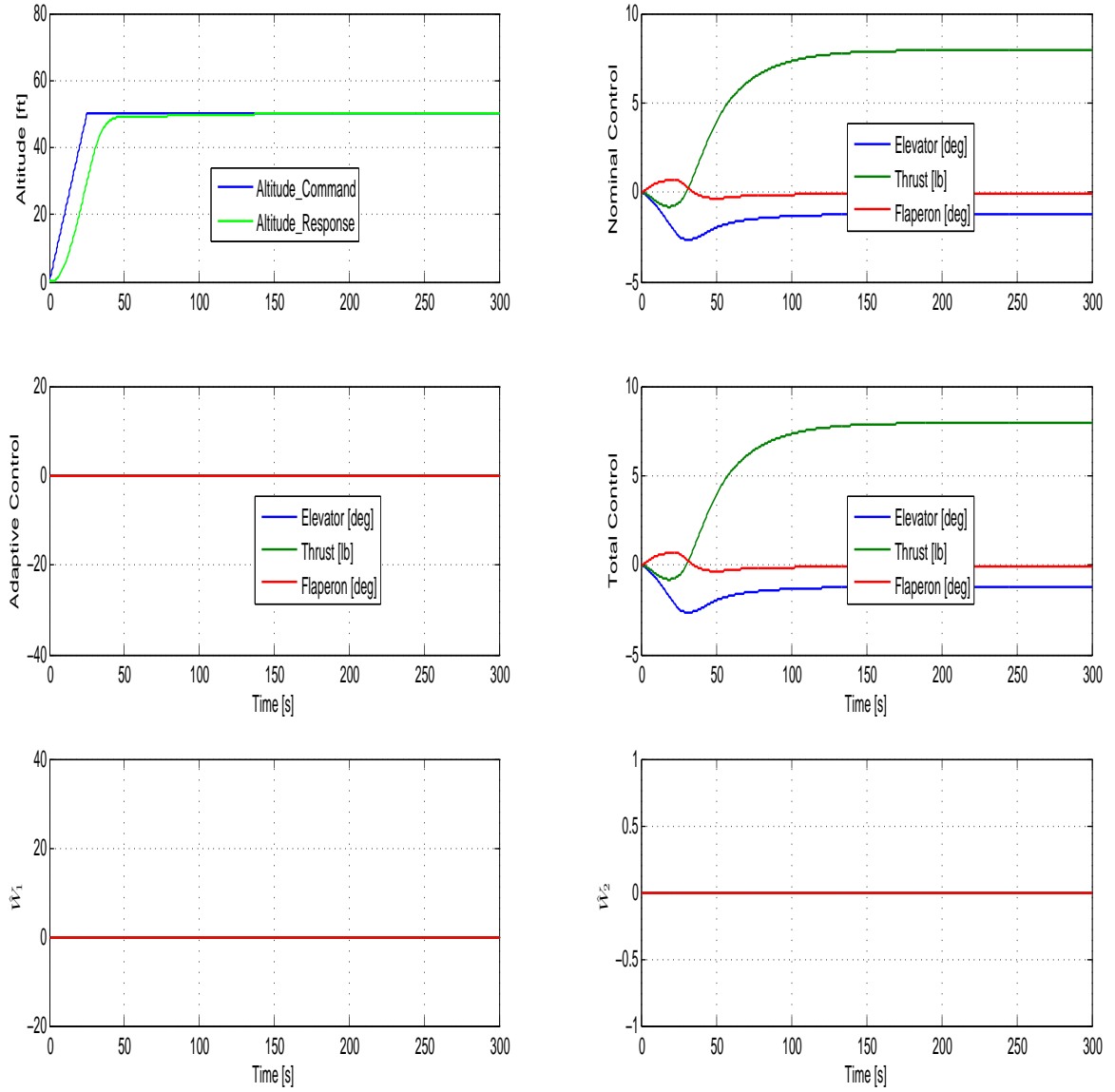


Figure 27: Response of the eight state UAV model under nominal control.

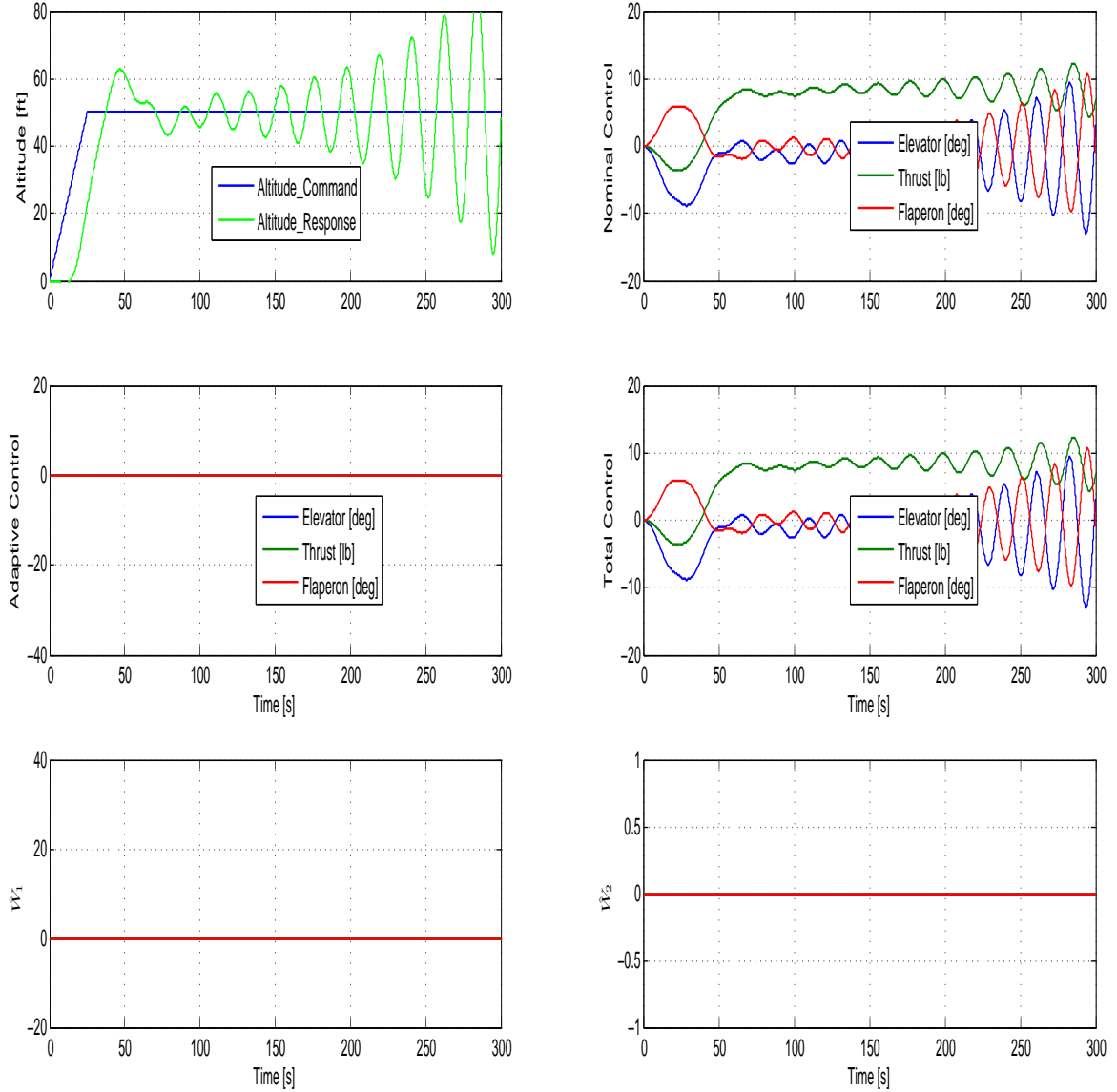


Figure 28: Response of the forty four state UAV model under nominal control.

5.4 Adaptive Control Design

An adaptive controller is developed using the method developed in Chapter 2 to augment the nominal control to improve robustness to the unmodeled flexible modes. Since there are forty five states in UAV model (44 states from the model augmented with the altitude state), $n - 1 = 44$ delayed values of the output, along with 41 delayed values of the inputs together with a bias are used with sigmoidal activation

function to form the basis vector. An activation potential of 0.5 for y and its delayed values and 2 for u and its delayed values are used. The activation potentials were chosen as before to be linear when signals are within their nominal ranges. Using Equation (2.29), the parameter $M = M_0$ is obtained as

$$M = \begin{bmatrix} 0.2472 & -0.0181 & 0.0190 & 0.0016 \\ -0.5874 & 0.0014 & -0.0053 & 0.0001 \\ -0.0289 & -0.7682 & 0.0347 & 0.0003 \end{bmatrix} \quad (5.20)$$

Using Potter's method, the resulting maximum allowable value for the parameter μ from Lemma 2.1 is $\bar{\mu} = 98.3$. Figure 29 shows that the system with adaptive augmentation using the weight update law given in Equation (2.31), with the adaptive control designed using $\gamma = 1000$, $\mu = 35$, $\sigma = 2.5 \times 10^{-5}$ and a delay of 0.004 seconds provides adequate tracking of commanded altitude in the presence of both the aero lag and flexible modes as opposed to the nominal control response seen in Figure 28 which goes unstable.

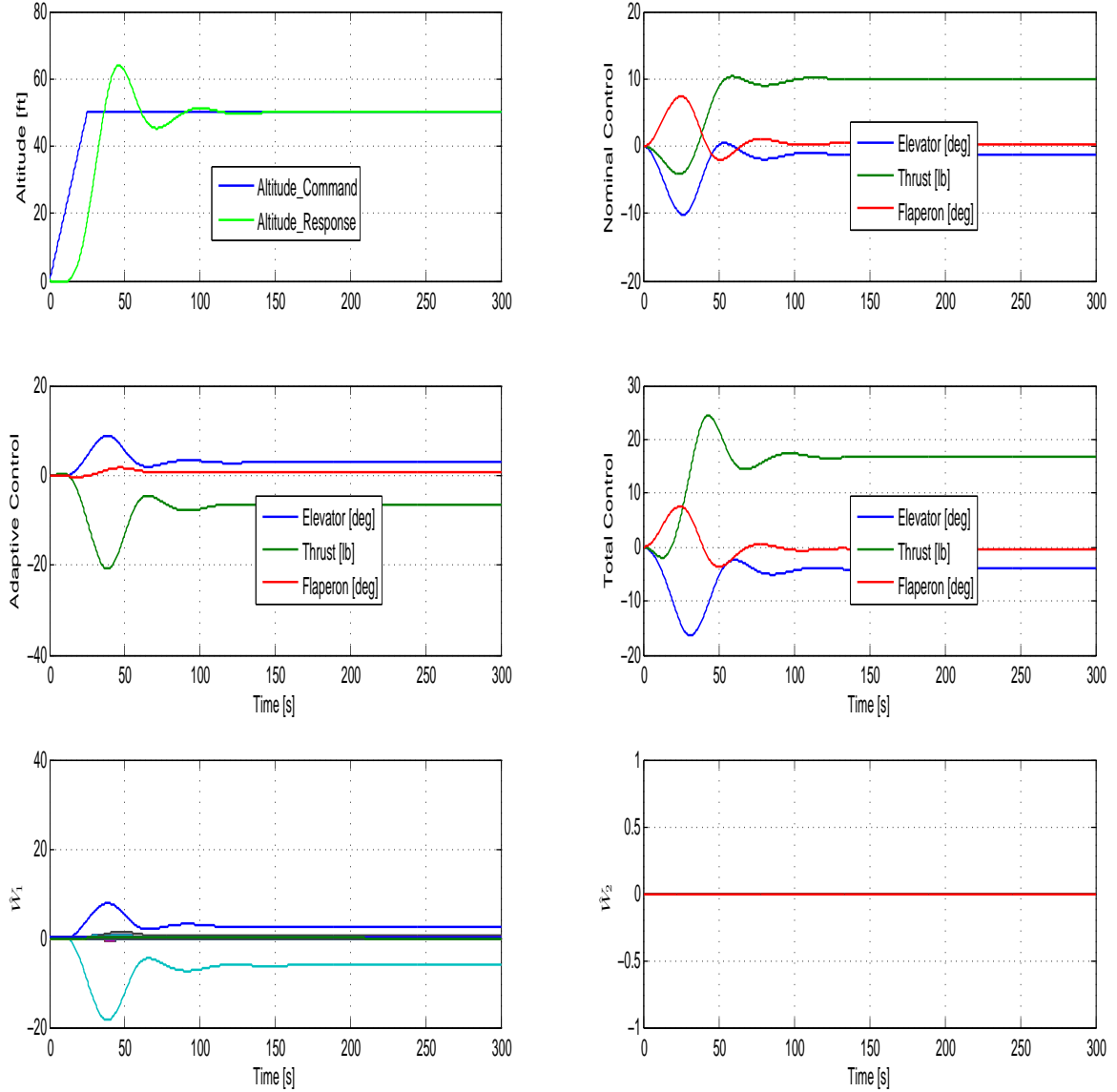


Figure 29: Response of the forty four state UAV model under adaptive control.

Next we consider the effect of noisy sensor measurements on the adaptive control designed above. Towards this end the measurements for $u(t)/U_0$ and $q(t)$ are corrupted with band limited white noise with a power spectral density of 1×10^{-3} . A simulation is first carried out with the adaptive control law used to obtain the results in Figure 29. Figure 30 shows that the weight histories and the adaptive portion of the control signal is extremely noisy.

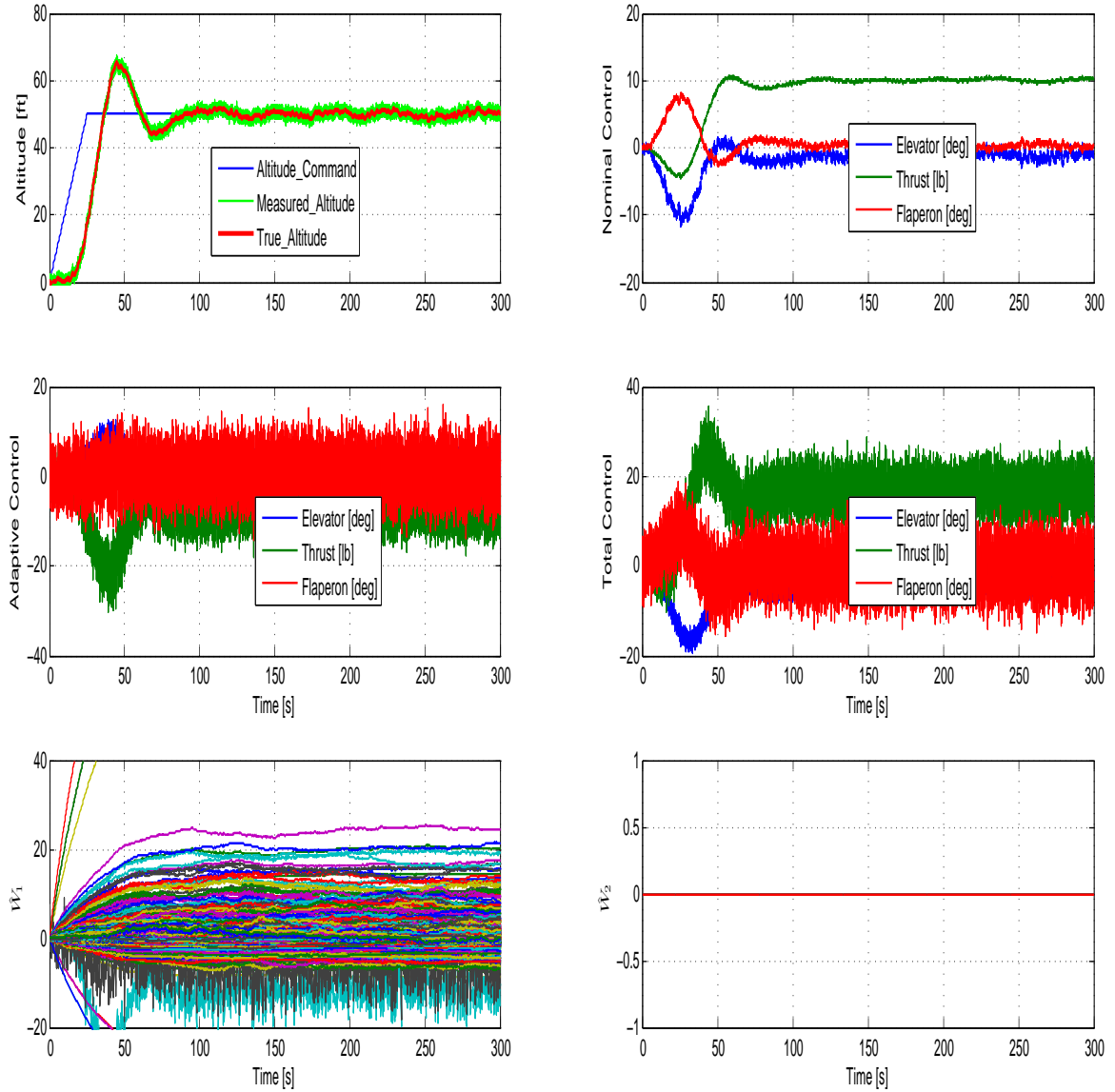


Figure 30: Response of the forty four state UAV model under adaptive control with noisy measurements.

Next we examine performance for the case where the weight update law given in Equation (3.1) is used to reduce the effect of sensor noise on adaptive control. The filtered error signal is obtained by passing the measured signals through a first order filter with a time constant of 0.1. As observed from Figure 31, the adaptive control using the filtered error signal in the weight update law provides tracking that is essentially the same as that shown in Figure 29 and the corresponding time histories

of the weights and the adaptive portion of the control are considerably less noisy.

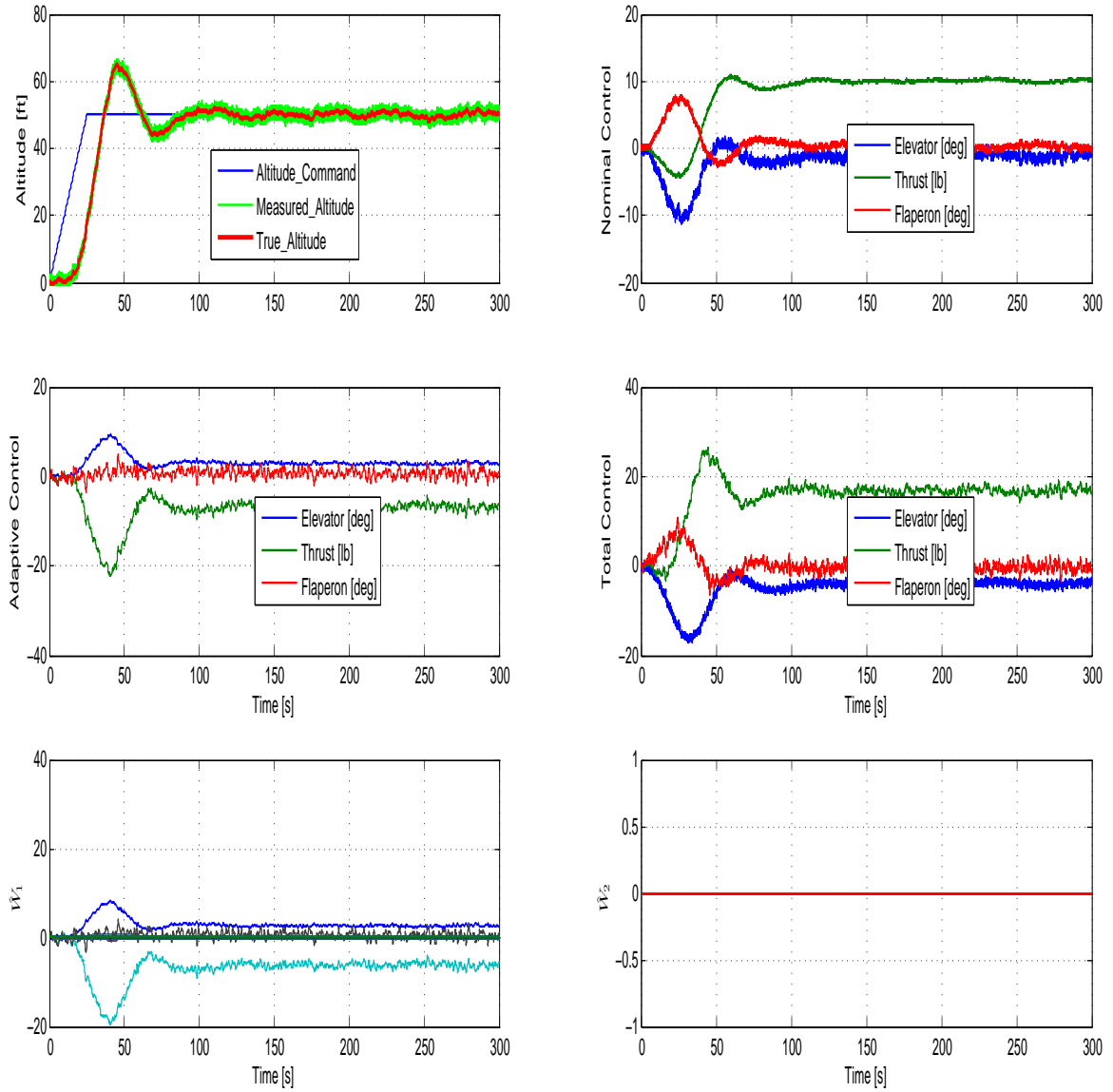


Figure 31: Response of the forty four state UAV model under adaptive control using filtered error signal in the adaptive law with noisy measurements.

5.5 Adaptive Control For Uncertain Control Effectiveness

In this section the performance of the adaptive control in the presence of uncertain control effectiveness is evaluated. Since $K_r = 0$, u_r is zero and hence the weight update law in Equation (4.20) is not used as part of the adaptive control design

process. Using the value of M in Equation (5.20) along with $\mu = 35$ the value of c in Equation (4.32) is 28.3 for $\bar{\Lambda} = 1.5$. This satisfies the condition that $c > 0$ as required by 4.3.1. As before $n_y = 44$ delayed values of y and $n_u = 43$ delayed values of u and \hat{x} together with a bias term are used to form the basis vector in Equation (4.19) with sigmoidal basis function. The activation potentials of the sigmoidal activation functions for y and u were chosen as in the previous section while the activation potential for \hat{x} is chosen as $1/50$. Figure 32 shows the resulting performance with an input uncertainty corresponding to $\Lambda = \text{diag}(1.5, 0.8, 1.3)$ using the weight update laws given by Equations (4.18),(4.19) with with $\gamma_{W_1} = 1000$, $\mu = 35$, $\sigma_{W_1} = 2.5 \times 10^{-5}$, $\gamma_{W_2} = 0$, $\sigma_{W_2} = 2.5 \times 10^{-5}$, $\gamma_d = 0$, $\sigma_{d_i} = 0$, and $d = 0.004$. Comparing this figure with the tracking performance in Figure 29, it is evident that with $\gamma_{W_2} = 0$ and $\gamma_d = 0$ the adaptive controller is robust to unmodeled flexible dynamics, but it is not robust to input uncertainty. Figure 33 shows the adaptive control result obtained for the same parameter settings and uncertainty set as in Figure 32, except that γ_d and γ_{W_2} are set to 0 and 10 respectively. This shows that the adaptive control provides adequate performance for both sources of uncertainty.

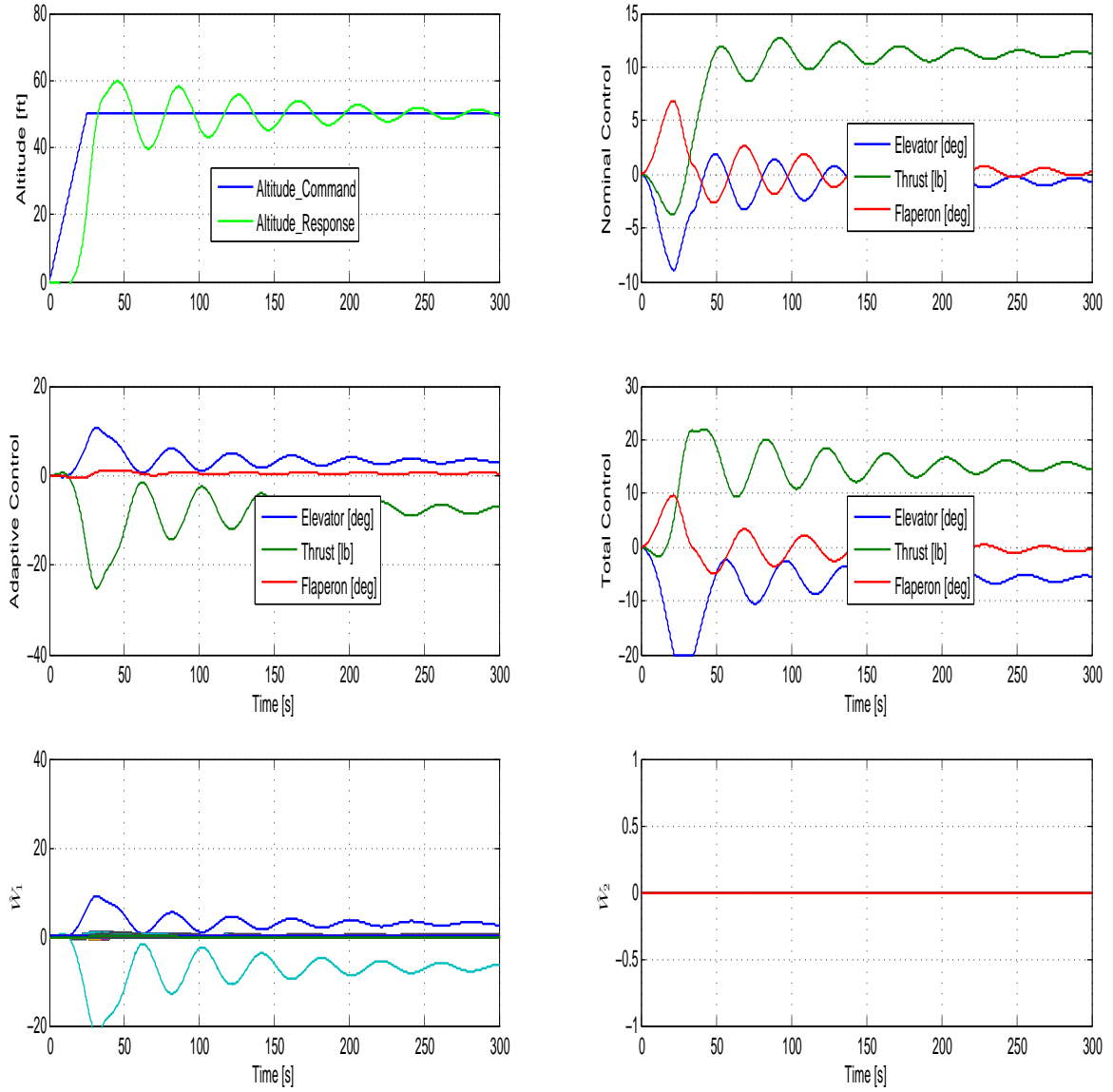


Figure 32: Response of the forty four state UAV model under adaptive control developed in Chapter 2 with input uncertainty.

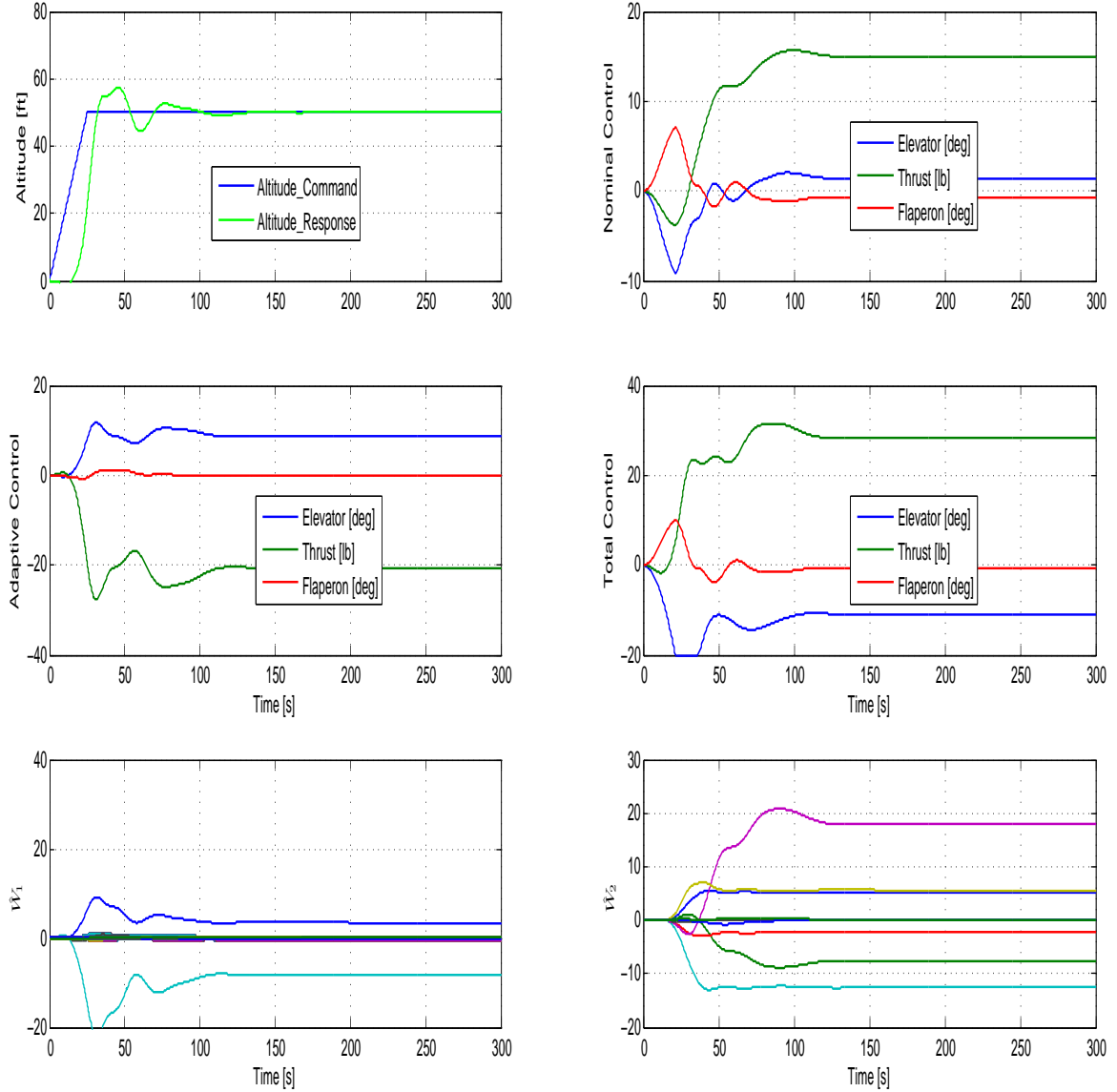


Figure 33: Response of the forty four state UAV model under adaptive control developed in Chapter 4 with Input Uncertainty.

Finally, the effect of sensor noise on the adaptive control is evaluated by corrupting the outputs with band limited white noise with spectral density of 1×10^{-7} . Figure 34 shows the effect of sensor noise in the presence of uncertain control effectiveness. As seen in Figure 34, the adaptive control signal is extremely noisy in the presence of sensor noise. Next the simulation is repeated with the filtered error signal being used in the weight update laws of Equation (4.18) and (4.19). As seen in Figure 35

the use of filtered error signal in the weigh update laws produces a response similar to that obtained in Figure 34 but with significantly less noisy weight and adaptive control time histories.

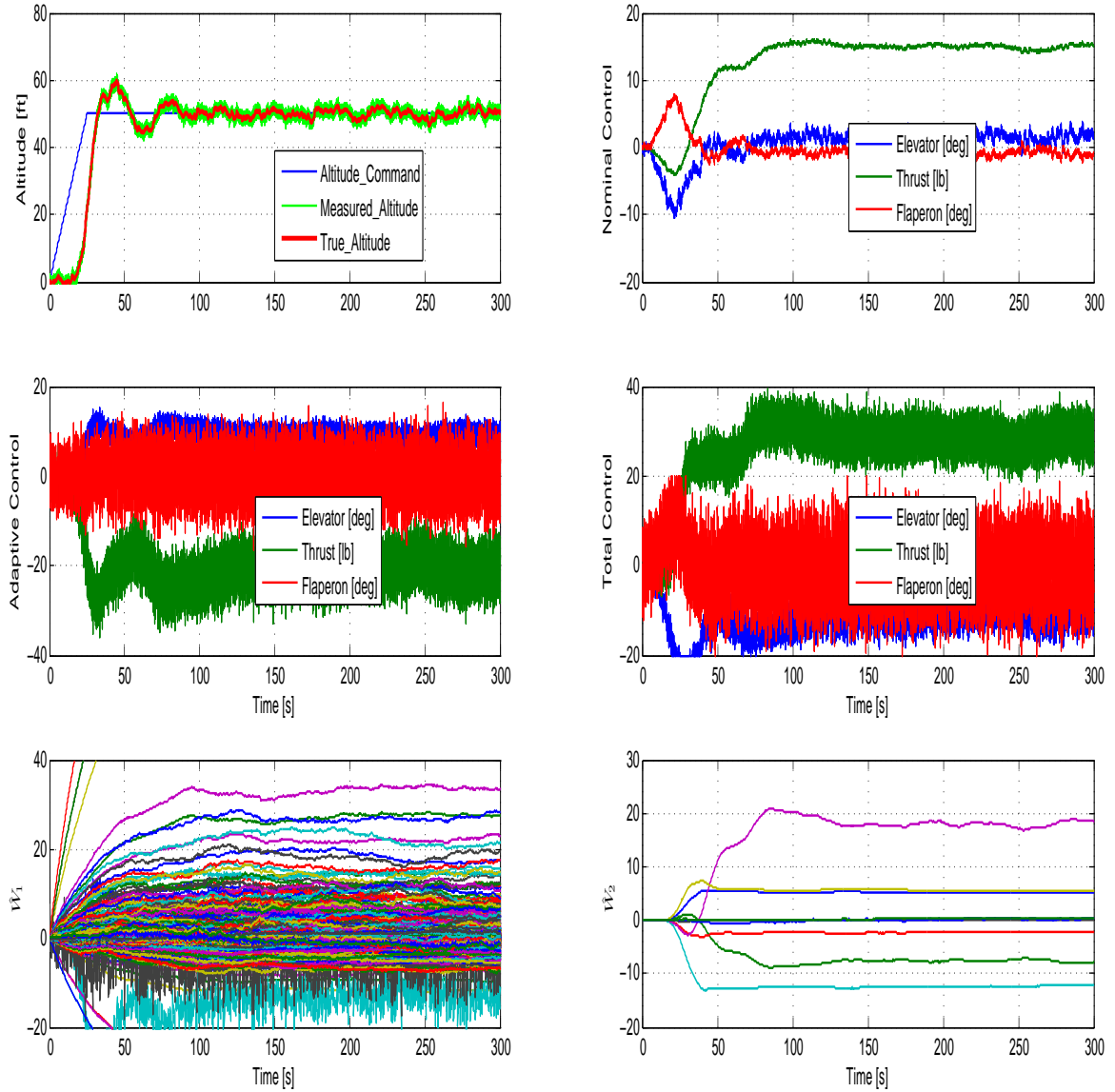


Figure 34: Response of the forty four state UAV model under adaptive control developed in Chapter 4 with noisy measurements.

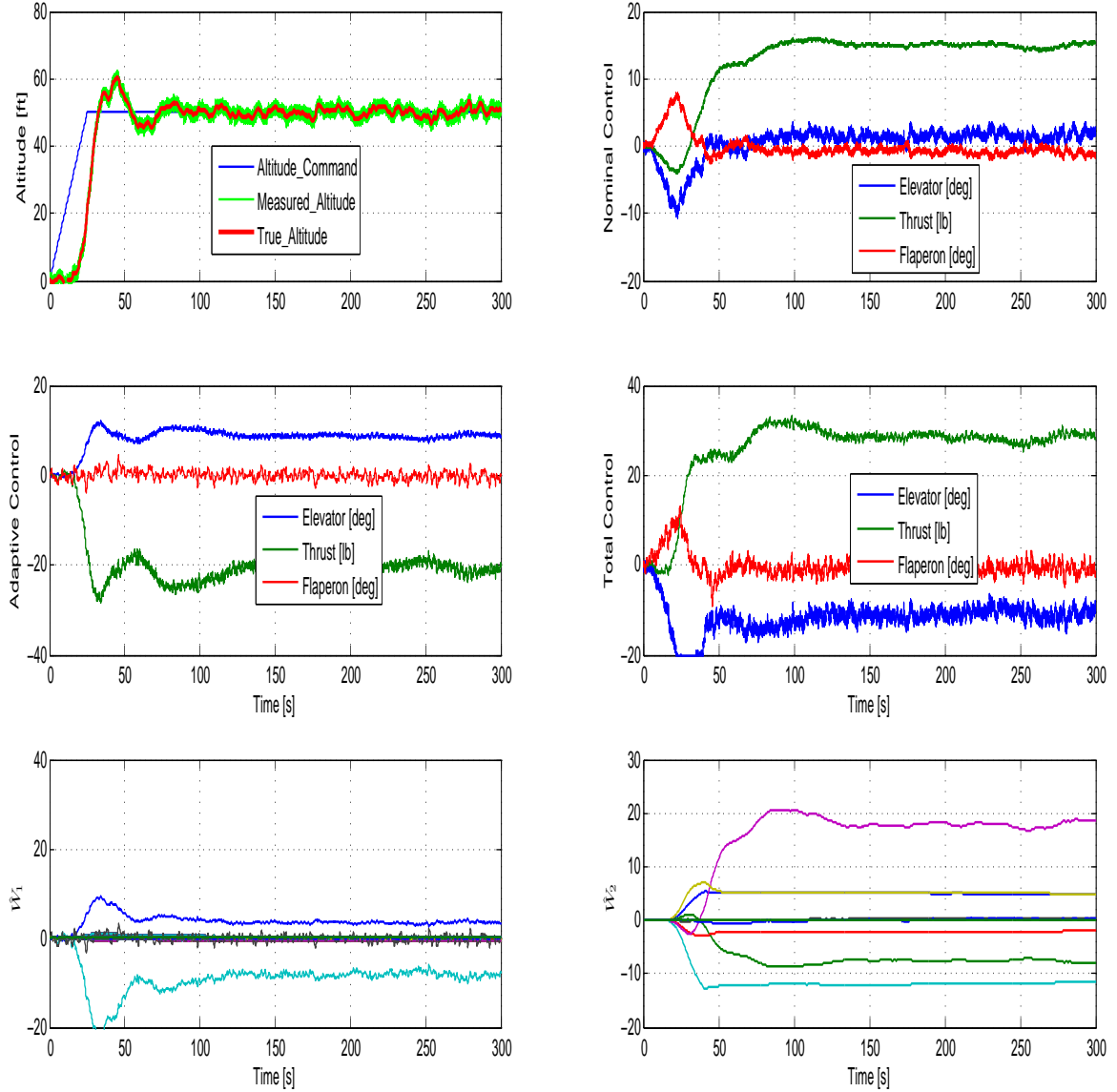


Figure 35: Response of the forty four state UAV model under adaptive control developed in Chapter 4 using filtered error signal with noisy measurements.

5.6 Conclusion

In this Chapter altitude control of a 44 state flexible UAV model is used to demonstrate the effectiveness of the methods for adaptive output feedback control design. An adaptive controller design that augments an observer based nominal controller with fixed gains is shown to be robust to unmodeled dynamics as well uncertain

control effectiveness. Adaptive control in the presence of noisy sensor signals is also considered by introducing noise on the measured outputs. The adaptive control approach uses the filtered error between the linear observer and the system output in the weight update law to reduce the effect of sensor noise propagating through the adaptive component of the control signal.

CHAPTER VI

SUMMARY AND FUTURE RESEARCH

In this thesis an output feedback adaptive controller design approach applicable to systems with matched uncertainty is presented. It is shown in Chapter 2 that the unique attributes of the proposed method are that it can be used to augment an existing linear controller without modifying the parameters of that controller, it is applicable to systems with unmodeled dynamics, it does not rely on the use of high gains neither in the adaptation law nor in the observer design, it is applicable to non-minimum phase systems and it does not require realization of a reference model. The stability properties of the adaptive system are established using a Lyapunov like stability analysis that relies on the existence of a positive definite solution of a parameter dependent Riccati equation. The effectiveness of the proposed approach are presented through simulations on a wing rock model appended with unmodeled dynamics, on attitude control of a flexible spacecraft with attitude feedback and altitude control of a flexible UAV model.

In Chapter 3 the effect of sensor noise in output feedback adaptive control is considered. Adaptive control theory provides a means for reducing the effects of modeling error but this comes at the cost of introducing a new pathway for sensor noise to enter the actuators, and therefore problems may arise with regard to actuator rate limits, energy consumption, and ultimately actuator failure. A simple but effective approach that filters the error signal in the weight update law of the adaptive control is employed. All the signals in the system are shown to be UUB using arguments from singular perturbation theory by treating the filter as a fast subsystem and the system dynamics together with weight update law as the slow system. Simulations on

the flexible spacecraft model corrupted with sensor noise are used to demonstrate the effectiveness of the proposed method in reducing the effect of sensor noise on adaptive control.

In Chapter 4, the approach is extended to systems with uncertainty in control effectiveness. A linear parameterization of the nominal control input is used to model uncertainty in control effectiveness. The adaptive control signal is composed of three different components. The first component is identical to that developed in Chapter 2. The other two components are based on the nominal control input and is shown to provide robustness to uncertain control effectiveness. Similar to what was done in Chapter 2, use of a filtered error signal in the weight update laws is shown to suppress the effect of sensor noise. Simulations on the flexible spacecraft model with uncertainty in control effectiveness and sensor noise are used to demonstrate the effectiveness of the method. As a variation on the nominal design employed in Chapter 2 for the example in this chapter, the underlying nominal control design is based on feedback inversion.

In Chapter 5, the adaptive controller developed in Chapters 2 to 4 is applied to the design of an altitude control of a forty four state flexible UAV model. The output feedback adaptive controller design that augments an observer based linear control design is shown to be robust to unmodeled dynamics as well uncertain control effectiveness. Adaptive control in the presence of noisy sensor signals is also considered by introducing noise on the measured outputs.

6.1 Future Research

Some of the areas that the adaptive control developed in this thesis can be extended are:

- 1) In this thesis we have considered only matched uncertainties. It would be of interest to extend the method to also account for unmatched uncertainties acting on

the system of the form

$$\begin{aligned}
\dot{x}(t) &= Ax(t) + B\Lambda [u(t) + G(x(t), x_d(t))] + G_u(x(t), x_d(t)), \\
y(t) &= Cx(t), \\
y_r(t) &= C_r x(t), \\
\dot{x}_d &= f_d(x(t), x_d(t))
\end{aligned} \tag{6.1}$$

2) In this thesis an output feedback adaptive control has been designed for systems with unmodeled dynamics wherein the output available for feedback is not dependent on the unmodeled dynamics. Another important area of extension would be to consider systems in which the outputs are corrupted by the unmodeled dynamics, i.e.

$$\begin{aligned}
\dot{x}(t) &= Ax(t) + B\Lambda [u(t) + G(x(t), x_d(t))], \\
y(t) &= Cx(t) + H(x(t), x_d(t)), \\
y_r(t) &= C_r x(t), \\
\dot{x}_d &= f_d(x(t), x_d(t))
\end{aligned} \tag{6.2}$$

3) In this thesis an output feedback adaptive controller is considered for systems with unmodeled dynamics wherein the unmodeled dynamics do not explicitly depend on the control input u . Extending the method to systems where the unmodeled dynamics depends on the control input u as considered in Ref. [15] is an area of worthy research.

4) Recent research has focused on improving transient response of systems under adaptive control [24, 25, 26, 27, 28]. The use of closed loop reference model as opposed to open loop response model has shown to provide stability and improved transient response of systems under adaptive control. This thesis has focussed on proving UUB of all the signals in the loop using a Lyapunov like stability analysis. It is of interest to extend the method presented to improve transient response. This extension will be based on the work done by Travis et al. [25] wherein the use of projection algorithm

along with the closed loop reference model adaptive controllers can be designed to be stable and have improved transient properties.

5) In this thesis output feedback adaptive control has been developed for systems with unmodeled dynamics. An area of recent research has been on designing adaptive controllers that have guaranteed performance in the presence of time delays which is inherently present in closed loop control implementations. Recent advances in adaptive control design have been shown to provide global boundedness of the overall adaptive system for a range of delays [1, 57, 58, 59]. An extension of the method presented in this thesis to account for time delays is an area of future research. This extension will be based on the research by Annaswamy et al. [1] wherein the authors develop three different approaches to improve robustness for the presence of time delays. It is of interest to consider the use of direct adaptive posicast controller along with the methodology developed in this thesis to deal with large system delays.

6) An alternative is to extend the approach in [8] where in a new modification term was developed for adaptive control that preserves the loop transfer properties of the reference model associated with the non-adaptive control for the case when only a subset of the states are available for feedback and in the presence of unmodeled dynamics. In this way the gain and phase margins (and time delay margin) of the nominal control design are preserved when augmented with an adaptive element. Flight test results can be found in Ref.[14].

7) In this thesis a linear parametrization was assumed to model the uncertainty acting on the system. Extending the method developed in this thesis to employ a nonlinear parameterizations to model the uncertainty, such as the form employed in [5], is an area worthy of further research.

8) Another area of research is to consider systems of the form

$$\begin{aligned}\dot{x}(t) &= Ax(t) + B\Lambda [(1 + \Delta(s))u(t)], \\ y(t) &= Cx(t), \\ y_r(t) &= C_r x(t)\end{aligned}\tag{6.3}$$

where $\Delta(s)$ represents the unmodeled dynamics such as actuators, filters acting on the system.

APPENDIX A

FLEXIBLE UAV MODEL

This appendix contains the different forms of the flexible UAV model used in the thesis to design and evaluate the different adaptive control laws presented in the thesis.

A.1 The Four State Longitudinal Model

The 4 state longitudinal model constructed using stability derivative data obtained from the rigidized flexible model of the UAV are given below

$$A = \begin{bmatrix} -0.0059 & 0.5280 & 0.1389 & -0.5529 \\ -0.9219 & -2.9445 & -0.0990 & -0.0091 \\ 0.0668 & -1.2083 & -2.7510 & 0 \\ 0 & 0 & 1 & 0 \end{bmatrix} \quad (\text{A.1})$$

$$B = \begin{bmatrix} -0.0001 & -0.0005 & -0.0001 \\ -0.0011 & 0 & -0.0229 \\ -0.0190 & -0.0001 & -0.0049 \\ 0 & 0 & 0 \end{bmatrix} \quad (\text{A.2})$$

$$C = \begin{bmatrix} 1 & 0 & 0 & 0 \\ 0 & 0 & 1 & 0 \end{bmatrix} \quad (\text{A.3})$$

where the states are $x = [u/u_0 \ \alpha \ q \ \theta]^T$, control inputs are $u = [\delta_e \ \delta_T \ \delta_f]^T$ and the outputs are $y = [u/u_0 \ q]^T$.

A.2 The Eight State Model

The eight state model after transformation to real form and augmented with the altitude state is given by:

$$A = \begin{bmatrix} A_1 & 0 & 0 \\ 0 & A_2 & 0 \\ A_{31} & A_{32} & 0 \end{bmatrix}$$

$$B = \begin{bmatrix} B_1 \\ B_2 \\ B_3 \end{bmatrix} \quad (\text{A.4})$$

$$C = \begin{bmatrix} C_1 & C_2 & C_3 \end{bmatrix} \quad (\text{A.5})$$

$$D = \begin{bmatrix} 0 & 0 & 0 \\ 0 & 0 & 0 \\ 0 & 0 & 0 \end{bmatrix} \quad (\text{A.6})$$

where

$$A_1 = \begin{bmatrix} -1.21e-01 & 5.87e-02 & 0.00e+00 & 0.00e+00 \\ -5.87e-02 & -1.21e-01 & 0.00e+00 & 0.00e+00 \\ 0.00e+00 & 0.00e+00 & -5.76e-02 & 2.98e-01 \\ 0.00e+00 & 0.00e+00 & -2.98e-01 & -5.76e-02 \end{bmatrix} \quad (\text{A.7})$$

$$A_2 = \begin{bmatrix} -1.15e+00 & 0.00e+00 & 0.00e+00 & 0.00e+00 \\ 0.00e+00 & -2.76e+00 & 7.04e-01 & 0.00e+00 \\ 0.00e+00 & -7.04e-01 & -2.76e+00 & 0.00e+00 \\ 0.00e+00 & 0.00e+00 & 0.00e+00 & -9.64e+00 \end{bmatrix} \quad (\text{A.8})$$

$$A_{31} = \begin{bmatrix} 9.54e-07 & -1.08e-06 & -4.16e-04 & -5.62e-04 \end{bmatrix} \quad (\text{A.9})$$

$$A_{32} = \begin{bmatrix} -1.19e-06 & -4.39e-05 & -1.08e-03 & -1.56e-06 \end{bmatrix} \quad (\text{A.10})$$

with

$$B_1 = \begin{bmatrix} -7.24e-02 & 2.14e-03 & 4.96e-03 \\ -1.11e-02 & -4.90e-04 & 9.63e-03 \\ 1.56e+02 & -4.04e+00 & 1.06e+01 \\ 1.61e+02 & 7.58e+00 & -9.48e+01 \end{bmatrix} \quad (\text{A.11})$$

$$B_2 = \begin{bmatrix} -1.70e-03 & 1.05e-03 & -1.37e-02 \\ -2.79e+03 & -7.73e+01 & -5.24e+02 \\ 2.70e+02 & 3.11e+01 & -3.40e+03 \\ -1.60e-01 & -2.17e-03 & 1.19e-01 \end{bmatrix} \quad (\text{A.12})$$

$$B_3 = \begin{bmatrix} 0.00e+00 & 0.00e+00 & 0.00e+00 \end{bmatrix} \quad (\text{A.13})$$

and

$$C_1 = \begin{bmatrix} -1.88e-07 & -8.17e-07 & -5.08e-05 & -3.46e-05 \\ 1.32e-11 & -2.90e-10 & -1.54e-07 & -7.44e-08 \\ 0.00e+00 & 0.00e+00 & 0.00e+00 & 0.00e+00 \end{bmatrix} \quad (\text{A.14})$$

$$C_2 = \begin{bmatrix} 8.99e-09 & 7.69e-07 & 1.33e-06 & 2.27e-09 \\ -2.21e-10 & 1.18e-07 & 3.02e-08 & 1.51e-10 \\ 0.00e+00 & 0.00e+00 & 0.00e+00 & 0.00e+00 \end{bmatrix} \quad (\text{A.15})$$

$$C_3 = \begin{bmatrix} 0.00e+00 \\ 0.00e+00 \\ 1.00e+00 \end{bmatrix} \quad (\text{A.16})$$

A.3 The Forty Four State Model

The forty four state model after transformation to real form and augmented with the altitude state is given by:

$$A = \begin{bmatrix} A_1 & 0 & 0 & 0 & 0 & 0 & 0 & 0 & 0 \\ 0 & A_2 & 0 & 0 & 0 & 0 & 0 & 0 & 0 \\ 0 & 0 & A_3 & 0 & 0 & 0 & 0 & 0 & 0 \\ 0 & 0 & 0 & A_4 & 0 & 0 & 0 & 0 & 0 \\ 0 & 0 & 0 & 0 & A_5 & 0 & 0 & 0 & 0 \\ 0 & 0 & 0 & 0 & 0 & A_6 & 0 & 0 & 0 \\ 0 & 0 & 0 & 0 & 0 & 0 & A_7 & 0 & 0 \\ 0 & 0 & 0 & 0 & 0 & 0 & 0 & A_8 & 0 \\ A_{91} & A_{92} & A_{93} & A_{94} & A_{95} & A_{96} & A_{97} & A_{98} & 0 \end{bmatrix} \quad (\text{A.17})$$

$$B = \begin{bmatrix} B_1 \\ B_2 \\ B_3 \\ B_4 \\ B_5 \\ B_6 \\ B_7 \\ B_8 \\ B_9 \end{bmatrix} \quad (\text{A.18})$$

$$C = \begin{bmatrix} C_1 & C_2 & C_3 & C_4 & C_5 & C_6 & C_7 & C_8 & C_9 \end{bmatrix} \quad (\text{A.19})$$

$$D = \begin{bmatrix} 0 & 0 & 0 \\ 0 & 0 & 0 \\ 0 & 0 & 0 \end{bmatrix} \quad (\text{A.20})$$

where

$$\begin{aligned}
 A_1 &= \begin{bmatrix} -1.15e-01 & -7.67e-02 & 0.00e+00 & 0.00e+00 & 0.00e+00 & 0.00e+00 \\ 7.67e-02 & -1.15e-01 & 0.00e+00 & 0.00e+00 & 0.00e+00 & 0.00e+00 \\ 0.00e+00 & 0.00e+00 & -6.17e-02 & -2.91e-01 & 0.00e+00 & 0.00e+00 \\ 0.00e+00 & 0.00e+00 & 2.91e-01 & -6.17e-02 & 0.00e+00 & 0.00e+00 \\ 0.00e+00 & 0.00e+00 & 0.00e+00 & 0.00e+00 & -1.30e+00 & 0.00e+00 \\ 0.00e+00 & 0.00e+00 & 0.00e+00 & 0.00e+00 & 0.00e+00 & -1.94e+00 \end{bmatrix} \\
 A_2 &= \begin{bmatrix} -1.94e+00 & 0.00e+00 & 0.00e+00 & 0.00e+00 & 0.00e+00 & 0.00e+00 \\ 0.00e+00 & -2.52e+00 & 5.57e-01 & 0.00e+00 & 0.00e+00 & 0.00e+00 \\ 0.00e+00 & -5.57e-01 & -2.52e+00 & 0.00e+00 & 0.00e+00 & 0.00e+00 \\ 0.00e+00 & 0.00e+00 & 0.00e+00 & -3.34e+00 & 0.00e+00 & 0.00e+00 \\ 0.00e+00 & 0.00e+00 & 0.00e+00 & 0.00e+00 & -3.99e+00 & 0.00e+00 \\ 0.00e+00 & 0.00e+00 & 0.00e+00 & 0.00e+00 & 0.00e+00 & -4.52e+00 \end{bmatrix} \\
 A_3 &= \begin{bmatrix} -5.19e+00 & 0.00e+00 & 0.00e+00 & 0.00e+00 & 0.00e+00 & 0.00e+00 \\ 0.00e+00 & -5.56e+00 & 0.00e+00 & 0.00e+00 & 0.00e+00 & 0.00e+00 \\ 0.00e+00 & 0.00e+00 & -5.89e+00 & 0.00e+00 & 0.00e+00 & 0.00e+00 \\ 0.00e+00 & 0.00e+00 & 0.00e+00 & -6.37e+00 & 0.00e+00 & 0.00e+00 \\ 0.00e+00 & 0.00e+00 & 0.00e+00 & 0.00e+00 & -6.53e+00 & 0.00e+00 \\ 0.00e+00 & 0.00e+00 & 0.00e+00 & 0.00e+00 & 0.00e+00 & -4.59e+00 \end{bmatrix} \\
 A_5 &= \begin{bmatrix} -4.59e+00 & 0.00e+00 & 0.00e+00 & 0.00e+00 & 0.00e+00 & 0.00e+00 \\ 0.00e+00 & -6.88e+00 & 0.00e+00 & 0.00e+00 & 0.00e+00 & 0.00e+00 \\ 0.00e+00 & 0.00e+00 & -7.46e+00 & 0.00e+00 & 0.00e+00 & 0.00e+00 \\ 0.00e+00 & 0.00e+00 & 0.00e+00 & -7.87e+00 & 0.00e+00 & 0.00e+00 \\ 0.00e+00 & 0.00e+00 & 0.00e+00 & 0.00e+00 & -8.15e+00 & 0.00e+00 \\ 0.00e+00 & 0.00e+00 & 0.00e+00 & 0.00e+00 & 0.00e+00 & -7.97e-01 \end{bmatrix}
 \end{aligned}$$

$$\begin{aligned}
A_6 &= \begin{bmatrix} -9.06e+00 & 0.00e+00 & 0.00e+00 & 0.00e+00 & 0.00e+00 & 0.00e+00 \\ 0.00e+00 & -9.41e+00 & 0.00e+00 & 0.00e+00 & 0.00e+00 & 0.00e+00 \\ 0.00e+00 & 0.00e+00 & -9.90e+00 & 0.00e+00 & 0.00e+00 & 0.00e+00 \\ 0.00e+00 & 0.00e+00 & 0.00e+00 & -1.01e+01 & 0.00e+00 & 0.00e+00 \\ 0.00e+00 & 0.00e+00 & 0.00e+00 & 0.00e+00 & -1.04e+01 & 0.00e+00 \\ 0.00e+00 & 0.00e+00 & 0.00e+00 & 0.00e+00 & 0.00e+00 & -1.05e+01 \end{bmatrix} \\
A_7 &= \begin{bmatrix} -1.08e+01 & 0.00e+00 & 0.00e+00 & 0.00e+00 & 0.00e+00 & 0.00e+00 \\ 0.00e+00 & -3.34e-01 & 1.09e+01 & 0.00e+00 & 0.00e+00 & 0.00e+00 \\ 0.00e+00 & -1.09e+01 & -3.34e-01 & 0.00e+00 & 0.00e+00 & 0.00e+00 \\ 0.00e+00 & 0.00e+00 & 0.00e+00 & -1.11e+01 & 0.00e+00 & 0.00e+00 \\ 0.00e+00 & 0.00e+00 & 0.00e+00 & 0.00e+00 & -1.12e+01 & 0.00e+00 \\ 0.00e+00 & 0.00e+00 & 0.00e+00 & 0.00e+00 & 0.00e+00 & -1.14e+01 \end{bmatrix} \\
A_8 &= \begin{bmatrix} -3.99e+00 & 1.08e+01 \\ -1.08e+01 & -3.99e+00 \end{bmatrix} \\
A_{91} &= \begin{bmatrix} -2.09e-06 & -5.69e-07 & -6.68e-04 & -4.08e-06 & -1.03e-06 & -7.91e-04 \end{bmatrix} \\
A_{92} &= \begin{bmatrix} -9.59e-04 & 4.47e-04 & -8.35e-04 & -4.02e-05 & -2.59e-03 & 5.44e-05 \end{bmatrix} \\
A_{93} &= \begin{bmatrix} 6.36e-03 & 5.33e-04 & 6.86e-03 & 5.89e-03 & 3.22e-03 & -2.28e-06 \end{bmatrix} \\
A_{94} &= \begin{bmatrix} -3.18e-06 & 5.31e-03 & 7.64e-04 & -4.55e-03 & -5.01e-04 & 5.16e-07 \end{bmatrix} \\
A_{95} &= \begin{bmatrix} -1.20e-07 & 1.66e-03 & 1.29e-06 & 2.12e-06 & -3.87e-04 & -2.80e-04 \end{bmatrix} \\
A_{96} &= \begin{bmatrix} 2.80e-04 & -8.66e-04 & 2.07e-04 & -3.40e-04 & 4.15e-05 & -4.61e-06 \end{bmatrix} \\
A_{97} &= \begin{bmatrix} -9.01e-06 & 2.32e-04 & -2.55e-04 & -8.65e-04 & 3.80e-05 & 6.18e-04 \end{bmatrix} \\
A_{98} &= \begin{bmatrix} -1.29e-03 & 6.52e-04 \end{bmatrix}
\end{aligned}$$

$$\begin{aligned}
B_1 &= \begin{bmatrix} 2.31e-02 & -1.34e-03 & -1.73e-03 \\ 1.19e-02 & -1.41e-03 & 7.48e-03 \\ -3.82e+01 & -8.71e+00 & 6.49e+01 \\ -2.25e+02 & -9.43e-01 & 2.04e+00 \\ -2.04e-02 & 1.73e-05 & -3.25e-02 \\ -1.59e+03 & -2.64e+01 & -3.18e+03 \end{bmatrix} \\
B_2 &= \begin{bmatrix} -3.96e+02 & 8.77e+00 & -1.40e+03 \\ 1.34e+03 & 2.60e+01 & 1.14e+03 \\ -4.25e+02 & -9.79e+00 & 5.56e+02 \\ -3.71e-02 & -6.17e-04 & -4.18e-02 \\ 2.55e+00 & 4.92e-01 & 5.19e+01 \\ -1.62e-02 & -1.21e-04 & -6.59e-03 \end{bmatrix} \\
B_3 &= \begin{bmatrix} 2.31e+01 & 9.14e-01 & -2.09e+01 \\ -4.01e-02 & -7.22e-04 & 5.20e-03 \\ -5.42e+01 & -1.54e+00 & 5.69e+01 \\ -1.53e+02 & 2.52e-01 & -1.52e+02 \\ 1.53e-01 & -2.51e-04 & 1.50e-01 \\ 4.15e-01 & 3.08e-03 & 5.69e-01 \end{bmatrix} \\
B_4 &= \begin{bmatrix} -8.01e-02 & -5.87e-04 & 2.36e-01 \\ 7.67e+00 & -4.64e-01 & 5.35e+01 \\ -4.92e-03 & -8.07e-06 & 9.11e-04 \\ 1.93e-01 & -1.12e-01 & 1.52e+01 \\ -1.07e-02 & 3.46e-05 & -9.75e-03 \\ -1.16e+00 & -3.06e-03 & -5.12e-01 \end{bmatrix}
\end{aligned}$$

$$\begin{aligned}
B_5 &= \begin{bmatrix} 7.64e-01 & -4.64e-02 & -2.26e-03 \\ 3.34e-02 & -1.04e-01 & 1.66e+01 \\ 1.03e-01 & -1.35e-03 & 5.83e-01 \\ -4.76e-02 & -2.36e-03 & -1.93e-01 \\ 2.97e+01 & 6.38e+00 & 4.00e+02 \\ 1.37e+01 & -1.22e+01 & 2.31e+03 \end{bmatrix} \\
B_6 &= \begin{bmatrix} -1.10e-03 & 6.05e-06 & 2.25e-03 \\ -5.62e-02 & -8.50e-02 & 1.52e+01 \\ 4.45e-03 & -5.72e-06 & -2.82e-04 \\ 3.22e-02 & 5.87e-02 & -1.18e+01 \\ 1.73e-03 & 5.80e-05 & 2.37e-03 \\ -8.68e-02 & 3.25e-03 & -7.94e-01 \end{bmatrix} \\
B_7 &= \begin{bmatrix} -1.88e-01 & -1.18e-02 & 2.57e+00 \\ -1.06e+00 & 8.40e+00 & 1.34e+02 \\ 5.32e+02 & -1.69e+02 & 1.13e+03 \\ -4.33e-02 & -5.02e-02 & 1.17e+01 \\ 1.63e-03 & -2.35e-05 & 2.57e-03 \\ -3.25e-02 & -6.09e-02 & 1.49e+01 \end{bmatrix} \\
B_8 &= \begin{bmatrix} -9.07e+01 & 4.76e+00 & -4.88e+02 \\ -4.17e+01 & -1.42e+01 & 2.44e+03 \end{bmatrix} \\
B_9 &= \begin{bmatrix} 0.00e+00 & 0.00e+00 & 0.00e+00 \end{bmatrix}
\end{aligned}$$

$$\begin{aligned}
C_1 &= \begin{bmatrix} -4.08e-07 & -8.97e-07 & -5.73e-05 & -2.23e-05 & 9.20e-09 & 1.35e-06 \\ -2.48e-10 & -3.36e-10 & -1.41e-07 & -7.77e-08 & -3.32e-10 & 3.09e-09 \\ 0.00e+00 & 0.00e+00 & 0.00e+00 & 0.00e+00 & 0.00e+00 & 0.00e+00 \end{bmatrix} \\
C_2 &= \begin{bmatrix} 3.30e-06 & -2.93e-06 & 2.15e-06 & 1.87e-07 & 9.42e-06 & -1.74e-07 \\ 1.17e-07 & -3.66e-07 & -6.74e-08 & 2.16e-08 & 8.91e-07 & -1.47e-08 \\ 0.00e+00 & 0.00e+00 & 0.00e+00 & 0.00e+00 & 0.00e+00 & 0.00e+00 \end{bmatrix} \\
C_3 &= \begin{bmatrix} -1.78e-05 & -1.41e-06 & -1.73e-05 & -1.38e-05 & -7.35e-06 & -6.01e-10 \\ -1.42e-06 & -1.12e-07 & -1.37e-06 & -1.08e-06 & -5.73e-07 & -6.46e-11 \\ 0.00e+00 & 0.00e+00 & 0.00e+00 & 0.00e+00 & 0.00e+00 & 0.00e+00 \end{bmatrix} \\
C_4 &= \begin{bmatrix} 9.73e-09 & -1.16e-05 & -1.52e-06 & 7.30e-06 & 8.99e-07 & -2.31e-10 \\ 6.62e-10 & -9.16e-07 & -1.20e-07 & 6.00e-07 & 7.21e-08 & -1.85e-11 \\ 0.00e+00 & 0.00e+00 & 0.00e+00 & 0.00e+00 & 0.00e+00 & 0.00e+00 \end{bmatrix} \\
C_5 &= \begin{bmatrix} -1.40e-09 & -2.78e-06 & 1.78e-10 & -3.54e-09 & 2.48e-07 & -2.07e-07 \\ -7.42e-11 & -2.31e-07 & 4.38e-11 & -2.58e-10 & 4.28e-09 & 1.75e-08 \\ 0.00e+00 & 0.00e+00 & 0.00e+00 & 0.00e+00 & 0.00e+00 & 0.00e+00 \end{bmatrix} \\
C_6 &= \begin{bmatrix} -4.27e-07 & 1.99e-06 & -2.40e-07 & 1.25e-06 & -3.58e-08 & -1.53e-08 \\ -3.69e-08 & 1.44e-07 & -2.63e-08 & 9.50e-08 & -5.34e-09 & 1.04e-09 \\ 0.00e+00 & 0.00e+00 & 0.00e+00 & 0.00e+00 & 0.00e+00 & 0.00e+00 \end{bmatrix} \\
C_7 &= \begin{bmatrix} -1.04e-07 & -3.47e-07 & -9.29e-07 & 1.97e-06 & -1.35e-07 & -1.67e-06 \\ 4.04e-09 & -2.24e-08 & -2.23e-08 & 1.31e-07 & -1.84e-09 & -1.13e-07 \\ 0.00e+00 & 0.00e+00 & 0.00e+00 & 0.00e+00 & 0.00e+00 & 0.00e+00 \end{bmatrix}
\end{aligned}$$

$$C_8 = \begin{bmatrix} 1.64e - 07 & 2.74e - 07 \\ 2.28e - 08 & 4.35e - 08 \\ 0.00e + 00 & 0.00e + 00 \end{bmatrix} \quad (\text{A.21})$$

$$C_9 = \begin{bmatrix} 0.00e + 00 \\ 0.00e + 00 \\ 1.00e + 00 \end{bmatrix}$$

The flexible UAV model used in this thesis is available as a companion to the thesis report on the Georgia Institute of Technology's SMARTech repository.

APPENDIX B

CONVERTING FROM MODAL FORM TO STATE SPACE

This appendix summarizes the steps followed in going from the modal form to state space model for control system design and simulation of closed loop system performance. The modal form of the model consists of a diagonal matrix made up of the eigenvalues of the flexible UAV model \bar{A} and the corresponding control input matrix \bar{B} . Also defined in the modal form are the matrices \bar{C} and \bar{D} that correspond to the accelerations measured at 18 different locations on the wing. The available control inputs u are ailerons, elevator, rudder, flaps, right spoiler, flaperons, symmetric throttle and anti-symmetric throttle. In this Thesis only altitude control of the flexible UAV is considered and so only the elevator, throttle and flaperons are used in the control design process. The ASWing model also provides the eigenvector matrix associated with the eigenvalues in \bar{A} . The rows of this matrix are used to construct outputs taken from a list of state variable outputs, which are also available. The eigenvector matrix is used to define outputs that are needed either for closing control loops and for simulation purposes. The eigenvector matrix provides the connection between the state variables of the reduced order model in modal form (which have no physical meaning) and the vehicle states defined which also include the control variables and the components of acceleration at the cg expressed in the body frame. Since the modal form results in a diagonal matrix having complex entries, the corresponding entries in \bar{B} , and \bar{C} matrices are also complex. Therefore, for control design purposes, it is necessary to transform the complex matrices obtained from ASWing model into the corresponding real form. The matlab inbuilt command `cdf2rdf` can be used to convert the complex matrices to real block Jordan form. The ASWing

\bar{A} and \bar{B} model data is converted to real form and used directly to define the plant dynamics, to design the controller gain matrix K_x and in the design of the observer. It is also necessary to transform the Eigenvector matrix to permit computation of the rows of \bar{C} in real form corresponding to the state variables that are to be fed back to the controller.

REFERENCES

- [1] ANNASWAMY, A., LAVRETSKY, E., DYDEK, Z., GIBSON, T. E., and MATSUTANI, M., “Recent results in robust adaptive flight control systems,” *Int. Journal of Adaptive Control and Signal processing*, vol. 27, no. 1-2.
- [2] ASTROM, K. J., “Interactions between excitation and unmodeled dynamics in adaptive control,” *The 23rd IEEE conference on Decision and Control*, pp. 1276–1281, 1984.
- [3] BORTOFF, S. A., KOHAN, R. R., and MILMAN, R., “Adaptive control of variable reluctance motors: a spline function approach,” *IEEE Transactions on Industrial Electronics*, vol. 45, no. 3, pp. 433–444, 1998.
- [4] CALISE, A. J., HOVAKIMYAN, N., and IDAN, M., “Adaptive output feedback control of nonlinear systems using neural networks,” *Automatica*, vol. 37, no. 8, pp. 1201–1211, 2001.
- [5] CALISE, A. J., LEE, S., and SHARMA, M., “Direct adaptive reconfigurable control of a tailless fighter aircraft,” *AIAA Journal of Guidance, Control, and Dynamics*, vol. 24, no. 5, pp. 896–902, 2001.
- [6] CALISE, A. J. and RYSZYK, R. T., “Nonlinear adaptive flight control using neural networks,” *IEEE Control Systems*, vol. 18, no. 36, p. 1425, 1998.
- [7] CALISE, A. J., YANG, B. J., and CRAIG, J. I., “Augmenting adaptive approach to control of flexible systems,” *Journal of Guidance Control and Dynamics*, vol. 27, pp. 387–396, May 2004.
- [8] CALISE, A. and YUCELEN, T., “Adaptive loop transfer recovery,” *Journal of Guidance Control and Dynamics*, vol. 35, pp. 807–815, May-June 2012.
- [9] CAMPION, G. and BASTIN, G., “Indirect adaptive state feedback control of linearly parametrized non-linear systems,” *International Journal of Adaptive Control and Signal Processing*, vol. 4, no. 5, pp. 345–358, 1990.
- [10] CHANDRAMOHAN, R., YUCELEN, T., and CALISE, A. J., “Flight test results for kalman filter and h2 modification in adaptive control,” *AIAA Guidance, Navigation, and Control Conference, Chicago*, 2009.
- [11] CHANDRAMOHAN, R., YUCELEN, T., CALISE, A. J., and JOHNSON, E. N., “Experimental evaluation of derivative-free model reference adaptive control,” *AIAA Guidance, Navigation, and Control Conference, Chicago*, 2009.

- [12] CHEN, B.-S. and CHENG, Y.-M., “Adaptive wavelet network control design for nonlinear systems,” *Proceedings of the 35th IEEE on Decision and Control, Kobe, Japan*, vol. 3, pp. 3224 – 3229, 1996.
- [13] CHEN, Y. and TENG, C., “A model reference control structure using a fuzzy neural network,” *Fuzzy sets and Systems*, vol. 73, no. 3, pp. 291–312, 1995.
- [14] CHOWDHARY, G., JOHNSON, E., CHANDRAMOHAN, R., KIMBRELL, M., and CALISE, A., “Guidance and control of airplanes under actuator failures and severe structural damage,” *Journal of Guidance Control and Dynamics*, vol. 36, pp. 1093–1104, May-June 2013.
- [15] DOGAN, K. M., YUCELEN, T., GRUENWALD, B. C., and MUSE, J. A., “On model reference adaptive control for uncertain dynamical systems with unmodeled dynamics,” *To appear at the IEEE conference on Decision and Control*, 2016.
- [16] DOYLE, J., DOVER, K., KHARGONEKAR, P., and FRANCIS, B., “State-space solutions to standard h_2 and h_∞ control problems,” *IEEE Transactions on Automatic Control*, vol. 34, no. 1, pp. 831–847, 1989.
- [17] DOYLE, J. and STEIN, G., “Multivariable feedback design: Concepts for a classical/modern synthesis,” *Automatic Control, IEEE Transactions on*, vol. 26, no. 1, pp. 4–16, 1981.
- [18] DRELA, M., “Aswing theory,” http://web.mit.edu/drela/Public/web/aswing/asw_theory.pdf, 2015.
- [19] ELZEBDA, J. M., NAYFEH, A. H., and MOOK, D. T., “Analytical study of the subsonic wing-rock phenomenon for slender delta wings,” *Journal of Aircraft*, vol. 26, no. 9, pp. 805–809, 1989.
- [20] ELZEBDA, J. M., NAYFEH, A. H., and MOOK, D. T., “Development of an analytical model of wing rock for slender delta wings,” *Journal of Aircraft*, vol. 26, no. 28, pp. 737–743, 1989.
- [21] FERRARI, S., *Algebraic and Adaptive Learning in Neural Control Systems*. PhD thesis, 2002.
- [22] FIORENTINI, L., SERRANI, A., BOLENDER, M. A., and DOMAN, D. B., “Non-linear robust adaptive control of flexible air-breathing hypersonic vehicles,” *Journal of Guidance Control and Dynamics*, vol. 32, no. 2, pp. 402–417, 2009.
- [23] GE, S. S., HANG, C. C., and ZHANG, T., “Adaptive neural network control of nonlinear systems by state and output feedback,” *IEEE Transactions on Systems, Man and Cybernetics Part B*, vol. 29, no. 6, pp. 818–828, 1999.
- [24] GIBSON, T. E., “Closed-loop reference model adaptive control: with application to very flexible aircraft,” *PhD Thesis*, February 2014.

- [25] GIBSON, T. E., ANNASWAMY, A., and LAVRETSKY, E., “Improved transient response in adaptive control using projection algorithms and closed loop reference models,” *AIAA Guidance, Navigation, and Control Conference, Minneapolis*, 2012.
- [26] GIBSON, T. E., ANNASWAMY, A., and LAVRETSKY, E., “Adaptive systems with closed-loop reference models, part i: Transient performance,” *American Control Conference, Washington D.C*, 2013.
- [27] GIBSON, T. E., ANNASWAMY, A., and LAVRETSKY, E., “Adaptive systems with closed-loop reference models, part i: Transient performance,” *IEEE Access*, vol. 1, pp. 703–717, 2013.
- [28] GIBSON, T. E., QU, Z., ANNASWAMY, A., and LAVRETSKY, E., “Adaptive output feedback based on closed-loop reference models,” *IEEE Transactions of Automatic Control*, vol. 60, no. 10.
- [29] GOLEAA, N., GOLEAA, A., and BENMAHAMMED, K., “Stable indirect fuzzy adaptive control,” *Fuzzy sets and Systems*, vol. 137, no. 3, pp. 353–366, 2003.
- [30] HOVAKIMYAN, N., CALISE, A. J., and MADYASTHA, V. K., “An adaptive observer design methodology for bounded nonlinear processes,” *Proceedings of the 41st IEEE Conference on Decision and Control*, vol. 4, pp. 4700 – 4705, 2002.
- [31] HOVAKIMYAN, N., LEE, H., and CALISE, A. J., “On approximate nn realization of an unknown dynamic function from its input output history,” *American Control Conference, Chicago*, vol. 2, pp. 919 – 923, June 2000.
- [32] HOVAKIMYAN, N., NARDI, F., and CALISE, A. J., “A novel error observer based adaptive output feedback approach for control of uncertain systems,” *IEEE transactions on Automatic Control*, vol. 47, pp. 1310–1314, 2002.
- [33] HOVAKIMYAN, N., YANG, B. J., and CALISE, A. J., “Adaptive output feedback control methodology applicable to non-minimumphase nonlinear systems,” *Automatica*, vol. 42, pp. 513–522, April 2006.
- [34] HSU, C. and LAN, C., “Theory of wing rock,” *Journal of Aircraft*, vol. 22, no. 10, pp. 920–924, 1985.
- [35] JIANG, Z.-P. and HILL, D. J., “A robust adaptive backstepping scheme for nonlinear systems with unmodeled dynamics,” *IEEE Transactions on Automatic Control*, vol. 4, pp. 1705–1711, June 1999.
- [36] JOHNSON, E. N. and CALISE, A. J., “Limited authority adaptive flight control for reusable launch vehicles,” *Journal of Guidance, Control and Dynamics*, vol. 26, no. 6, pp. 926–913, 2003.

- [37] JOHNSON, E. N., CHOWDHARY, G., CHANDRAMOHAN, R., and CALISE, A. J., “Uav flight control using flow control actuators,” *AIAA Guidance, Navigation, and Control Conference, Minnesota*, 2011.
- [38] KHALIL, H. K., *Nonlinear Systems*. Prentice Hall, 1996.
- [39] KIM, B. S. and CALISE, A. J., “Nonlinear flight control using neural networks and feedback linearization,” *Proceedings of the First Regional Conference on Aerospace Control Systems*, 1993.
- [40] KIM, K., YUCELEN, T., and CALISE, A. J., “K modification in adaptive control,” *AIAA Infotech Conference, Atlanta*, 2010.
- [41] KIM, K., YUCELEN, T., and CALISE, A. J., “A parameter dependent riccati equation approach to output feedback adaptive control,” *AIAA Guidance, Navigation, and Control Conference, Portland, Oregon*, 2011.
- [42] KIM, K., YUCELEN, T., CALISE, A. J., and NGUYEN, N., “Adaptive output feedback control for an aeroelastic generic transport model: A parameter dependent riccati equation approach,” *AIAA Guidance, Navigation, and Control Conference, Portland, Oregon*, 2011.
- [43] KIM, N., CALISE, A., HOVAKIMYAN, N., PRASAD, J., and CORBAN, E., “Adaptive output feedback for high-bandwidth flight control,” *AIAA Journal of Guidance, Control and Dynamics*, vol. 25, no. 6, pp. 993–1002, 2002.
- [44] KIM, Y. and LEWIS, F., *High Level Feedback Control with Neural Networks*. World Scientific, N.J, 1998.
- [45] KOSTARIGKA, K. A. and ROVITHAKIS, G. A., “Adaptive dynamic output feedback neural network control of uncertain mimo nonlinear systems with prescribed performance,” *IEEE Transactions on Neural Networks and Learning Systems*, vol. 23, no. 1, pp. 138–148, 2012.
- [46] KRISTIC, M., KANELAKOPOULOS, I., and KOKOTOVIC, P., *Nonlinear and Adaptive Control Design*. Wiley, New York, 1995.
- [47] KUTAY, A. T., CALISE, A. J., and MUSE, J. A., “A 1-dof wind tunnel experiment in adaptive flow control,” *AIAA Guidance, Navigation, and Control Conference*, 2006.
- [48] LAVRETSKY, E., “Combined/composite model reference adaptive control,” *Automatic Control, IEEE Transactions on*, vol. 54, no. 11, pp. 2692–2697, 2009.
- [49] LAVRETSKY, E., “Adaptive output feedback design using asymptotic properties of lqg / ltr controllers,” *IEEE Transactions on Automatic Control*, vol. 57, no. 6, pp. 1587–1591, 2012.

- [50] LAVRETSKY, E., HOVAKIMYAN, N., and CALISE, A. J., “Upper bounds for approximation of continuous-time dynamics using delayed outputs and feedforward neural networks,” *IEEE transactions on Automatic Control*, vol. 48, no. 9, pp. 1606–1610, 2003.
- [51] LEE, K. W. and KHALIL, H. K., “Adaptive output feedback control of robot manipulators using high-gain observer,” *International Journal of Control*, vol. 67, no. 6, pp. 869–889, 1997.
- [52] LEWIS, F. L., “Neural network control of robot manipulators,” *IEEE Expert*, vol. 11, no. 3, pp. 64–75, 1996.
- [53] LEWIS, F. W., JAGANNATHAN, S., and YESILDIRAK, A., *Neural Network Control Of Robot Manipulators And Non-Linear Systems*. CRC Press, 1998.
- [54] LIGHTBODY, G. and IRWIN, G. W., “Direct neural model reference adaptive control,” *IEEE Proceedings on Control Theory and Applications*, 1998.
- [55] LUO, J. and LAN, E. C., “Control of wing-rock motion of slender delta wings,” *Journal of Guidance, Control and Dynamics*, vol. 16, no. 22, pp. 225–231, 1993.
- [56] MARINO, R. and TOMEI, P., *Nonlinear Control Design: Geometric, Adaptive and Robust*. Prentice-Hall, Englewood Cliffs, N.J, 1995.
- [57] MATSUTANI, M., ANNASWAMY, A., GIBSON, T. E., and LAVRETSKY, E., “Trustable autonomous systems using adaptive control,” *IEEE Conference on Decision and Control and European Control Conference, Orlando*.
- [58] MATSUTANI, M., ANNASWAMY, A., and LAVRETSKY, E., “Guaranteed delay margins for adaptive control of scalar plants,” *IEEE Conference on Decision and Control*, 2012.
- [59] MATSUTANI, M., ANNASWAMY, A., and LAVRETSKY, E., “Guaranteed delay margins for adaptive systems with state variable access,” *American Control Conference, Washington D.C*, 2013.
- [60] MCFARLAND, M. B. and CALISE, A. J., “Nonlinear adaptive control of agile anti-air missiles using neural networks,” *AIAA Missile Sciences Conference*, 1996.
- [61] MUSE, J. A., KUTAY, A. T., BRZOZOWSKI, D. P., CULP, J. R., CALISE, A. J., and GLEZER, A., “Dynamics flight maneuvering using trapped vorticity flow control,” *AIAA Aerospace Sciences Meeting, January*, 2008.
- [62] MUSE, J. A., TCHIEU, A. A., KUTAY, A. T., CHANDRAMOHAN, R., and LEONARD, A., “Vortex model based adaptive flight control using synthetic jets,” *AIAA Guidance, Navigation, and Control Conference, Chicago*, 2009.

- [63] NAIDU, D. and CALISE, A., “Singular perturbations and time scales in guidance and control of aerospace systems, a survey,” *Journal of Guidance Control and Dynamics*, vol. 24, pp. 1057–1078, Nov-Dec 2001.
- [64] NARENDRA, K. and VALAVANI, L., “Direct and indirect model reference adaptive control,” *Automatica*, vol. 15, no. 6, pp. 653–664, 1978.
- [65] NARENDRA, K. and VALAVANI, L., “Stable adaptive controller design—direct control,” *IEEE Transactions on Automatic Control*, vol. 23, no. 4, pp. 570–583, 1978.
- [66] NGYUEN, L. T., “Control-system techniques for improved departure/spin resistance for fighter aircraft,” *NASA TP*, 1980.
- [67] PONNUSAMY, S. S. and GUIB, J. B., “Adaptive output feedback control of aircraft flexible modes,” *Communications, Computing and Control Applications (CCCA), 2012 2nd International Conference on*, December 2012.
- [68] POTTER, J. E., “Matrix quadratic solutions,” *SIAM Journal on Applied Mathematics*, vol. 14, no. 3, pp. 496–501, 1966.
- [69] QU, Z., ANNASWAMY, A. M., and LAVRETSKY, E., “Adaptive output-feedback control for a class of multi-input-multi-output plants with applications to very flexible aircraft,” *IEEE American Control Conference, Boston, MA*, July 2016.
- [70] ROHRS, C., VALAVANI, L., ATHANS, M., and STEIN, G., “Robustness of continuous-time adaptive control algorithms in the presence of unmodeled dynamics,” *Automatic Control, IEEE Transactions on*, vol. 30, no. 9, pp. 881–889, 1985.
- [71] SESHAGIRI, S. and KHALIL, H. K., “Output feedback control of nonlinear systems using rbf neural networks,” *IEEE Transactions on Neural Networks*, vol. 11, no. 1, pp. 69–79, 2000.
- [72] SICILIANO, B., YUAN, B., and BOOK, W. J., “Direct and indirect model reference adaptive control,” *Automatica*, vol. 15, no. 6, pp. 653–664, 1978.
- [73] SINGH, S., YIM, W., and WELLS, W., “Direct adaptive and neural control of wingrock motion of slender delta wings,” *Journal of Guidance, Control and Dynamics*, vol. 18, pp. 25–30, 1995.
- [74] SINGLA, P., SUBBARAO, K., and JUNKINS, J., “Adaptive output feedback control for spacecraft rendezvous and docking under measurement uncertainty,” *Journal of Guidance Control and Dynamics*, vol. 29, pp. 892–902, July 2006.
- [75] SMAIN, D. and BRAHIM, B., “Modelling and simulation of an aeroelastic airfoil using lqr, lqg/ltr, h2 and h_∞ controllers,” *International Conference on Electrical and Electronic Engineering*, 2009.

- [76] SPALL, J. C. and CRISTION, J. A., “A neural network controller for systems with unmodeled dynamics with applications to wastewater treatment,” *IEEE transactions on Systems, Man and Cybernetics partB*, vol. 27, no. 3, pp. 369–375, 1997.
- [77] SUARE, C. J., KRAMER, B. R., AYERS, B., and MALCOLM, G. N., “Forebody vortex control for suppressing wing rock on a highly-swept wing configuration,” *Journal of Aircraft*, vol. 26, no. 9, pp. 805–809, 1992.
- [78] TAYLOR, D. G., KOKOTOVIC, P. V., MARINO, R., and KANNELLAKOPOULOS, I., “Adaptive regulation of nonlinear systems with unmodeled dynamics,” *Automatic Control, IEEE Transactions on*, vol. 34, no. 4, pp. 405–412, 1989.
- [79] TUZCU, I., *Dynamics and Control of Flexible Aircraft*. PhD thesis, 2001.
- [80] XIAO, B., QINGLEI, H., and YOUJIN, Z., “Fault-tolerant attitude control for flexible spacecraft without angular velocity magnitude measurement,” *Journal of Guidance, Control and Dynamics*, vol. 34, no. 5, pp. 1556–1561, 2011.
- [81] YANG, B. J., HOVAKIMYAN, N., and CALISE, A. J., “Output feedback control of an uncertain system using an adaptive observer,” *Proceedings of the 42nd Conference on Decision and Control, Maui*, 2003.
- [82] YUCELEN, T., “Advances in adaptive control theory: Gradient and derivative-free approaches,” *PhD Thesis*, May 2012.
- [83] YUCELEN, T. and CALISE, A. J., “Derivative-free model reference adaptive control,” *Journal of Guidance, Control and Dynamics*, vol. 34, no. 4, pp. 933–950, 2011.
- [84] YUCELEN, T. and CALISE, A. J., “Robustness of a derivative-free adaptive control law,” *Journal of Guidance Control and Dynamics*, vol. 37, no. 5, pp. 1583–1594, 2014.
- [85] YUCELEN, T., CALISE, A. J., MUSE, J. A., and YANG, B. J., “A loop recovery method for adaptive control,” *AIAA Guidance, Navigation, and Control Conference, Chicago*, 2009.
- [86] YUCELEN, T., KIM, K., and CALISE, A. J., “Derivative-free output feedback adaptive control,” *AIAA Guidance, Navigation, and Control Conference, Portland, Oregon*, 2011.
- [87] YUCELEN, T., KIM, K., CALISE, A. J., and NGUYEN, N., “Derivative-free output feedback adaptive control of an aeroelastic generic transport model,” *AIAA Guidance, Navigation, and Control Conference, Portland, Oregon*, 2011.
- [88] ZHANG, T., GE, S. S., and HANG, C. C., “Adaptive neural network control for strict-feedback nonlinear systems using backstepping design,” *Automatica*, vol. 36, no. 2, pp. 1835–1846, 2000.

VITA

Rajeev Chandramohan obtained his bachelors degree in Electronics and Communication Engineering from Bangalore University, India in 2001. He obtained his Masters in Aerospace Engineering from Wichita State University in 2007. His areas of interest include robust control, optimal control theory and adaptive control theory with application to both manned and unmanned fixed wing vehicles.